

**Phylogenetic and electrophysiological characterization
of new ion channel subunits from *Hydra
magnipapillata* belonging to the DEG/ENaC gene
family**

der Fakultät für Biologie
der EBERHARD KARLS UNIVERSITÄT TÜBINGEN

zur Erlangung des Grades eines Doktors
der Naturwissenschaften

Andjelko Golubovic
aus Ehingen/ Do.
vorgelegte
D i s s e r t a t i o n

2007

Tag der mündlichen Prüfung: 26. Oktober 2007

Dekan: Prof. Dr. F. Schöffl

1. Berichterstatter: Prof. Dr. S. Gründer

2. Berichterstatter: Prof. Dr. H. A. Mallot/ Prof. Dr. H. Herbert

ABSTRACT

The degenerin (DEG)/epithelial sodium channel (ENaC) gene family represents a class of sodium selective ion channels found in nearly all multicellular animals (Metazoa). The members of this ion channel family are functionally diverse, however, nothing is known about the evolutionary origin and the primitive characteristics. In contrast to K^+ , Cl^- or water channels, DEG/ENaC ion channels are neither present in unicellular organisms nor in plants. Since cnidarians are the simplest metazoans having a nervous system, we used the model cnidarian *Hydra magnipapillata* to isolate cDNA for four different DEG/ENaC subunits, HyNaC1-4. The present work had two purposes: first the phylogenetic classification of the newly cloned *Hydra* proteins within the diverse family of DEG/ENaC channels and second the characterization of the activation mechanism and of the electrophysiological properties of HyNaC ion channels.

The phylogenetic analysis showed that HyNaCs are close relatives of vertebrate ASICs and BLINaCs/INaC, whereas ENaCs and the FMRFamide-gated FaNaCs are more distant relatives of HyNaCs. ASICs are proton-gated ion channels mainly expressed in the mammalian nervous system. BLINaCs are a subgroup of the DEG/ENaC superfamily with an unknown ligand, expressed in the brain, liver and intestine of mouse and rat and INaC is the human orthologue found exclusively in the intestine.

We could evoke robust currents in oocytes expressing HyNaC2 and 3 by application of HydraRFamides I or II, which are common neuropeptides in *Hydra*. The activation was dose-dependent with similar potency for both peptides ($EC_{50} \sim 25 \mu M$). HyNaC2/3 was unselective for monovalent cations and was blocked by amiloride with a rather low affinity ($IC_{50} \sim 500 \mu M$). Inhibition of G-proteins as well as altering expression of hemi gap junctions did not change current amplitudes, suggesting direct channel activation.

Using in situ hybridization, we located the HyNaC expressing cells adjacent to the HydraRFamide expressing neurons in the hypostome region at the bases of the tentacles, suggesting that the peptides are the natural ligands for this channel. Moreover, peptide interaction seems to be a common feature of DEG/ENaC channels since we could show that HydraRFamides can also modulate proton-activated ASIC currents.

Our results show that the simple nervous systems of *Hydra* uses neuropeptides for fast neurotransmission, suggesting that neuropeptides were among the first ligands for ion

channels. Furthermore, close relationship of HyNaCs to both human INaC and ASIC4, for which the activating stimulus is not yet known, opens the possibility that ligands for these two channels are among RFamide-like peptides.

ZUSAMMENFASSUNG

Die DEG/ENaC (Degenerine/epitheliale Natrium Kanäle) Gen-Familie ist eine Klasse Natrium-selektiver Ionenkanäle, deren Vertreter in fast allen tierischen Vielzellern (Metazoa) vorkommen. Die einzelnen Untergruppen sind funktionell sehr unterschiedlich, es ist jedoch nichts über den Ursprung und die ursprünglichen Eigenschaften der Kanäle bekannt. Im Gegensatz zu K^+ -, Cl^- - oder Wasserkanälen kommen DEG/ENaC Ionenkanäle weder in einzelligen Lebewesen noch in Pflanzen vor. Da Cnidarier die primitivsten Metazoen sind, die ein Nervensystem besitzen, haben wir die cDNA von 4 DEG/ENaC Untereinheiten aus dem Modell-Cnidarier *Hydra magnipapillata* isoliert: HyNaC1-4.

Diese Arbeit hatte zwei Ziele: zum einen die phylogenetische Einordnung der neu klonierten *Hydra* Proteine in die Familie der DEG/ENaC Kanäle und zum zweiten die Charakterisierung des Aktivierungsmechanismus` und der elektrophysiologischen Eigenschaften der *Hydra* Ionenkanäle.

Die phylogenetische Analyse zeigte, daß ASICs und BLINaCs/INaC nahe Verwandte von HyNaCs sind, wohingegen ENaCs und die FMRFamid-aktivierten FaNaCs entfernter stehen. ASICs sind Protonen-aktivierte Ionenkanäle, die hauptsächlich im Nervensystem von Säugern exprimiert werden. BLINaCs sind eine Untergruppe der DEG/ENaC Superfamilie mit unbekanntem Liganden; sie werden im Gehirn, der Leber und dem Verdauungstrakt von Mäusen und Ratten exprimiert, während INaC, das Ortholog im Menschen, nur im Darm gefunden wird.

Durch Applikation der *Hydra*-Neuropeptide HydraRFamid I und II konnten wir in Frosch-Oozyten, die HyNaC2 und 3 exprimierten, große Ströme hervorrufen. Die Aktivierung war dosisabhängig, wobei beide Peptide in etwa die gleiche Affinität besaßen ($EC_{50} \sim 25 \mu M$). HyNaC2/3 Kanäle waren unselektiv gegenüber monovalenten Kationen und wurden durch Amilorid mit einer geringen Affinität blockiert ($IC_{50} \sim 500 \mu M$). Die Inhibierung von G-Proteinen und die Veränderung der Expressionsstärke von Hemi Gap Junctions führten zu keiner Veränderung der Stromamplituden, was auf eine direkte Kanalaktivierung schließen lässt.

Durch in-situ-Hybridisierungen konnten wir zeigen, daß in der Hypostom-Region, direkt an den Basen der Tentakel, Zellen, die HyNaCs exprimieren, neben Neuronen liegen, die HydraRFamide exprimieren. Dies lässt vermuten, daß die Peptide die natürlichen Liganden

der HyNaC Kanäle sind. Desweiteren scheint die Interaktion mit Peptiden ein allgemeines Merkmal der DEG/ENaC Kanäle zu sein, da wir zeigen konnten, daß Protonen-aktivierte ASIC-Ströme ebenfalls durch HydraRFamide moduliert werden.

Unsere Ergebnisse zeigen, daß das einfache Nervensystem von *Hydra* Neuropeptide zur schnellen Signalübertragung benutzt, was darauf schliessen lässt, daß Peptide eine der ersten Liganden für Ionenkanäle in Metazoen überhaupt waren. Desweiteren eröffnet die enge Verwandtschaft von HyNaCs zu INaC und ASIC4, deren beider Aktivierungsstimulus noch nicht gefunden wurde, die Möglichkeit, daß die Liganden dieser beiden Kanäle unter den RFamid-artigen Peptiden zu suchen sind.

ACKNOWLEDGEMENTS

I would like to thank many people and I think I should do this in German.....

Zuallererst möchte ich mich bei meinem Betreuer Prof. Dr. Stefan Gründer bedanken, ohne ihn wäre diese Arbeit nicht zustande gekommen, und überhaupt hätte ich mir keinen besseren Betreuer vorstellen können.

Des Weiteren möchte ich folgenden Leuten für die tolle Kooperation danken: Herrn Dr. Kalbacher und Herrn Prof. Dr. Grimmelikhuijzen und den jeweiligen Mitarbeitern für die Bereitstellung der Hydra-Peptide, ebenso Herr Prof. Dr. Holstein und seinem Team für die in-situ Hybridisierungen.

Ganz besonders möchte ich auch Herr Prof. Dr. Mallot und Herrn Prof. Dr. Herbert herzlich danken, dass Sie so kurzfristig als Gutachter und Prüfer eingesprungen sind und bin dabei in Gedanken bei der Familie von Herrn Prof. Dr. Werner Schmidt.....

Natürlich darf ich meine Kollegen und Freunde aus dem Labor nicht vergessen. Ich danke unseren TA's Maria Siba und Patricia Seeberger, daneben Lilia, Ivan, Dominik, Xuanmao und Martin für die große Unterstützung und eine tolle Zeit.

Daneben gibt es eine Reihe von Menschen, die ich hier nicht namentlich erwähne, die aber, wenn sie diese Zeilen lesen wissen werden, dass sie eigentlich auch hier rein gehören.

Zum guten Schluss möchte ich den beiden Frauen danken ohne die ich nicht wäre was ich jetzt bin. Zum einen meiner lieben Mama, die mich mit ihrer mütterlichen Liebe in allem was ich tat unterstützt hat und immer für mich da war, und zum anderen natürlich auch meiner Kuschelmaus, die mich auch in Zeiten, in denen es nur zäh voranging immer wieder aufgefangen hat und mir mit Ihrer Liebe den nötigen Rückhalt gab. Meine kleine Kuschelmaus, die bisherige Zeit mit Dir war wunderschön und ich freue mich schon auf die vielen gemeinsamen Jahre, die noch kommen werden....

TABLE OF CONTENTS

Abstract	I
Zusammenfassung	III
Acknowledgements	V
Table of contents	VI
List of abbreviations	X
I. Introduction	1
1.1 The DEG/ENaC Ion Channel Superfamily	1
1.1.1 History	1
1.1.2 Phylogeny and sequence comparison	2
1.1.3 General features and structure	3
1.1.4 Subfamilies	6
1.1.4.1 ASICs (acid-sensing ion channels)	6
1.1.4.2 ENaCs (epithelial sodium channels)	7
1.1.4.3 BLINaCs/INaC (brain liver intestine sodium channels)	7
1.1.4.4 FaNaCs (FMRFamide-gated sodium channels)	8
1.1.4.5 DEGs (degenerins)	8
1.1.4.6 RPK/PPKs (ripped pocket/pickpocket proteins)	10
1.1.4.7 FLRs (fluoride resistant mutation proteins)	11
1.1.5 Modulation by FMRFamide-related neuropeptides	11
1.2 Cnidaria and <i>Hydras</i>	14

1.2.1 General features	14
1.2.2 Neurotransmission and neuropeptides in cnidarians	18
1.3 Aims of this study.....	21
II. Materials and methods	23
2.1 Phylogenetic analysis	23
2.2 Electrophysiological measurements	24
2.2.1 <i>Xenopus laevis</i> oocyte expression system	24
2.2.1.1 Preparation of the oocytes	25
2.2.1.2 Properties of the oocytes	25
2.2.1.3 Injection	26
2.2.1.4 cDNA and cRNA synthesis	27
2.2.2 Voltage clamp technique	27
2.2.2.1 Two electrode voltage clamp in oocytes	29
2.2.2.2 Intracellular electrodes	30
2.2.2.3 Fast solution exchange set-up	30
2.2.3 Solutions	32
2.2.4 Data analysis	33
III. Results	35
3.1 Sequence comparison between HyNaCs and other DEG/ENaC proteins and phylogenetic analysis	35
3.1.1 The primary structure of HyNaCs shares all domains characteristic for DEG/ENaC family members	35
3.1.2 HyNaCs are close relatives of ASICs and BLNaC/INaC	37

3.2 Electrophysiological characterization of HyNaC DEG-mutant currents .	39
3.2.1 Expression of HyNaC2 G429T evokes small constitutive currents that are strongly increased by co-expression of HyNaC3 G430T	39
3.2.2 Co-injection of HyNaC3 G430T alters the properties of HyNaC2 G429T homomeric currents	43
3.3 Electrophysiological analysis of HyNaC wild-type currents	47
3.3.1 Removal of Ca ²⁺ and Mg ²⁺ evokes large currents in oocytes co-expressing HyNaC2 and HyNaC3	47
3.3.2 HyNaC2/3 currents evoked by removal of divalent cations are inhibited by acidic pH	50
3.3.3 Neuropeptides from <i>Hydra</i> evoke currents in oocytes co-expressing HyNaC2 and HyNaC3	52
3.3.4 Peptide-activated HyNaC currents exhibit tachyphylaxis, which is suppressed by pre-application of acidic pH	53
3.3.5 Peptide-activated HyNaC currents are blocked by low pH	55
3.3.6 HydraRFamide I and II activate heteromeric HyNaC2/3 currents with similar potency, which is enhanced by removal of Ca ²⁺	56
3.3.7 Peptide-activated HyNaC currents are unselective and can be blocked by amiloride with low affinity	58
3.3.8 Unselective currents activated by HydraRFamides are not evoked by the opening of hemi gap junctions	61
3.3.9 HyNaC2/3 heteromers form ion channels that are directly activated by the <i>Hydra</i> neuropeptides	64
3.4 Modulation of ASIC currents by HydraRFamides	68
IV. Discussion	70
4.1 HyNaCs are members of the DEG/ENaC family with ASICs and BLINaC/INaC as closest relatives	70
4.2 HyNaCs are directly activated by <i>Hydra</i> neuropeptides	72

4.3 Properties of peptide-evoked HyNaC2/3 currents and their evolutionary implications	74
4.4 Neuropeptides and DEG/ENaC ion channels	77
V. References.....	80
VI. Appendix	95
5.1 Complete alignment of HyNaC2-4 together with selected members of the DEG/ENaC ion channel superfamily.....	96
5.2 Trimmed alignment used for phylogenetic analysis.....	98
5.3 Phylogenetic tree created with PAUP4.0b10 using the neighbor joining method.....	101
5.4 Phylogenetic tree created with PAUP4.0b10 using the parsimony method.....	102
5.5 Phylogenetic tree created with ClustalX 1.81 using the neighbor joining method.....	103
5.6 In situ hybridizations reveal co-localization of HydraRFamides and HyNaC2-4 in the hypostome region	104
5.7 List of accession numbers for the sequences used in the phylogenetic analysis	105
Lebenslauf	110

LIST OF ABBREVIATIONS

μA	microampere
μl	microliter
μM	micromoles per liter
τ	time constant
A	alanine
Ach	acetyl choline
amil.	amiloride
AMP	adenosine monophosphate
2-APB	2-aminoethoxydiphenyl borate
ASIC	acid-sensing ion channel
AS-1-l	long version of antisense oligonucleotide against <i>Xenopus</i> pannexin-1
ATP	adenosine triphosphate
BAPTA	1,2-bis(2-aminophenoxy)ethane-N,N,N',N'- tetraacetic acid
BLINaC	brain-liver-intestine sodium channel
BNC/BNaC	brain sodium channel
C	cysteine
$^{\circ}\text{C}$	degree Celsius
Ca^{2+}	calcium

CaCl ₂	calcium chloride
<i>C.elegans</i>	<i>Caenorhabditis elegans</i>
cAMP	cyclic AMP
cDNA	complement DNA
Cl ⁻	chloride
cm	centimeter
C _m	membrane capacitance
CNS	central nervous system
COO ⁻ (H)-	carboxy-terminus
CRD	cysteine-rich-domain
cRNA	complement RNA
D	aspartic acid
DEG	degenerin
DEL	degenerin-like protein
DEPC	diethylpyrocarbonate
DNA	deoxyribonucleic acid
DRG	dorsal root ganglion
ECM	extracellular matrix
EC ₅₀	ligand concentration necessary for half-maximal activation
EDTA	ethylenediaminetetraacetic acid
ENaC	epithelial sodium channel

ERD	extracellular regulatory domain
F	phenylalanine
FaNaC	FMRamide-gated sodium channel
FFA	flufenamic acid
Fig.	figure
FLR-1	fluoride resistant mutant-1
FMRamide	phenylalanine-methionine-arginine-phenylalanine amide
G	glycine
G _i	inhibitory G-protein
GABA	gamma-aminobutyric acid
GDP-β-S	guanosine 5`-(β-thio)diphosphate
GPCR	G-protein coupled receptor
h	hour
H ⁺	proton
HG	histidine-glycine
H ₃ N ⁺ -	amino terminus
5-HT	5-hydroxytryptamine (serotonin)
HEDTA	N-(2-hydroxyethyl)ethylene-diamine-N,N',N'-triacetic acid
HEPES	4-(2-hydroxyethyl)-1-piperazineethanesulfonic acid

Hym-301	peptide 301 cloned from <i>Hydra magnipapillata</i>
HyNaC	<i>Hydra</i> sodium channel
I	current
IBMX	3-isobutyl-1-methyl-xanthin
I _c	capacitative current
IC ₅₀	ligand concentration necessary for half-maximal inhibition
ID	inner diameter
I _i	ionic current
I _m	membrane current
I _{max}	maximal current
INaC	intestinal sodium channel
INX	innexin
IRK-1	inward rectifying potassium channel-1
K	lysine
K ⁺	potassium
KCl	potassium chloride
kDa	kiloDalton
L	leucine
L-DOPA	3,4-dihydroxy-L-phenylalanine
Li ⁺	lithium
LiCl	lithium chloride

M	methionine
MEC	mechanosensitive mutations
MES	2-(N-morpholino)ethanesulfonic acid
MDEG	mammalian degenerin
mg	milligram
Mg ²⁺	magnesium
MgCl ₂	magnesium chloride
min	minute
ml	milliliter
mm	millimeter
mM	millimoles per liter
mRNA	messenger ribonucleic acid
mV	millivolt
MSD	membrane spanning domain
MΩ	MegaOhm
N	asparagine
n	number
Na ⁺	sodium
NaCl	sodium chloride
ng	nanogram
Na ₂ HPO ₄	di-sodium hydrogen phosphate
NH ₂ ⁻	amino terminus

NJ	neighbor joining
nm	nanometer
NMDA	N-methyl-D-aspartic acid
NMDG ⁺	D(-)-N-Methylglucamin
NO	nitric oxide
NPAF	neuropeptide AF
NPFF	neuropeptide FF
NPSF	neuropeptide SF
OD	outer diameter
OR-2	oocyte ringer's solution 2
OTC-20	oocyte testing carousel - 20
P	proline
P	probability
PANX	pannexin
PMA	phorbol ester 12-O-tetradecanoylphorbol-13-acetate
PNS	peripheral nervous system
post-TM1	post-transmembrane domain 1
PVP	polyvinylpyrrolidone
PPK	pickpocket
pyro-Glu	pyro-glutamate
P ₂ X ₇	purinergic receptor that opens in response to extracellular ATP

Q	glutamine
Q_m	membrane charge
R	arginine
R_i	resistance of the current electrode
RNA	ribonucleic acid
RPK	ripped pocket
S	serine
SD	standard deviation
sec	second
SEM	standard error of mean
SLP	stomatin-like protein
S-S	disulfide bridge
T	threonine
Tab.	table
TEVC	two electrode voltage clamp
TM	transmembrane domain
trunc.	truncated
UNC	uncoordinated locomotion mutant
V	voltage
V	valine
V_{hold}	holding potential
V_m	membrane potential

W tryptophan

Y tyrosine

CHAPTER I

Introduction

1.1 The DEG/ENaC Ion Channel Superfamily

1.1.1 History

The epithelial sodium channel (ENaC)/degenerin (DEG) gene family represents a class of sodium selective ion channels that was discovered in the early 1990s. The members of this ion channel superfamily are widely distributed throughout the animal kingdom and functionally highly diverse. The ion channel family was named after a dominant negative mutation that when present in *deg-1* and other genes of *C.elegans*, led to the degeneration of specific touch sensitive neurons (Chalfie 1990). At about the same time the α -subunit of the epithelium sodium channel (ENaC) was cloned and functionally expressed in *Xenopus laevis* oocytes (Canessa 1993). It was already known that ENaC plays a crucial role in sodium reabsorption in epithelia of different mammalian organs. The authors recognized the high sequence similarity between the gene encoding ENaC and the genes encoding the degenerins in *C.elegans* and proposed a new gene family encoding for cation channels.

Soon, additional members forming a new subgroup inside this emerging ion channel family were cloned by sequence homology. At the beginning, they were named mammalian degenerins (MDEG) (Waldmann 1996) or brain sodium channels (BNC, BNaC) (Price 1996; Garcia-Anoveros 1997), because they were mainly found in the central and peripheral nervous system of mammals. After the discovery that these channels could be activated by extracellular protons, they got their today's name: acid-sensing ion channels (ASICs) (Waldmann 1997).

At about the same time, a novel member of the DEG/ENaC superfamily was cloned from the snail *Helix aspersa* (Lingueglia 1995). It was called FaNaC (FMRFamide-activated Na⁺-channel) and forms a subgroup on its own within the DEG/ENaC ion channel family. Until today FaNaC is the only known ion channel that is directly activated by a peptide. Some 3 years later, in 1998, members of two new invertebrate subgroups were cloned,

FLR-1 from *C.elegans* (Take-Uchi 1998) and RPK/PPK from *Drosophila melanogaster* (Darboux 1998). In 1999, Lazdunski et al. screened a rat cDNA library for novel members of the DEG/ENaC family and found a gene encoding for a degenerin-related protein that is expressed mainly in the brain, liver and intestine of the rat (Sakai 1999). It was named BLINaC, and one year later the same group cloned the human homolog, called INaC (intestinal Na⁺-channel) (Schaefer 2000). Until today, the stimulus to activate BLINaC/INaC and their function are still unknown.

1.1.2 Phylogeny and sequence comparison

Members of the DEG/ENaC superfamily are found in insects, snails, nematodes and several vertebrates, including humans. They are distributed in tissues as diverse as kidney epithelia, muscles and neurons and are, depending on their function, constitutively open or activated by different ligands like protons or neuropeptides. Although DEG/ENaC channels are found in almost all groups of metazoans where they participate in diverse biological processes and are activated in response to markedly distinct stimuli, the overall secondary structure of channel subunits encoded by this gene superfamily is highly conserved.

In Figure 1 the most important members of the DEG/ENaC ion channel family are shown. At the moment, seven major subgroups can be distinguished: ENaCs, ASICs and BLINaC/INaC, which are only found in vertebrates, the DEG/MEC-group and FLR-1 found in *C.elegans*, the peptide-gated FaNaCs present in different snails, and the RPK/PPK-group in *Drosophila melanogaster*. Not much is known about the evolutionary relationships between the subfamilies. There are only few works concerning the phylogeny of the superfamily, most of them with contradictory data, but it seems clear that ASICs and BLINaC are close relatives, also ENaCs and DEGs (see Fig. 1). Until today, nothing is known about the origin and the precursor of the DEG/ENaC channels. The amino acid sequence identity between the different DEG/ENaC subfamilies is about 15-20%, but is higher within the different subgroups. The amino acid identity between the four ASIC subunits is in the range of 45-60%, about 30% between the ENaCs and also between the DEGs. RPK and PPK from *Drosophila* share 38% amino acid identity, and the FaNaC orthologues are 65% identical on the amino acid level.

In contrast to the evolutionary older potassium, chloride or water channels, the DEG/ENaC

genes are only present in complex animals with specialized organs or structures for coordination, digestion and reproduction. The wide tissue distribution from transporting epithelia to excitable neurons is accompanied by a high degree of functional heterogeneity between the DEG/ENaC family members, which is unusual for the other known ion channel gene families.

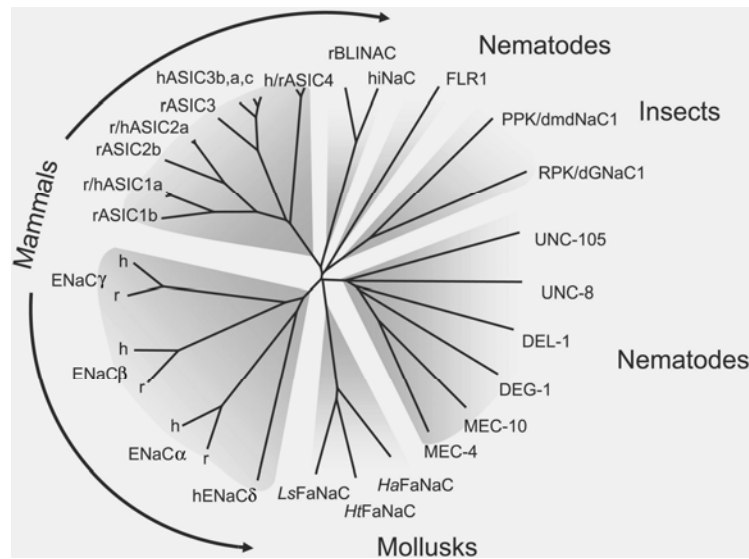


Fig. 1: Phylogenetic tree of the DEG/ENaC ion channel superfamily.
(From Kellenberger 2002.)

Depending on their function, DEG/ENaC ion channels are constitutively open like ENaCs, mechanically gated like MEC-10 and MEC-4 in *C. elegans* or activated by ligands like protons and peptides, as it is the case for ASICs and FaNaCs, respectively. The functional heterogeneity and the fact that the DEG/ENaC subgroups only appear in either protostomes or deuterostomes indicate that the evolution of the DEG/ENaC gene family is widely ramified and diverged very early in history.

1.1.3 General features and structure

Functional members of the DEG/ENaC superfamily are cation channels with a high selectivity for Na^+ over K^+ . They can all be blocked by amiloride with an IC_{50} in the low μM range. DEG/ENaC ion channels are probably multimeric, with several subunits forming a pore through the cell membrane. Most works concerning the stoichiometry of DEG/ENaC

ion channels postulate tetrameric assemblies as it is shown in Figure 2 (Firsov 1998; Coscoy 1998; Kosari 1998; Dijkink 2002), whereas Snyder et al. favor ion channels composed of 9 subunits (Synder 1998).

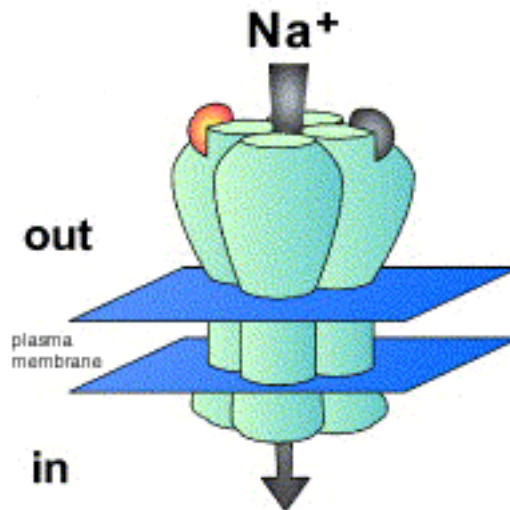


Fig. 2: Tetrameric structure of DEG/ENaC ion channels. The orange and grey structures on the subunits indicate potential binding sites for ligands or agonists.

(Adapted from Lingueglia 2006.)

The size of single subunit proteins varies between ~500 and ~1000 amino acids and all members have several domains of high sequence similarity in common, indicating important functional roles. Figure 3 shows a schematic illustration of the DEG/ENaC subunit topology with the conserved domains. All members of the DEG/ENaC superfamily possess two hydrophobic membrane-spanning domains (MSD1 and MSD2) and a large extracellular loop situated between the transmembrane segments. The NH₂-terminus and the short COOH-terminus are intracellular. The cytoplasmic pre-MSD1 region, in near proximity to the membrane-spanning domain 1, contains a conserved HG (His-Gly) motif and the extracellular post-MSD1 region contains a FPxxTxC motif. The extracellular loop makes up more than 50% of the channel protein and represents a structural feature unique to the DEG/ENaC family members. It contains at least two cysteine-rich domains (CRDs), CRD2 and CRD3 that are likely to be involved in the formation of disulfide bonds to maintain the tertiary structure of the large extracellular loop. For ENaCs, two cysteine-pairs

have already been identified that are important for the trafficking of the protein to the plasma membrane (Firsov 1999). Other domains in the extracellular loop are conserved only within subfamilies of the DEG/ENaC superfamily, for example the CRD1 and the extracellular regulatory domain (ERD) that are present only in the degenerin subfamily of *C.elegans*.

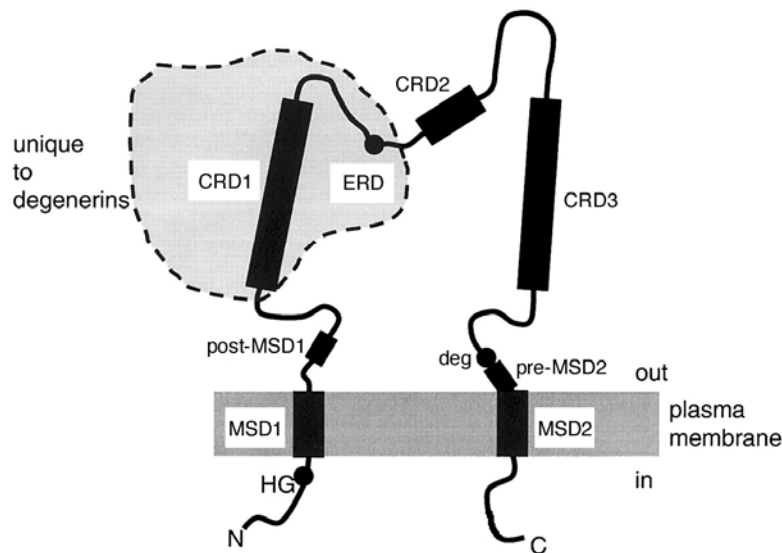


Fig. 3: Schematic transmembrane topology common for proteins within the DEG/ENaC ion channel superfamily. (Adapted from Kellenberger 2002.)

The membrane-spanning domain 2 (MSD2) together with the pre-MSD2 is highly conserved among the DEG/ENaC family members. Several lines of evidence suggest that the latter is partially embedded in the membrane and forms the outer mouth of the hydrophilic pore. It was shown for ENaC subunits that amino acid residues in the pre-MSD2 are important for the ion selectivity and also for the binding of amiloride (Schild 1997; Sheng 2000; Kellenberger 1999 and 2001; Fuller 1997). The pre-MSD2 region also includes a key position occupied by variable amino acids with short side chains. Substitution of this residue by amino acids with larger side chains causes hyperactivity in most of the DEG/ENaC family members. This site was first identified in *C.elegans* degenerins, where the mutation caused degeneration of specific touch-sensitive neurons (Driscoll 1991; Chalfie 1990), giving the gene family its name. Mutations in this position are known as “DEG-mutations”.

1.1.4 Subfamilies

1.1.4.1 ASICs (acid-sensing ion channels)

Acid-sensing ion channels (ASICs) are a proton-activated subgroup of the DEG/ENaC superfamily. The recent cloning of proton insensitive lamprey and shark ASICs indicated that the proton sensitivity arose during the development of bony fishes, some 400 million years ago and that activation by protons is characteristic only for ASICs of higher vertebrates (Coric 2005).

In mammals, there are 6 members: ASIC1a and 1b, ASIC 2a and 2b, ASIC3 and ASIC4, encoded by four genes; *asic1* and *asic2* encode for two different splice variants of the same gene, differing in their N-termini (Lingueglia 1997; Chen 1998; Bässler 2001). In heterologous expression systems, ASICs can form homo- and heteromeric channels generating fast activating transient sodium currents when extracellular pH is rapidly decreased. The only exception is ASIC4, which can not be activated by protons and also does not alter the properties of other subunits when co-expressed. Mammalian ASICs are almost exclusively found in the nervous system, although they have also been detected in other tissues (Babinski 1999; Gründer 2000; Ishibashi 1998; Jahr 2005). ASICs are involved in a variety of physiological functions and pathologies. ASIC1a, the most prominent ASIC subunit in the brain, is believed to play a role in long-term potentiation, spatial learning and fear conditioning (Wemmie 2002 and 2003). Due to its Ca²⁺ permeability, activation of ASIC1a also contributes to neuronal death during acidosis associated with brain ischemia (Gao 2005; Xiong 2004). In the peripheral nervous system, ASIC-like currents seem to be involved in the perception of pain (Jones 2004; Chen 2002; Ugawa 2002), cutaneous mechanical sensitivity (Price 2000 and 2001) and visceral mechanotransduction (Jones 2004 and 2005; Page 2004 and 2005). Due to its ability to generate sustained currents in addition to the transient component and due to its high sensibility to lactic acid, ASIC3 is believed to play a major role in triggering angina and other ischemic pain (Yagi 2006; Immke 2001; Immke 2003; Sutherland 2000; Benson 1999).

1.1.4.2 ENaCs (epithelial sodium channels)

The constitutively open ENaCs are another subfamily of DEG/ENaC ion channels exclusively expressed in vertebrates. There are four subunits known: α ENaC, β ENaC, γ ENaC and δ ENaC with isoforms existing for all 4 subunits. In 2003, a new subunit was cloned from *Xenopus laevis* that is no isoform or species orthologue of any known subunit; it was called ϵ ENaC (Babini 2003). In heterologous expression systems, only the co-expression of the α -, β - and γ -subunit together generates constitutive currents that are comparable to native currents (Canessa 1994). Quantitative analysis of cell surface expression and functional assays based on differential sensitivities to channel blockers point to a 2:1:1 stoichiometry between the ENaC subunits, meaning that the α -subunit is two times more abundant in functional ENaCs compared to the β - and γ -subunits (Firsov 1998; Kosari 1998).

ENaC is involved in the regulation of Na^+ -balance, of blood volume and of blood pressure. It is localized in the apical membrane of polarized epithelial cells where it plays a major role in Na^+ -transport across the epithelia. ENaC is mainly expressed in kidney, lung, gastrointestinal tract, salivary glands, and skin (Kellenberger 2002). In the kidney, it is expressed in the distal nephron, where it mediates an electrogenic Na^+ -absorption related to K^+ -secretion into the tubule lumen. In lung and in salivary glands, ENaC contributes to the volume of the luminal fluid, saliva and the alveolar fluid (Kellenberger 2002). In humans, Liddle's syndrome (Hansson 1995 and 1995; Inoue 1998; Lifton 1995) and pseudohypoaldosteronism type I (Chang 1996; Schild 1996) are two hereditary diseases caused by mutations in the genes encoding ENaC, emphasizing the important role of ENaC in Na^+ -and K^+ -homeostasis.

1.1.4.3 BLINaCs/INaC (brain liver intestine sodium channels)

The BLINaC/INaC group is the most mysterious subfamily of the DEG/ENaCs. Only two members are cloned, BLINaC from the rat (Sakai 1999) and INaC from humans (Schaefer 2000). Phylogenetic analyses put them in close proximity to ASICs, but until today, the right stimulus for activation of heterologously expressed BLINaC/INaC is not found.

Currents can only be generated by introducing the DEG-mutation. The RNA for *blinac* is mainly expressed in the small intestine, the liver and the brain of rats, whereas *inac* is found almost exclusively in the small intestine of humans (Sakai 1999; Schaefer 2000).

1.1.4.4 FaNaCs (FMRFamide-gated sodium channels)

FaNaCs are a subgroup of the DEG/ENaC family that is exclusively found in snails. The first FaNaC was cloned from the snail *Helix aspersa* in 1995 (Lingueglia 1995). Today, FaNaCs from three other snail species have been cloned: from *Helisoma trivolvis* (Jeziorski 2000), *Lymnaea stagnalis* (Perry 2001) and *Aplysia kurodai* (Furukawa 2006). Heterologously expressed FaNaCs can be activated by FMRFamide, a common peptide in the nervous system of snails. These currents have similar properties to native FMRFamide-evoked currents recorded from snail neurons (Green 1994; Harris 1995; Jeziorski 2000). FMRFamide activates FaNaC in the μM range and generates sodium selective transient currents that desensitize only partially (see Fig. 5). Thus, FaNaC is the first, and to date unique, ion channel that is directly gated by peptides. In snails, FaNaCs are exclusively expressed in neurons (Davey 2001). Their physiological role is unknown, there are speculations about the participation in fast synaptic transmission (Lingueglia 2006), but this remains to be established.

1.1.4.5 DEGs (degenerins)

DEGs or degenerins are a subgroup of the DEG/ENaC superfamily of ion channels that are found exclusively in *Caenorhabditis elegans*. Their name refers to the fact that specific mutations in different subunits cause swelling and degeneration of specific touch sensitive neurons (Chalfie 1990; Driscoll 1991). At least 9 candidate genes encoding for proteins of this subgroup are known in the *C.elegans* genome. The already cloned members are: MEC-4 (Driscoll 1991), MEC-10 (Huang 1994), DEG-1 (Chalfie 1990), UNC-105 (Liu 1996), DEL-1 and UNC-8 (Tavernarakis 1997). Phylogenetic analysis showed that degenerins are closely related to mammalian ENaCs (Kellenberger 2002; Syntichaki 2004), both gave this whole ion channel superfamily their name. MEC-4 and MEC-10 build the core of a mechanosensitive complex in touch sensitive neurons of *C.elegans*. Mutations in both

genes lead to touch-insensitive worms (Huang 1994 and 1995; Driscoll 1991; Hong 1994). Figure 4 shows a model of the touch receptor mechanotransducing complex with all other proteins that are supposed to be involved in sensing touch. MEC-2, a stomatin-like protein, is proposed to link the transduction channel, composed of MEC-4 and MEC-10 subunits, to the intracellular tubulins MEC-7 and MEC-12 (Tavernarakis 1997). On the outer side of the plasma membrane the touch sensitive neurons are surrounded by an extracellular matrix (ECM) and extracellular proteins, like MEC-1 and MEC-5, are tethered to the transduction channel. Recent results demonstrate an important role of these extracellular structures in organizing the precise location of the channel (Emtage 2004). It was shown that *mec-6* encodes for a single-pass membrane-spanning protein with limited similarity to paraoxonases and that it is required for punctate MEC-4 expression along touch-neuron processes (Chelur 2002); its precise role is not yet known.

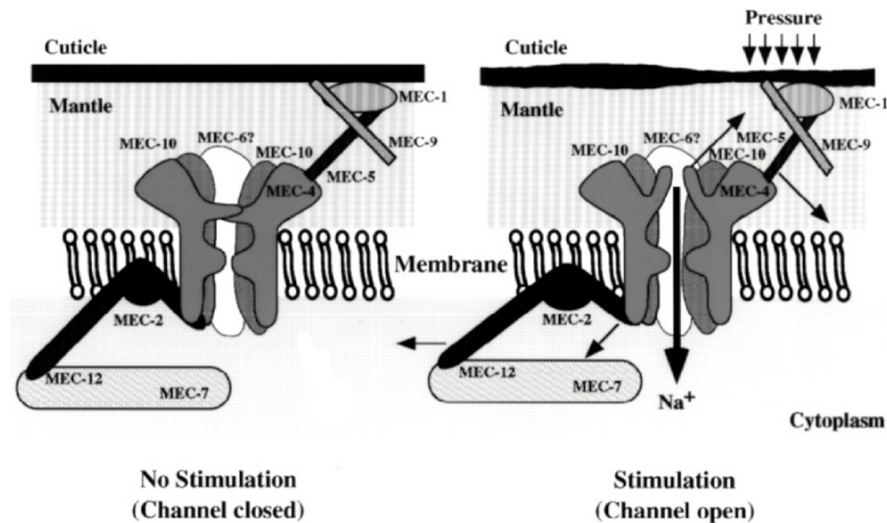


Fig. 4: Schematic arrangement of the supposed proteins participating in the mechanosensitive complex in touch-sensitive neurons of *C.elegans*.
(From Tavernarakis and Driscoll 1997.)

The model shown in Figure 4 proposes that exertion of pressure on the cuticle opens the transduction channel either by deformation of the intracellular microtubule network or of the connections in the ECM (Tavernarakis 1997). When expressed in oocytes, MEC-4 and MEC-10 generate only very small constitutive currents that can be increased by introducing DEG-mutations. However, the co-expression of MEC-2 and MEC-6 dramatically potentiates MEC-4/10 currents (Goodman 2002; Chelur 2002). There are some indications

that also other members of the DEG/ENaC family, particularly ASICs, are involved in different forms of mechanosensitivity (Price 2000 and 2001), and a recent work also showed that a stomatin-related protein, called SLP-3, is involved in mechanotransduction in the mouse and directly interacts with ASICs (Wetzel 2006).

UNC-8 and DEL-1, two other degenerins that are co-expressed in motoneurons of *C.elegans*, are also thought to form ion channels in mechanosensitive complexes (Kellenberger 2002), but this is speculative and has to undergo further investigation. Nevertheless, it was shown that UNC-8, which is also expressed in sensory neurons and interneurons, plays a role in regulation of the worm's locomotion (Tavernarakis 1997).

UNC-105, another member of the degenerins, is not expressed in neurons, but in muscles of *C.elegans*. UNC-105 contributes to proprioception by monitoring muscle stretch (Kellenberger 2002). Introducing the DEG-mutation creates permanently open channels, either when expressed heterologously in *Xenopus* oocytes (Garcia-Anoveros 1998) or in native tissue, which causes muscle hypercontraction (Liu 1996; Park 1986).

1.1.4.6 RPK/PPKs (ripped pocket/pickpocket proteins)

The RPK/PPKs are a rather diverse subgroup of the DEG/ENaC family from *Drosophila melanogaster*. There are about 25 candidate DEG/ENaC genes in the *Drosophila* genome, but so far, not all of them have been investigated with regard to their function and tissue distribution. Today, 16 members are cloned: RPK (Darboux 1998), PPK1 (Darboux 1998), PPK4, PPK7, PPK10-14, PPK16, PPK19-21, PPK23 and PPK28 (Liu 2003). A phylogenetic analysis made by Liu et al. showed that the cloned *Drosophila* members are more closely related to each other than to DEG/ENaC subunits from other species, which suggests RPK/PPKs to be a distinct subfamily within the DEG/ENaC superfamily (Liu 2003). RPK is the only member of the RPK/PPK subgroup that generates currents when heterologously expressed in *Xenopus* oocytes (Adams 1998). Transcripts of RPK are found exclusively in the fly gonads and are maternally deposited into the embryo, where they are found in the PNS, indicating that RPK is involved in maturation and early embryonic development (Darboux 1998; Adams 1998). All PPKs cloned until today do not generate currents when expressed in *Xenopus* oocytes. The expression patterns of the single members vary. *ppk1*, which is the PPK-subunit that was cloned first, is expressed

exclusively in multidendritic (md) sensory neurons in the larval body wall and in some bipolar brain neurons (Adams 1998). A recent study revealed that *ppk1* null mutant larvae show an altered crawling behavior, indicating that PPK1 plays an essential role in controlling rhythmic locomotion (Ainsley 2003). *ppk11* and *ppk19* are both expressed in the larval taste-sensing terminal organ and on the taste bristles of the labellum, the legs, and the wing margins in adult flies. Liu et al. showed that knockout of the two genes affects the flies behavior in salt detection and salt discrimination (Liu 2003). The same group found that 9 of the PPK subunits are expressed in the tracheal system of *Drosophila* and may be important to clear liquid and generate an air-filled tubule system, similar to ENaCs in mammals (Liu 2003).

1.1.4.7 FLRs (fluoride resistant mutation proteins)

In the *C.elegans* genome there are at least 7 putative *flr* candidate genes, but until today, only FLR-1 was cloned (Take-Uchi 1998). In 1998, it was found that *flr-1* encodes a protein belonging to the DEG/ENaC ion channel family (Take-Uchi 1998), but no functional experiments in heterologous expression systems have been done to date. The name resulted from the first isolation of *flr-1* mutants by resistance to fluoride ions (Katsura 1994). It was shown that *flr-1* is expressed in the intestine of *C. elegans* and that mutations in *flr-1* affect the worm's defecation rhythm (Iwasaki 1995; Take-Uchi 1998).

1.1.5 Modulation by FMRFamide-related neuropeptides

In the nervous system, the transmission of electrical information between neurons occurs via electrical or chemical synapses. The latter usually use small molecule transmitters, like dopamine or adrenaline that are released from the presynaptic neurons into the synaptic cleft, and bind to receptors in the plasma membrane of the postsynaptic neurons, where they activate ion channels. Besides these classical, fast working small molecule messengers, there is also a multiplicity of neuroactive peptides that are pharmacologically active in the nervous system. Most of them have only modulatory functions in synaptic transmission, but some serve as neurotransmitters in slow neuronal transmission processes by activating G-protein coupled receptors (GPCRs), for example Substance-P. Thus,

usually neuropeptides do not act directly on ion channels. However there are exceptions in the DEG/ENaC ion channel family.

In the early 1990s, it was shown by Cottrell and colleagues that FMRFamide could elicit fast depolarization of C2-neurons from the snail *Helix aspersa*, which was triggered by Na^+ -influx (Cottrell 1990; Green 1994). Only short time after this finding, Lingueglia et al. cloned FaNaC from *Helix* and showed that it was directly activated by FMRFamide in *Xenopus* oocytes (see Fig. 5; Lingueglia 1995). In the meantime, 3 more FMRFamide-sensitive FaNaCs have been cloned from different snail species (Jeziorski 2000; Perry 2001; Furukawa 2006). Until today, they are the only known ion channels that are directly gated by a neuropeptide.

FMRFamide and related peptides comprise a family of neuropeptides that are abundant in many invertebrates, including snails, worms and flies. In these organisms, FMRFamide-like neuropeptides are supposed to act as neurotransmitters and neuromodulators (Price 1977; Roumy 1998).

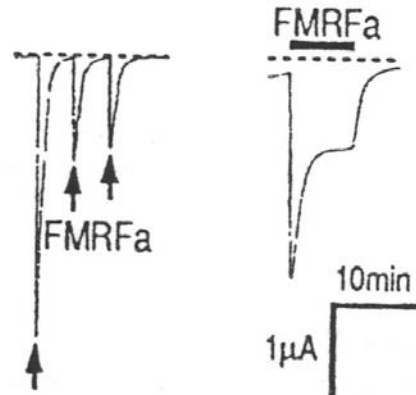


Fig. 5: Currents elicited by FMRFamide in oocytes injected with FaNaC cRNA.
(From Lingueglia 1995.)

Although FMRFamide itself has not been discovered in mammals, at least one gene encoding a precursor protein for FMRFamide-related peptides is found in the mammalian genome. Neuropeptide FF (NPFF), Neuropeptide AF (NPAF) and Neuropeptide SF (NPSF) all are mammalian FMRF-like neuropeptides derived from this common precursor protein that is mainly expressed in the mammalian CNS (Deval 2003). These neuropeptides are supposed to be involved in a variety of physiological functions, including pain modulation, opiate function and cardiovascular regulation (Deval 2003). In mammals, some of the

effects exerted by FMRF-like peptides are mediated through opioid receptors, since they can be blocked by naloxone (Kavaliers 1985 and 1987; Raffa 1988; Gouarderes 1993; Roumy 1998). However, there are also effects that are insensitive to naloxone (Gayton 1982; Raffa 1986; Kavaliers 1987; Raffa 1988; Allard 1989; Roumy 1998). Thus, after the finding that FaNaC is activated by FMRFamide, people hoped to find the non-opioid receptors for the FMRF-like neuropeptides within the mammalian DEG/ENaC members. In 2000, Askwith and colleagues showed for the first time that ASIC currents are modulated by FMRFamide and NPPF in DRG neurons (see Fig. 6; Askwith 2000).

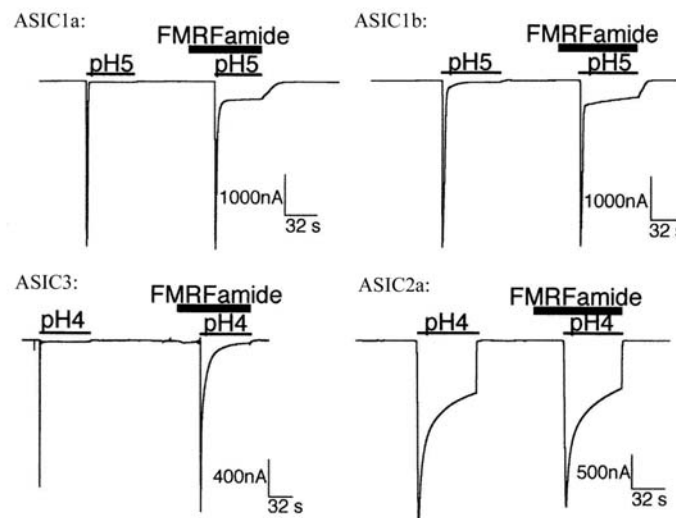


Fig. 6: Modulation of homomeric ASIC-currents by FMRFamide, recorded from *Xenopus* oocytes. (Adapted from Askwith 2000.)

Heterologous expression of ASIC in *Xenopus* oocytes and knockout experiments revealed that only ASIC1 and ASIC3 containing channels are modulated by these two peptides (Askwith 2000; Catarsi 2001; Xie 2003). It is supposed that the modulation of ASIC1 and ASIC3, both expressed in sensory neurons, could be important in regulating neuronal excitability, particularly under inflammatory conditions (Deval 2003; Chen 2006). With regard to the phylogenetic distance between ASICs and FaNaCs within the DEG/ENaC superfamily, it is conceivable that modulation or activation by neuropeptides has developed rather early in the history of DEG/ENaC ion channels and that at least modulation by peptides may be a rather common feature of DEG/ENaC channels.

1.2 Cnidaria and *Hydras*

1.2.1 General features

Porifera (sponges), Ctenophora (comb jellies) and the Cnidaria are the only surviving diploblast groups in the animal kingdom. They are supposed to predate the protostome/deuterostome divergence, thus, representing the base of the multicellular animals (Metazoa). Besides the Ctenophora, members of the phylum Cnidaria are the simplest animals within the Metazoa having a real nervous system, and thus are regarded as sister group to the overwhelming number of bilaterian species (see Fig. 7).

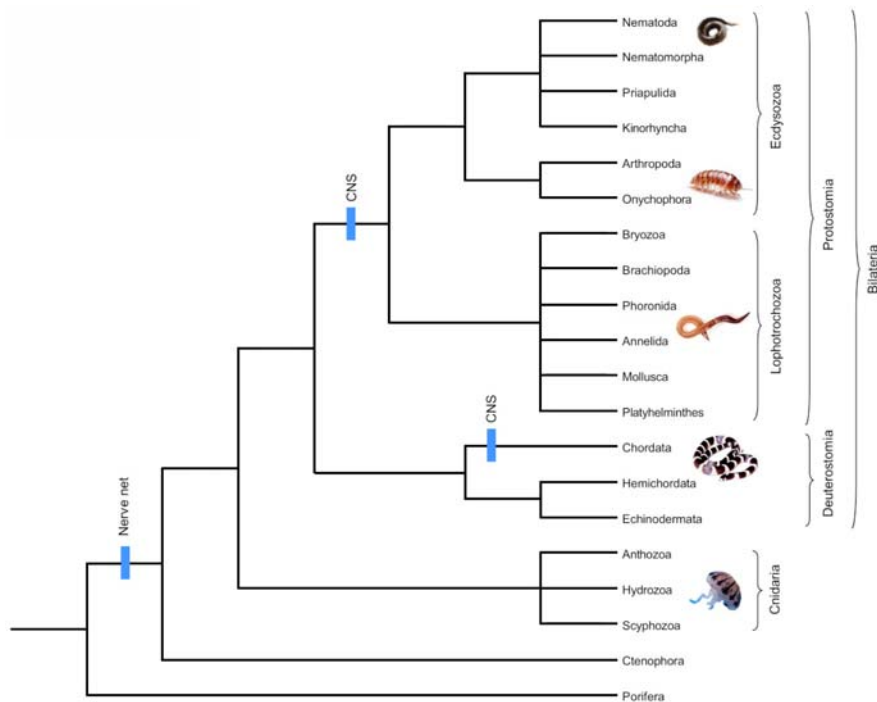


Fig. 7: Phylogeny of the Metazoa.
(Adapted from Sanetra 2005.)

Today, about 10.000 species are known, which are subdivided into 4 major classes: Anthozoa, Scyphozoa, Cubozoa and Hydrozoa. Cnidarians are found exclusively in aquatic, mostly marine, environments. Theoretically, they have life-cycles that alternate between asexual, sessile polyps and sexual, free-swimming forms called medusae. In reality there is a vast variation within the life-cycles of cnidarians.

The uniting and name-giving feature is the cnidocyte, also called nematocyte. Cnidocytes

are very complex, specialized cells containing subcellular organelles called cnidocysts, which carry a hollow coiled thread-like structure that can be fired off (see Fig. 8). This firing is triggered by an interesting structure called cnidocil. The cnidocil is a fixed cilium surrounded by several stereocilia similar to hair bundles that serve as mechanoreceptive structures in vertebrates (see Fig. 8). There are over 30 types of cnidocytes found in different cnidarians, where they serve as weapons primarily used for prey-capture.

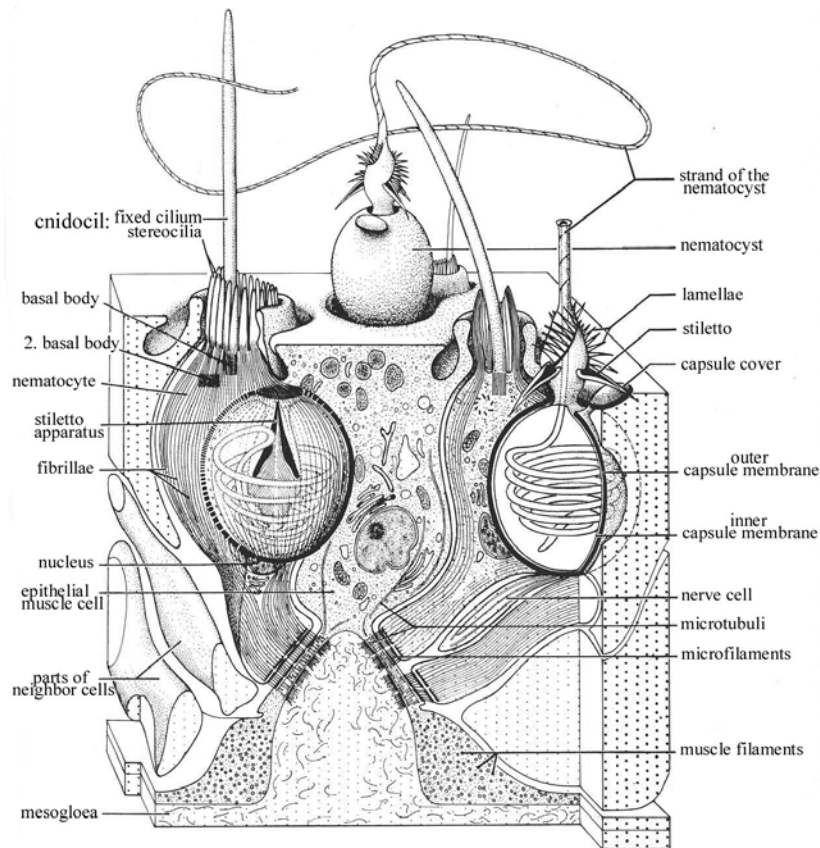


Fig. 8: Schematic nematocytes of *Pelmatohydra oligactis* within the epithelial association. Nematocysts are drawn too small in relation to the cells, particularly to the cnidocils.

(Adapted from Storch and Welsch 1996.)

Cnidarians possess a rather easy body plan. Only two epithelial layers assemble the body: the ecto- and the entoderm (see Fig. 9).

The outer ectoderm is forming the body cover and the inner entoderm surrounds the gastrovascular cavity, which is the site where digestion takes place. Ciliated cells of the entoderm and contraction of the body wall arrange the dispersal of the nutrients, which are

taken up by diffusion. Cnidarians have only a single opening that serves as mouth and anus. Ectoderm and entoderm embed the mesogloea, a jelly-like layer primarily composed of glycoproteins and proteoglycans that are secreted from the epithelial cells. The mesogloea acts as a structural support in the water as cnidarians lack bones or other means of support.

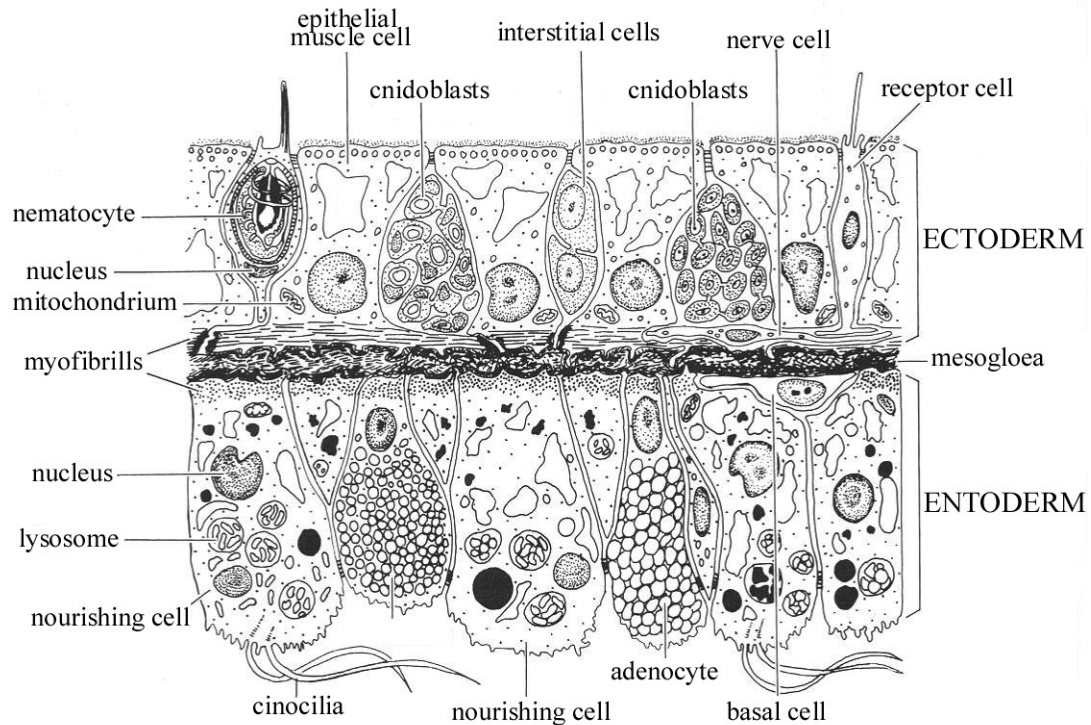


Fig. 9: Cellular composition of the body wall of *Hydra*.
(Adapted from Storch and Welsch 1996.)

The muscular system is composed of longitudinal and concentric elements. The myofibrils are found in the prolonged bases of specialized ento- and ectodermal cells, which are called muscular epithelial cells (see Fig. 9). The nervous system consists of two components: a network of bi- and multipolar nerve cells at the base of the epithelial cells and sensory neurons situated between the epithelial cells. The latter ones possess a ciliated process projecting into the surrounding space (see Fig. 9). Close-by to these ciliated neurons clustered groups of sensory neurons can form also sensory regions that are sensitive to light or touch.

Another important cell type are the interstitial cells (see Fig. 9), which are pluripotent cells that can transform into other cell types such as cnidoblasts, spermatozoa, adenocytes or

nerve cells. These give many cnidarians an extraordinary capacity for regeneration. In particular the genus *Hydra* serves as a model for the research of pattern formation processes.

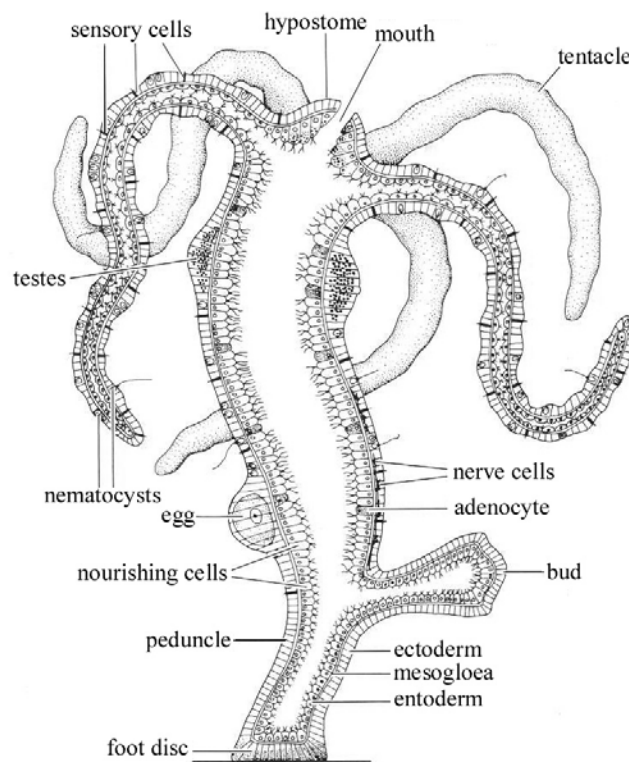


Fig. 10: Schematic, longitudinal section through *Hydra viridissima*.
(Adapted from Storch and Welsch 1996.)

Hydras are freshwater polyps belonging to the class of Hydrozoa within the Cnidaria. They are small, sessile animals with a body length of 1-30 mm. Their life-cycle is characterized by the lack of a medusoidal stage. *Hydras* reproduce either sexually or asexually by budding. Five regions are distinguished in the body plan of *Hydra*: the head region, the gastric region, the budding region, the peduncle and the foot region (see Fig. 10).

Hydra's mouth region, called hypostome, is surrounded by tentacles. They are used primarily for prey-capture and thus are equipped with up to 30.000 nematocysts. Figure 10 shows a schematic cross-section through the body wall of *Hydra*, showing the major cell types already discussed above.

1.2.2 Neurotransmission and neuropeptides in cnidarians

DEG/ENaC proteins are not found in plants or unicellular organisms, like bacteria and protists. Since cnidarians, where *Hydra* belongs to, are simple multicellular animals that diverged very early in history from all other metazoans, one can assume that the DEG/ENaC subunits from *Hydra* should have a high similarity to the common ancestor of all DEG/ENaC family members that existed hundreds of million years ago.

Besides the Ctenophora, cnidarians are considered to be the most basal animal group having a nervous system. It is a loose network of neurons without ganglia or brain-like structures (see Chapter 1.2.1), but for example in *Hydra*, the neuronal network is strongly condensed in the head and foot region (Storch and Welsch 1996). Until 1970, when Westfall and co-workers described synaptic vesicles in sea anemones and *Hydra* (Westfall 1970, 1971 and 1973), the scientific world doubted the existence of a nervous system in cnidarians. However, since that time much effort was invested to investigate neuronal structures and to identify transmitters involved in neurotransmission, which would allow us to draw conclusions about the origins and evolution of our own nervous system. The most debated question in this respect was and is still today: which types of neurotransmitter do cnidarian synapses use?

At the beginning, the emphasis was put on the search for classical fast and slow non-peptidergic neurotransmitters known from the vertebrate nervous system. Already in the 1960s, histochemical studies described epinephrine, norepinephrine and 5-HT in the nervous system of *Hydra* (Wood 1963; Wood and Lentz 1964; Wood and Barnett 1965). At about the same time, regeneration and behavioral studies pointed to the importance of classical vertebrate neurotransmitters like acetylcholin, norepinephrine, serotonin, and histamine for cnidarian morphogenesis and behavior (Lentz and Barnett 1961, 1962 and 1963; Singer 1964; Wood and Lentz 1964; Lentz 1966). However, until today, it is very hard to proof that these chemicals indeed work as neurotransmitters. Ultrastructural studies, mainly immunogold labeling, have shown that various types of synaptic vesicles in sea anemones contain the slow non-peptidergic transmitters L-DOPA and 5-HT (Carlberg 1989; Westfall 2000). The latter was also detected in dense vesicles of ectodermal sensory cells of *Hydra attenuata* (Carlberg 1992). Additional immunohistochemical and biochemical works have confirmed the presence of catecholamines and 5-HT in various

cells of all cnidarian subgroups, but also the presence of fast transmitters like acetylcholine, glutamate or GABA (Kass-Simon 2007). While the mainly histochemical evidence for cholinergic transmission in Cnidaria remains equivocal, immunocytochemical and biochemical evidence for glutamate, NMDA-, GABA- and glycine receptors has been far more convincing (Kass-Simon 2007). Classical, non-peptidergic neurotransmitters are thought to be involved in various cnidarian physiological functions. ACh, GABA and glutamate were shown to increase the discharge probability in certain types of nematocysts of *Hydra*. Various behavioral and electrophysiological studies showed that non-peptidergic neurotransmitters also play a role in the control of muscle contraction, in the pacemaker systems, the feeding responses and light perception of different cnidarians (Kass-Simon 2007).

In the last years, small-molecule short-lived transmitters, like NO, ATP and different eicosanoids turned out to be interesting candidates as potential neurotransmitters in cnidarians. Biochemical, histochemical and physiological data begin to accumulate mainly for NO that it could work as an intercellular messenger. It was shown that NO is involved in the recruitment of the tentacles in prey capture in *Hydra vulgaris* (Colasanti 1997), but also in the nematocyst discharge and the swimming behavior in different sea anemones (Salleo 1996; Moroz 2004).

Today, the most promising and most investigated group of potential transmitters are neuropeptides. The growing importance of neuropeptides in the central nervous system of vertebrates stimulated a search for similar peptides in cnidarians. To date a total of 35 neuropeptides from the Hydrozoa, Anthozoa and Scyphozoa have been isolated and sequenced (Hansen 2002). Pioneering work in the detection of neuropeptides was done by Grimmelikhuijzen and co-workers, who reported a FMRF-like immunoreactivity in *Hydra vulgaris* already in 1982 (Grimmelikhuijzen 1982). Subsequently, a series of studies produced compelling evidence for the ubiquitous presence of RFamides and RFamide-related peptides in cnidarian nervous systems. In the genome of *Hydra*, there are at least 7 genes encoding for different neuropeptide precursor proteins, called preprohormones. Each preprohormone gives rise to neuropeptides having 2 specific amino acids next to the C-terminus. Figure 11 shows a list of the known RFamide- and RFamide-related peptides from *Hydra* with their corresponding preprohormone and their distribution: Hydra-RFamide I-IV arise from preprohormone A, B and C, whereas preprohormone D gives rise

to various Hydra-LWamides. Hydra-KVamide results from preprohormone E, Hydra-RGamide from preprohormone F and the recently discovered Hym-301 from preprohormone G. In situ hybridization studies have shown that all preprohormones show specific expression patterns and that adjacent populations of neurons express different preprohormones. Nevertheless, two-color double-labeling in situ hybridization experiments demonstrated that there are populations of neurons in *Hydra*, where different neuropeptides are co-expressed (Hansen 2000 and 2002). To date, all light microscopic studies point on a homogenous distribution of cnidarian peptides throughout neurons and there is little evidence for synaptic peptide accumulations and synaptic peptidergic transmitter activity.

Preprohormone	Peptides	Location	
A	<EWLGGRF-NH ₂	Hydra-RFa-I	Hypostome Upper gastric region Peduncle
	<EWFNGRF-NH ₂	Hydra-RFa-II	
	KPHLRGRF-NH ₂	Hydra-RFa-III	
	HLRGRF-NH ₂	Hydra-RFa-IV	
B	<EWLGGRF-NH ₂	Hydra-RFa-I	Hypostome Upper gastric region
	<EWFNGRF-NH ₂	Hydra-RFa-II	
C	<EWLGGRF-NH ₂	Hydra-RFa-I	Tentacle
D	GPPLGLW-NH ₂	Hydra-LWa-I (Hym-331)	Foot Gastric region Hypostome Tentacle
	EPLPIGLW-NH ₂	Hydra-LWa-II (Hym-248)	
	KPIPLGLW-NH ₂	Hydra-LWa-III (Hym-249)	
	NPYPGLW-NH ₂	Hydra-LWa-IV (Hym-53)	
	GPMTGLW-NH ₂	Hydra-LWa-V (Hym-54)	
	KPNAYKGLPIGLW-NH ₂	Hym-370	
E	APFIFPGPKV-NH ₂	Hydra-KVa (Hym-176)	Upper gastric region Peduncle
F	FPQSFLPRG-NH ₂	Hydra-RGa (Hym-355)	Foot Gastric region Hypostome Tentacle
G	KPPRRCYLNGYCSP-NH ₂	Hym-301	Tentacle zone Hypostome

Fig. 11: RFamides and related neuropeptides arising from preprohormones A-G in *Hydra*.

Nevertheless, there are a few ultrastructural and immunogold labeling studies showing neuropeptide immunoreactivity in synaptic and non-synaptic vesicles of different sea

anemones and *Hydra* (Koizumi 1989; Westfall and Grimmelikhuijzen 1993; Westfall 1995; Carlberg 1989). Behavioral studies have shown that a variety of peptides have excitatory and inhibitory effects on cnidarian muscles (McFarlane and Grimmelikhuijzen 1991; McFarlane 1987, 1991, 1992 and 1993; Anctil 1987; Pierobon 1989). For example, Pierobon et al. demonstrated that bath-applied substance P stimulate tentacle contractions and nematocyst movement in tentacle battery cells of *Hydra* (Pierobon 1989). In electrophysiological studies it was shown that external application of neuropeptides in different cnidarians evoke Ca^{2+} inward currents and inhibitory outward currents in myoepithelial cells and swimming motoneurons, respectively (Spencer 1991; Cho and McFarlane 1996). However, although a multitude of neuropeptides have been found in cnidarians and the list continues to grow, there is strong indication that in cnidarians, as in higher vertebrates and invertebrates, also the known classical transmitters, eicosanoids, and small, short-lived molecules, like NO, are involved in the physiology of neuronal communication and transmission system.

1.3 Aims of this study

Our group had cloned 3 full-length cDNAs for ion channel subunits belonging to the DEG/ENaC gene family from *Hydra magnipapillata* (HyNaCs). The first aim of this work was to generate a detailed phylogenetic analysis including most of the known DEG/ENaC family members, which would allow us to make better assumptions on the evolutionary relation to other DEG/ENaC subgroups, like ASICs or ENaCs.

The second aim of this work was a functional analysis of HyNaC ion channels heterologously expressed in *Xenopus* oocytes. For this purpose, we searched for a stimulus that activated currents in oocytes expressing HyNaC subunits. Moreover, since *Hydra* did not change very much in appearance and lifestyle during the last hundreds of million years, it is likely that also the HyNaC ion channels are functionally rather conserved. Thus, electrophysiological characterization of HyNaCs would allow us to predict ancient properties of a DEG/ENaC precursor ion channel and give deeper insights into the origins of the gene family. Furthermore, electrophysiological studies on HyNaCs, in combination with the phylogenetic analysis, would give us the chance to make functional predictions with respect to other DEG/ENaC members that are poorly understood, like, for example,

the BLINaC/INaC group or ASIC4.

CHAPTER II

Materials and methods

2.1 Phylogenetic analysis

By homology cloning, our group isolated four different cDNAs from *Hydra magnipapillata* containing regions characteristic for DEG/ENaC ion channel family members. The proteins that are encoded by the new *Hydra* cDNAs were named HyNaC1-4 (*Hydra* sodium channels) and the sequences were deposited in the GenBankTM/EBI data base. Accession numbers are AM393879 for HyNaC1, AM393878 for HyNaC2, AM393880 for HyNaC3 and AM393881 for HyNaC4. Amino acid sequences from other DEG/ENaC subunits used for the phylogenetic analysis were identified by BLAST SEARCH and downloaded from NCBI data base (for accession numbers see Appendix 7). The selected sequences were aligned in the program ClustalX and subsequently, regions lacking a certain degree of consensus were identified and deleted. The truncated sequences were again aligned and the resulting alignment (see Appendix 2) was used for creating different phylogenetic trees.

Three approaches were applied to calculate phylogenetic trees: neighbor joining, parsimony analysis and maximum-likelihood analysis. Depending on the method, different programs were used to calculate phylogenetic relationships: the programs ClustalX and PAUP for creating neighbor joining trees. PAUP was also used to create parsimony trees, whereas Tree-Puzzle was used to create maximum-likelihood trees.

Neighbor joining (NJ) is a distance method, meaning that distances are expressed as the fraction of sites that differ between two sequences in a multiple alignment. From the original matrix, NJ first calculates for each taxon its net divergence from all other taxa as the sum of the individual distances from the taxon. This net divergence is used to calculate a corrected distance matrix. NJ then finds the pair of taxa with the lowest corrected distance and calculates the distance from each of those taxa to the node that joins them. A new matrix is then created in which the new node is substituted for those two taxa. NJ does not assume that all taxa are equidistant from the root.

Like NJ, the parsimony method is also a minimum change method. It is based on the

assumption that the most likely tree is the one that requires the fewest number of changes to explain the data in the alignment. Parsimony analysis always assumes that taxa sharing a common characteristic do so because they inherited that characteristic from a common ancestor. It operates by selecting the tree or trees that minimize the number of evolutionary steps, including homoplasies (reversal, convergence and parallelism), required to explain the data. For protein sequences each site in the alignment is a character.

The maximum likelihood analysis evaluates a hypothesis about evolutionary history in terms of the probability that the proposed model and the hypothesized history would give rise to the observed data set. The supposition is that a history with a higher probability of reaching the observed state is preferred to a history with a lower probability. The method searches for the tree with the highest probability or likelihood.

2.2 Electrophysiological measurements

2.2.1 *Xenopus laevis* oocyte expression system

Xenopus laevis, the South African clawed frog (see Fig. 12), is a member of the anuran family Pipidae. There are four subspecies of *Xenopus laevis*, all of them are aerobic but entirely aquatic. Frogs within the genus *Xenopus* are characterized by the presence of three toes with claws on each hind foot.

In 1971, the *Xenopus* oocyte expression system has been introduced by Gurdon (Gurdon 1971) and was refined by Miledi and co-workers, who showed that injection of mRNA led to expression of various types of ion channels and receptors (Barnard 1982).

Xenopus oocytes are an ideal expression system for ion channels and receptors because they contain only few endogenous channels. Another advantage is the uncomplicated handling due to their size and robustness. However, channels expressed heterologously in oocytes may function differently because posttranslational modification may be different in their native environment and associated or auxiliary proteins could miss in oocytes. Nevertheless, despite their disadvantages, *Xenopus* oocytes have become an ideal expression system to investigate the main aspects of structure and function of ion channels and receptors.

Xenopus oocytes undergo six different development stages, termed stages I to VI. All

stages are found in the ovarian lobes, which are located in the abdominal cavity of the frog and can be removed surgically for experimental purposes. For our studies only mature stage V and VI oocytes were used.



Fig. 12: *Xenopus laevis*.

2.2.1.1 Preparation of the oocytes

Xenopus laevis were kept individually in an aquarium after their first operation. Aquariums had water temperatures around 21°C and were exposed to dark-light rhythm of 12h/12h. About 45 minutes before operation, the frog was put on ice. After anaesthetization, the frog was placed on its back and a small cut along the body axis (about 2 cm) was made into the abdominal skin and into subcutaneous body musculature. A sufficient number of oocytes was removed through this incision and put in a dish containing OR-2 medium. The cut was stitched up and the frog was put back into the aquarium. The same frog can be operated 3-6 times, but the interval between the operations should be at least 3 months (Goldin 1992).

2.2.1.2 Properties of the oocytes

Oocytes are cells with a diameter of approximately 1 mm that are surrounded by a glycoprotein matrix called vitelline membrane (see Fig. 13). The vitelline membrane is covered by a follicle cell layer that was removed before mRNA injection or recording. The

removal was done by a combination of treatment with 1mg/ml collagenase Type IIA (SIGMA Chemical Company) solution before injection and manual removal with forceps the day after injection. After collagenase treatment the oocytes were carefully washed with OR-2 medium and only the healthy looking oocytes were selected for injection.



Fig. 13: Single oocytes from *Xenopus laevis*.

The animal pole of oocytes is dark colored and contains the nucleus, while the vegetal pole is white. Different populations of mRNA are located in both halves, but to date there is nothing known about the connection between the site of RNA injection and the location on the oocyte membrane of the expressed channels.

2.2.1.3 Injection

For injection, pulled glass capillaries (1.14 mm OD and 0.5 mm ID, World Precision Instruments, Inc.) were used. Capillaries were pulled with an automatic Puller (Flaming/Brown Micropipette Puller Model P-97; Sutter Instrument Co.) and afterwards, the pulled tips were broken manually under a microscope to a diameter of about 10-20 μm , which allowed more easily penetration of the oocyte membrane. In order to reduce the air volume and water evaporation from the RNA solution, capillaries were filled with paraffin oil before the attachment to the injector.

A hand-driven coarse manipulator (Nanoliter 2000, World Precision Instruments, Inc.) was used to pilot the injection. The oocytes were kept in a scratched petri dish filled with OR-2 solution during the injection and were manipulated with fire polished Pasteur pipettes whose tips had been broken to enlarge the opening (Stühmer 1998).

The cRNA stock solutions with a concentration of 200 ng/ μ l were stored in aliquots of 2-5 μ l/tube at -80 °C. Before injection, cRNAs were diluted with autoclaved doubly distilled water that had been treated with diethylpyrocarbonate (DEPC H₂O). A total volume of about 40 nl of diluted cRNA was injected for each oocyte. The cRNAs were diluted as follows: all HyNaC cRNAs 1:3 or 1:4; cRNAs for *Hydra* innexin-1, stomatin and antisense-oligonucleotide against *Xenopus* pannexin-1 (AS-1-l) all 1:2; cRNA for ASIC1a 1:1000; for ASIC1b 1:10; for ASIC2a and ASIC 3 1:20.

2.2.1.4 cDNA and cRNA synthesis

As *hynac1* is probably a pseudogene, only cRNAs of HyNaC2-4 were expressed in *Xenopus* oocytes. The coding sequence of HyNaC1-4 was cloned in the oocyte expression vector pRSSP containing the 5'-untranslated region from *Xenopus* β -globulin and a poly (A) tail.

HyNaC point mutations were constructed by recombinant PCR using Pwo DNA polymerase (Roche Molecular Biochemicals). All PCR-derived fragments were entirely sequenced.

cDNA containing plasmids were linearized with appropriate enzymes and capped cRNA was synthesized by SP6 polymerase using the mMessage machine kit (Ambion).

2.2.2 Voltage clamp technique

Generally, an electric capacitor is defined as two conductive materials that are separated by an isolator. Cellular membranes are excellent capacitors. Basic characteristic of a capacitor is its ability to store positive and negative charges simultaneously on its surface. Capacitance of membranes (C_m) is the ability to store charge (Q) when there is a voltage change (ΔV) across the two sides of the membrane:

$$Q = C_m * \Delta V_m$$

The capacitance of all biological membranes (C_m) is about $1\mu\text{F}/\text{cm}^2$. Since C is constant, the current flow through the capacitor is proportional to the voltage change with time:

$$I_c = \Delta Q_m / \Delta t = C_m * \Delta V_m / \Delta t$$

The total current I_m flowing through the membrane is the sum of the resistance or ionic current I_i and the capacitive current I_c :

$$I_m = I_i + I_c$$

If V_m does not change, Q_m is constant and there is no capacitive current I_c flowing through the membrane. In this case, measured I_m is nearly equal to I_i , flowing exclusively through ion channels in the membrane.

Applying above-mentioned principles, Marmont and Cole (1949) invented the voltage-clamp technique to overcome the problem of disturbing capacitive currents. With this method they uncoupled the opening and closing of voltage dependent ion channels from the membrane potential. In voltage clamp measurements it is possible to control the membrane voltage (clamping the voltage) and measure the transmembrane current that is required to maintain the clamped voltage. As mentioned above, elimination of capacitive currents is a big advantage of this system and that's why the current flowing through the membrane is only proportional to the number of open channels and, thus, can be correctly measured.

The voltage clamp is a negative feedback mechanism where the membrane potential is kept stable and the current necessary for keeping that potential is measured. In the two electrode voltage clamp technique, two intracellular electrodes are used, one to pass the feedback current and the other to measure the membrane potential (see Fig. 14). Latter (V_m) is recorded by a unity-gain amplifier (A1) connected to the voltage-recording potential electrode (v). A second high-gain differential amplifier (A2) compares V_m to the command potential (V_{hold}) and adjusts the difference between V_m and V_{hold} . The voltage at the output of A2 forces the current to flow through the current-passing microelectrode (i) into the cell (see Fig. 14).

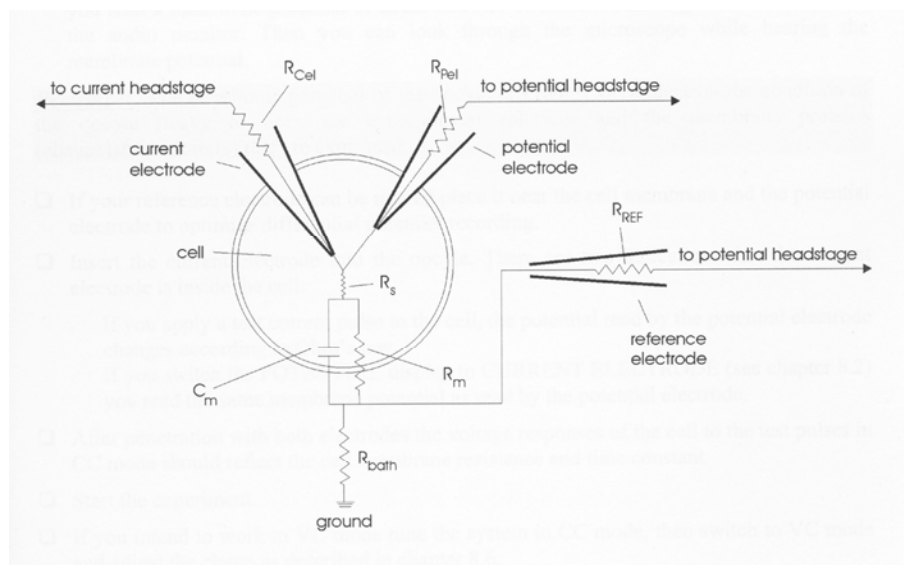


Fig. 14: Model circuit for Two Electrode Voltage Clamp (TEVC) technique. C_m : membrane capacity, R_m membrane resistance, R_{CEL} : current electrode, R_{PEL} : potential electrode resistance, R_{REF} : reference electrode resistance, R_S : series resistance.

(From NPI TURBO TEC-03X product instructions.)

Thus, there is a negative feed back loop: the membrane potential is clamped at a determined value by the command voltage. So, current is produced via the clamping amplifier output if the membrane potential is different from this command voltage and this current flows through the microelectrode i to compensate the difference. This compensating current is the measured parameter.

An additional potential recording electrode (reference electrode) was used for bath solution in our voltage clamp studies to avoid polarization errors that arise from the current passing through the ground electrode. In this configuration, the difference between the intracellular potential electrode and the reference electrode was equated with the transmembrane potential.

2.2.2.1 Two electrode voltage clamp in oocytes

Several considerations have to be made when measuring big cells, like *Xenopus* oocytes, with the two electrode voltage clamp technique. The most important is that oocytes possess a large surface of around $10^6 \mu\text{m}^2$ that has to be charged in order to clamp the cell. Additionally, invaginations of the surface are doubling or tripling the amount of membrane

compared to an ideal spherical oocyte. Another point is that injection of mRNA, depending on the protein, can lead to high expression levels. Currents up to 50 μA or even larger can cause enormous resistance errors.

Since the response time (τ) of a voltage clamp to a step voltage change is,

$$\tau = R_i * C_m / A$$

where R_i is the resistance of the current electrode, C_m is the membrane capacitance, and A is the gain of the command amplifier, the lowest R_i and the largest A possible are usually used to achieve fast clamping of the oocyte.

2.2.2.2 Intracellular electrodes

To achieve above-mentioned low resistance we usually used electrodes, formed by a solution filled glass pipette, which contained an AgCl-coated Ag wire. The pipettes used were borosilicate capillaries (0.7 mm - 1.0 mm, Science Products GmbH, Germany) pulled with an automatic Puller (Flaming/Brown Micropipette Puller Model P-97; Sutter Instrument Co.). If necessary, pipette tips were manually broken to achieve resistances in the range of 0.3- 1.0 $\text{M}\Omega$. The glass pipettes were filled with 3 M KCl to further reduce the electrode resistance. The electrical contact to the electrode filling solution was made through the above-mentioned silver chloride wire. The electrodes could be used repeatedly during the day as they had rather large tip openings and did not plug very often. Oocyte penetration was achieved by advancing the electrode to the cell surface until it broke the membrane and then visibly popped into the oocyte.

2.2.2.3 Fast solution exchange set-up

For my measurements I used the OTC-20 system (NPI, Electronic Instruments). An advantage of this system is the fast solution exchange within less than 1 sec (Madeja 1995). This is achieved because the solution is drawn by suction into a very small “Maltese cross” bath chamber, where the oocyte is located. Solution exchange is controlled by an automated

valve (see Fig. 15). Opening of the valve and rotation of the dishes was directed by the software Cell works 5.1.1 (NPI, Electronic Instruments).

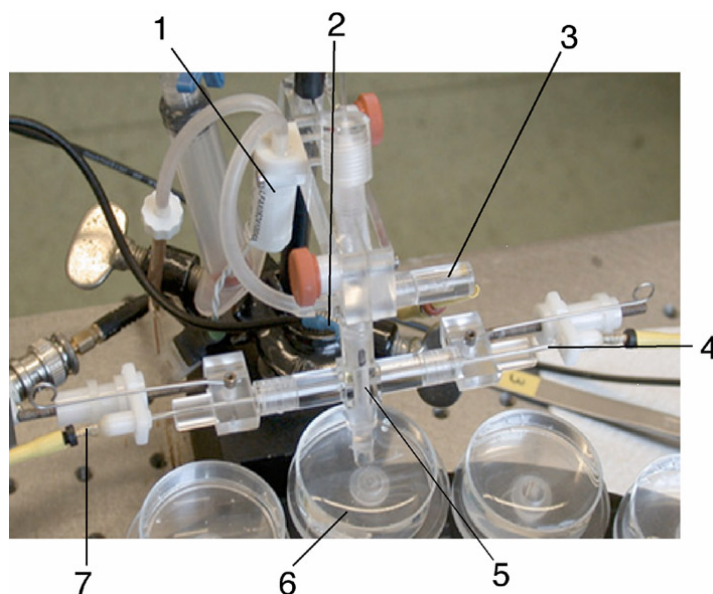


Fig. 15: Experimental chamber of the carousel solution exchange system. 1: Automated valve for the solution exchange; 2: Ground electrode; 3: Reference electrode; 4: Voltage electrode; 5: “Maltese cross” bath chamber containing the oocyte; 6: Solution containing dish; 7: Current electrode

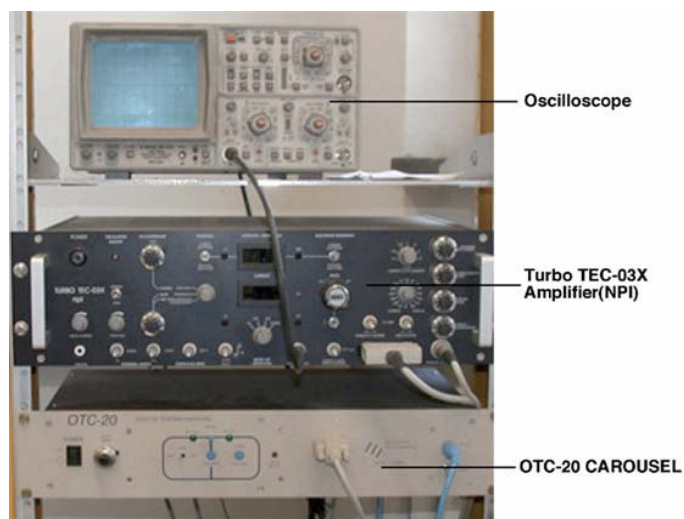


Fig. 16: OTC-20 interface, amplifier and oscilloscope.

The whole set-up (see Fig. 16) was made up of an interface OTC-20 (NPI, Electronic

Instruments), a Turbo Tec 03X amplifier (NPI, Electronic Instruments), an oscilloscope HM507 (Hameg instruments) and a computer (Macintosh G4). Acquisition of the data was also managed by Cellworks 5.1.1 software (NPI, Electronic Instruments).

2.2.3 Solutions

Standard bath solution (pH 7.4) contained:

NaCl	140.0 mM
HEPES	10.0 mM
CaCl ₂	1.8 mM
MgCl ₂	1.0 mM

The Na⁺ concentration and the concentration of the divalent cations were changed according to the different experimental protocols. HEPES was replaced by MES buffer for acidic solutions.

Usually, pH-adjustment was done by adding NaOH or HCl, respectively. In solutions containing a low concentration of divalent cations (≤ 0.1 mM CaCl₂, 0 mM MgCl₂), 0.1 mM flufenamic acid (Sigma) was added in order to block the large conductance induced in oocytes by divalent-free extracellular solutions.

For incubation of oocytes expressing HyNaC wildtype subunits OR-2 solution (Oocyte Ringer solution 2) was used. It was adjusted to pH 7.3 and contained:

NaCl	82.5 mM
KCl	2.5 mM
Na ₂ HPO ₄	1.0 mM
MgCl ₂	1.0 mM
CaCl ₂	1.0 mM
HEPES	5.0 mM
polyvinylpyrrolidone (PVP)	0.5 g/l

As already mentioned in the introduction, DEG-mutations introduced into DEG/ENaC-

family members usually generate constitutive open channels. Therefore, in order to avoid a strong Na^+ loading, a low Na^+ OR-2 solution (pH 7.3) was used for incubation of oocytes expressing HyNaC DEG-mutations. It contained:

NaCl	5.0 mM
NMDG	77.5 mM
KCl	2.5 mM
Na_2HPO_4	1.0 mM
MgCl_2	1.0 mM
CaCl_2	1.0 mM
HEPES	5.0 mM
polyvinylpyrrolidone (PVP)	0.5 g/l
amiloride	1 mM

For determination of the ion selectivity, NaCl was replaced by equimolar concentrations of LiCl or KCl concentrations. Solutions containing different Ca^{2+} and Mg^{2+} concentrations were used to determine the affinity for divalent cations. Solutions with Ca^{2+} or Mg^{2+} concentrations beneath $100\mu\text{M}$ contained either EDTA or HEDTA buffer. All solutions used for determining divalent cation affinity contained 0.1 mM flufenamic acid (Sigma). Free concentrations of divalent cations were calculated by the software Cabuf (downloaded from www.kuleuven.be/fysio/trp/cabuf.php).

2.2.4 Data analysis

Data acquisition in the fast solution exchange set-up was managed using Cellworks 5.1.1 software (NPI Electronic Instruments). Data were stored on hard disk and analyzed using IgorPro 4.02A software (Wave Metrics, Lake Oswego, OR). The figures were created using the program Canvas 7 (Deneba Systems, Inc.). Voltage was clamped at -70 mV if not mentioned otherwise.

Dose response curves (for peptide activation, amiloride affinity, affinity for divalent cations) were fitted to the Hill function:

$$I = a + (I_{\max} - a) / (1 + (C_{50} / [L])^n) \quad \text{Eq.1}$$

Where I_{\max} is the maximal current, a is the residual current, $[L]$ is the concentration of the ligand, C_{50} is the concentration at which half-maximal response occurs, and n is the Hill coefficient. The desensitization time constants of HyNaC2/3 were determined using a monoexponential fit.

For the peptide dose response curves, currents were normalized to the current obtained by applying 120 μM peptide. Inhibition dose response curves for Ca^{2+} , Mg^{2+} and amiloride were obtained by normalizing inhibited currents to the maximal current. Results are reported, in the text, as means \pm SD or, on the figures, as means \pm SEM.

CHAPTER III

Results

3.1 Sequence comparison between HyNaCs and other DEG/ENaC proteins and phylogenetic analysis

3.1.1 The primary structure of HyNaCs shares all domains characteristic for DEG/ENaC family members

By homology cloning, our group isolated 4 cDNAs for novel DEG/ENaC subunits from *Hydra magnipapillata* that we called HyNaC (*Hydra* sodium channel) 1 to 4. cDNAs for HyNaC2, 3 and 4 encode proteins that are between 468 and 471 amino acids in size (see Appendix 1). HyNaC1 has no initiator methionine at the N-terminus, although it has a stop codon there. Thus, it is likely that *hynac1* is a pseudogene and therefore we decided not to express it, but to include it into the phylogenetic analysis, since the conserved domains characteristic for DEG/ENaC family members were all present, except for the HG-motif preceding the first transmembrane domain.

HyNaC2, 3 and 4 share about 15-30% amino acid identity with other members of the DEG/ENaC superfamily. Table 1 shows the percentage of identity on the amino acid level between the HyNaC subunits and selected DEG/ENaC members. The identity between ASICs, BLINaC and HyNaCs lies in the range of 20-30%, whereas ENaCs, FaNaC and MECs share only 15-20% of the amino acids with the *Hydra* proteins. Sequence identity between the three HyNaC subunits varies strongly. 65% of the amino acids of HyNaC3 and HyNaC4 are identical, whereas HyNaC2 shares only about 28% with the other two HyNaC subunits (see Tab. 1).

The most conserved domains characteristic for DEG/ENaC ion channel subunits are all present in HyNaCs2-4. Appendix 1 shows a complete sequence alignment for HyNaC2-4 together with selected members of the DEG/ENaC family. Similar to other DEG/ENaC subunits, a N-terminal cytoplasmic HG (histidine-glycine)-motif precedes the first transmembrane domain (TM1) in HyNaCs2-4. TM1 is followed by the conserved post-TM1 domain, containing the FPAXTxCN motif, where the x positions are occupied by nonpolar, hydrophobic amino acids. In HyNaCs, the

post-TM1 motif is conserved, the hydrophilic threonine (T) is conservatively substituted by a serine (S).

In the extracellular loop, HyNaCs possess CRDs (cysteine-rich-domains) II and III (see Introduction). CRD I, which can be seen in the MEC-4 sequence (Appendix 1) and which is characteristic for *C. elegans* DEG/MECs, is missing.

In CRD II, 2 cysteines (C) are conservatively replaced by threonine (T) and glutamine (Q) (Appendix 1, blue asterisks), whereas another C-residue in the N-terminal part of CRDII is not present at all (Appendix 1, red asterisks) in HyNaCs.

	rASIC1a	rASIC3	rASIC2a	H.a.FaNaC	HyNaC4	HyNaC3	HyNaC2	rENaCalpha	rENaCbeta	rENaCgamma	rBLINaC	MEC4		
1	██████	51.8	65.9	22.8	25.2	27.2	26.8	18.8	22.4	20.5	27.4	19.9	1	rASIC1a
2	51.8	██████	49.1	21.3	25.6	25.7	27.2	21.7	20.2	21.2	27.6	20.0	2	rASIC3
3	65.9	49.1	██████	21.6	24.6	24.6	27.0	20.5	23.2	21.1	27.2	20.1	3	rASIC2a
4	22.8	21.3	21.6	██████	18.8	20.2	19.8	16.9	15.8	17.1	20.8	18.4	4	H.a.FaNaC
5	25.2	25.6	24.6	18.8	██████	65.0	27.8	18.2	17.9	18.2	23.3	17.5	5	HyNaC4
6	27.2	25.7	24.6	20.2	65.0	██████	28.1	18.5	15.5	19.3	24.6	17.0	6	HyNaC3
7	26.8	27.2	27.0	19.8	27.8	28.1	██████	20.0	19.1	18.9	20.2	19.1	7	HyNaC2
8	18.8	21.7	20.5	16.9	18.2	18.5	20.0	██████	29.9	31.3	17.1	16.0	8	rENaCalpha
9	22.4	20.2	23.2	15.8	17.9	15.5	19.1	29.9	██████	34.0	21.6	17.7	9	rENaCbeta
10	20.5	21.2	21.1	17.1	18.2	19.3	18.9	31.3	34.0	██████	21.8	20.9	10	rENaCgamma
11	27.4	27.6	27.2	20.8	23.3	24.6	20.2	17.1	21.6	21.8	██████	24.0	11	rBLINaC
12	19.9	20.0	20.1	18.4	17.5	17.0	19.1	16.0	17.7	20.9	24.0	██████	12	MEC4
	1	2	3	4	5	6	7	8	9	10	11	12		

Percent Identity

Tab. 1: Amino acid identity between HyNaCs2-4 and selected members of the DEG/ENaC ion channel family. Numbers indicate the percentage of identical amino acids.

Characteristic for the amino acids at the DEG-position are short side chains. Substitution by amino acids with long side chains leads to gain-of-function mutants. In HyNaCs, there is a glycine (G) at the DEG-position, as it is the case in ASICs. In FaNaC, BLINaC and MEC-4 a short-chain hydrophobic amino acid (A, alanine) is positioned at this site, whereas ENaCs have a short-chain hydrophilic serine (S) there. A residue between the DEG-position and second transmembrane domain was shown to be crucial for amiloride binding. Mutation of the amino acid corresponding to S583 in rat α ENaC led to a less potent block by amiloride (Kellenberger 2003). HyNaCs and all other DEG/ENaC subunits shown in Appendix 1, except for above

mentioned rat α ENaC, carry a G (glycine) at this position. Furthermore, Kellenberger and co-workers identified a G/SxS motif downstream of the amiloride binding site that is crucial for ion selectivity in ENaCs (Kellenberger 1998, 1999 and 2001; Sheng 2000). Mutations in this region cause loss of Na⁺ selectivity and make the channels also permeable to K⁺. Only α ENaC has a serine (S) at the first position of this triple amino acid motif, whereas all other subunits in Appendix 1 have a G (glycine) at this site. The S (serine) at the last position is highly conserved, also in HyNaC2, but interestingly, HyNaC3 and 4 both have a G (glycine) at this site.

3.1.2 HyNaCs are close relatives of ASICs and BLINaC/INaC

After comparison of the sequences, we performed phylogenetic analyses using different programs and methods to investigate relationships within the DEG/ENaC superfamily, especially with regard to the HyNaC subunits. The phylogenetic tree calculated with Treepuzzle-50 using the maximum-likelihood method is shown in Figure 17. It is representative for the other trees, calculated with PAUP4.0b10 and ClustalX1.81, which are added in Appendices 3-5. Due to the poor knowledge about the origins of the DEG/ENaC channels and the lack of an adequate outgroup candidate, all trees are shown as unrooted phylograms.

In all four trees HyNaC1-4 are consistently placed near the ASICs and BLINaCs, these three subgroups forming a monophyletic assemblage. As it was expected from the sequence analysis, in all four phylogenetic trees HyNaC3 and 4 are put in close relationship. Also, the position of the more distantly related HyNaC2 as sister protein to the HyNaC3/4 pair is consistent in all calculations. However, the phylogenetic rank of HyNaC1 within the ASIC/BLINaC/HyNaC assemblage is more controversial. Treepuzzle puts HyNaC1 together with the other HyNaC subunits into a real monophyletic HyNaC subfamily, with ASICs and BLINaCs as sister groups (see Figure 17). However, in the trees of ClustalX and PAUP calculated with the neighbor joining method, HyNaC1 is placed as sister protein to the ASIC group, and the other three HyNaCs as sister group to the ASIC/HyNaC1 assemblage (Appendices 3 and 5). A third variant results from the PAUP calculation that applies the parsimony approach, where HyNaC2-4 form the sister group to ASICs and HyNaC1 is put in a sister relationship to the ASIC/HyNaC2-4 group (Appendix 4).

Besides the ASIC/BLINaC/HyNaC assemblage, there is another major branch consistent in all four phylogenetic trees. It is composed of ENaCs, FaNaCs and DEG/MECs from *C. elegans*.

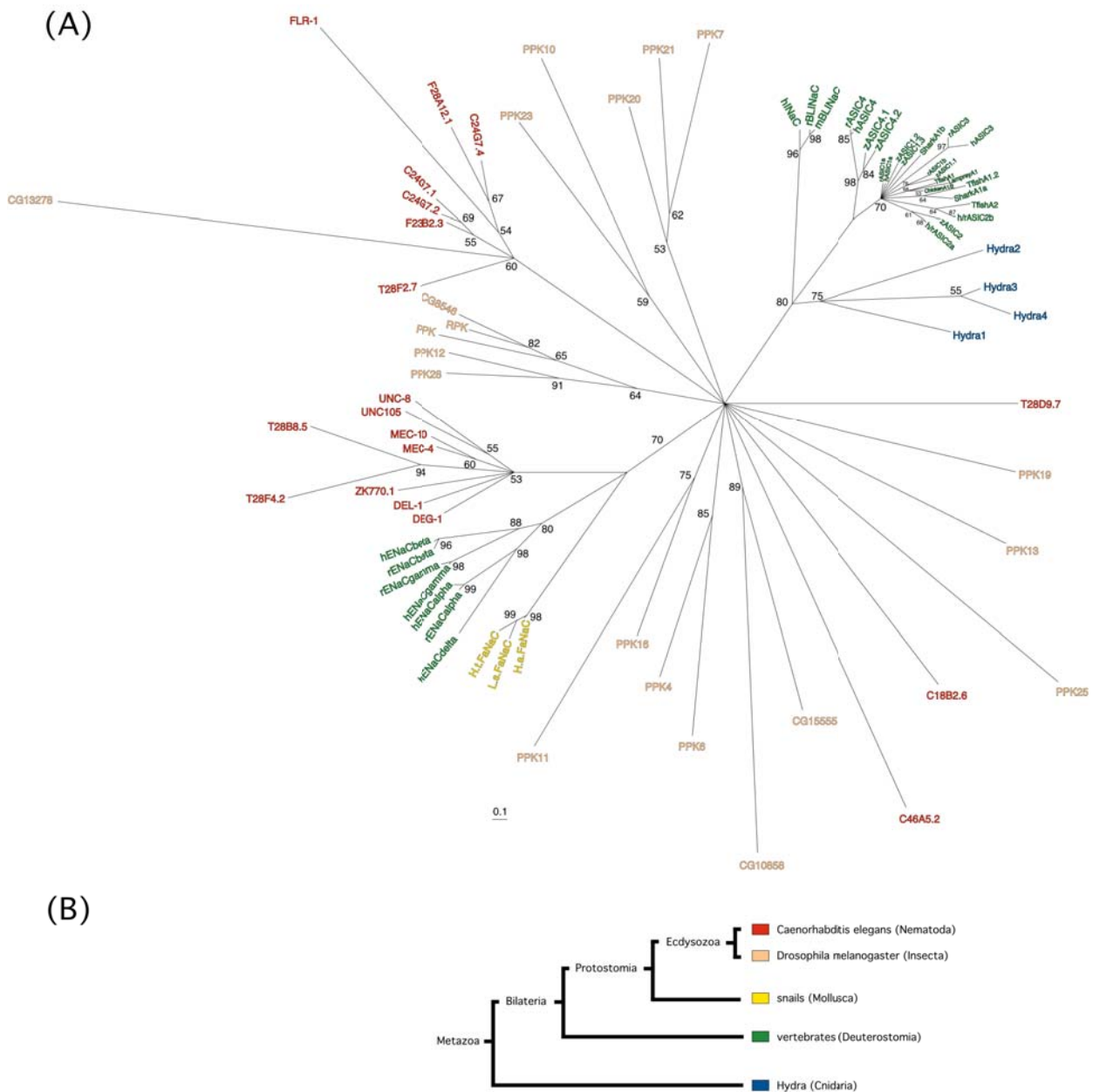


Fig. 17: HyNaCs are closely related to vertebrate ASICs and INaC/BLINaCs. (A) Phylogenetic tree created with Treepuzzle-50 using the maximum-likelihood method. The numbers show the confidence of bifurcations in percent. The branches are drawn so that their lengths are proportional to the evolutionary distance along that branch. The scale at the bottom relates the length of the branches to the distance, the number indicates the substitutions per site. The colors represent animal groups from which the subunits were cloned (see B). (B) Cladogram showing general relationships of the animal groups from which the DEG/ENaC subunits in A were cloned. Only monophyletic assemblages important for the phylogenetic tree in (A) are shown.

While the neighbor joining method of PAUP and ClustalX puts FaNaCs and DEG/MECs together as a monophyletic sister group (Appendices 3 and 5), this is the case for ENaCs and DEG/MECs in the PAUP parsimony tree (Appendix 4). In Treepuzzle (maximum likelihood),

the three subfamilies are forming sister groups that are in equal distance to each other (see Fig. 17). The additional DEG/ENaC members from *C. elegans* and *Drosophila* that were included into this analysis form very diverse arrangements. For example, the PPKs from *Drosophila* do not form a monophyletic assemblage, instead they are split into many different subgroups that are mixed with members from *C. elegans* or comprise only a single protein (see Fig. 17).

3.2 Electrophysiological characterization of HyNaC DEG-mutant currents

3.2.1 Expression of HyNaC2 G429T evokes small constitutive currents that are strongly increased by co-expression of HyNaC3 G430T

At the beginning of our studies, we tried various stimuli in order to activate currents in oocytes expressing HyNaCs. Among these stimuli were substances like protons, serotonin, ATP, substance P, histamine, taurine, FMRFamide, sodium butyrate, PMA and 2-APB, but also osmotic stress and variation in the ionic composition. None of these stimuli could activate HyNaCs. Therefore, we introduced the DEG-mutations in all three HyNaC subunits to see whether these mutations constitutively activate HyNaCs. We replaced the glycine (G) by the large side chain amino acid threonine (T) and expressed the three HyNaC DEG-mutations, HyNaC2 G429T, HyNaC3 G430T and HyNaC4 G430T, either alone or in all possible combinations and looked for constitutive currents that could be inhibited by 1 mM amiloride. Figure 18A shows the mean currents inhibited by 1 mM amiloride for the different HyNaC DEG-mutant combinations. Generally, HyNaC2 G429T expressing oocytes had a depolarized membrane potential that was shifted from about -30 mV in non-injected oocytes to up to $+20$ mV (data not shown). In these oocytes amiloride blocked small currents with mean amplitudes of 0.26 ± 0.23 μ A ($n = 10$), whereas in oocytes injected with either HyNaC3 G430T or HyNaC4 G430T amiloride did not inhibit any current. The co-injection of HyNaC3 G430T together with HyNaC2 G429T led to a 20-fold increase of the amiloride-sensitive current (mean: 5.3 ± 2.52 μ A; $n = 10$). In contrast, the co-expression of HyNaC4 G430T did not significantly alter the amplitudes of the amiloride-sensitive currents of HyNaC2 G429T (mean: 0.20 ± 0.15 μ A; $n = 10$; $p = 0.49$) or of HyNaC2 G429T/HyNaC3 G430T (mean: 7.07 ± 2.85 μ A; $n = 10$; $p = 0.22$; see Fig. 18A). These results suggest that HyNaC2 can form a functional homomeric channel. Furthermore, the results suggest that HyNaC2 and HyNaC3 form heteromeric channels that are

more efficiently expressed on the cell surface than homomeric HyNaC2.

C-terminal di-lysine or KKXX-motifs are known to be common retention sequences for membrane proteins (Nilsson 1989; Teasdale 1996) impairing their trafficking to the plasma membrane. The KKKS-site at the C-terminus of HyNaC2 (see Appendix 1) resembles such a retention motif and therefore we truncated these four amino acids in HyNaC2 G429T to see whether the constitutive current was enlarged in the truncated form. However, we could not observe any significant differences in the mean current amplitudes between HyNaC2 G429T and its KKKS-truncated form (mean: $0.18 \pm 0.16 \mu\text{A}$; $n = 10$; $p = 0.09$; see Fig. 18A).

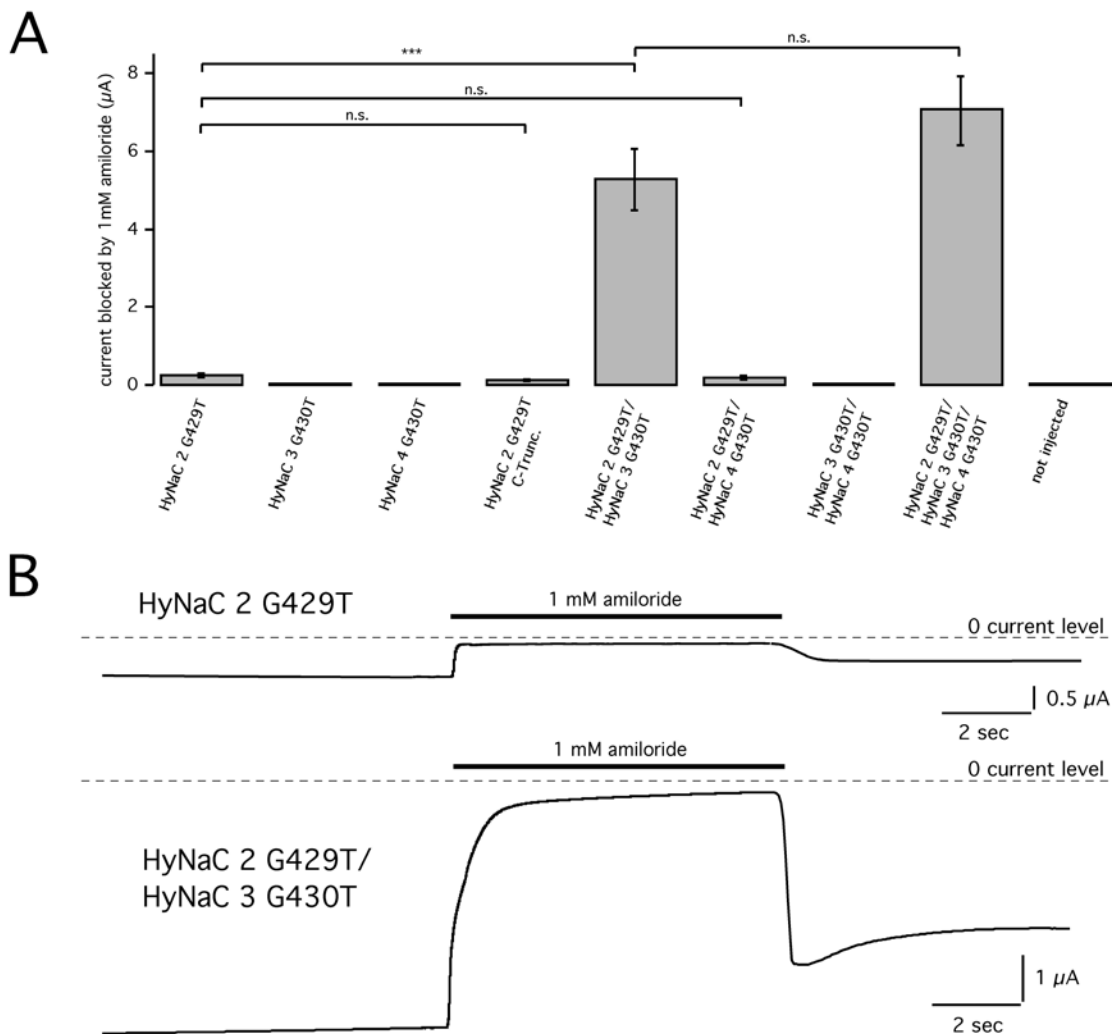


Fig. 18: Co-injection of HyNaC3 G430T enhances the constitutive currents of HyNaC2 G429T homomers. (A) Oocytes injected with cRNA for HyNaC 2 G429T showed small constitutive currents that could be largely increased by co-injection of HyNaC3 G430T. n.s.: not significant; ***, $p \leq 0.001$. (B) Example traces for HyNaC2 G429T homomeric currents and HyNaC2 G429T/ HyNaC3 G430T heteromeric currents that are blocked by 1 mM amiloride.

Figure 18B shows representative current traces for HyNaC2 G429T and for HyNaC2 G429T/HyNaC3 G430T that were blocked by 1 mM amiloride. Kinetics of the onset and offset of the amiloride block varied strongly. In Figure 18B the HyNaC2 G429T trace is an example for a rapid onset and a slow offset of the amiloride block, whereas for the trace of the heteromeric channel it is the other way around. In most measurements, after washing out amiloride, currents did not return to the initial level and sometimes, we could observe for HyNaC2 G429T and HyNaC2 G429T/ HyNaC3 G430T that maximal current amplitude reached immediately after the washout of amiloride partially declined. This decline was variable in amplitude and time course (see Fig. 18B).

After we had examined the current amplitudes of the HyNaC DEG-mutations, we next wanted to investigate whether the co-expression of wildtype subunits would alter current amplitudes of the HyNaC DEG-mutants. Oocytes which co-expressed the HyNaC2 wildtype together with the HyNaC3 G430T mutant had a depolarized membrane potential that was in the range of 0 mV (data not shown), similar to HyNaC2 G429T expressing oocytes. Figure 19A shows the mean current amplitudes that could be blocked by 1 mM amiloride.

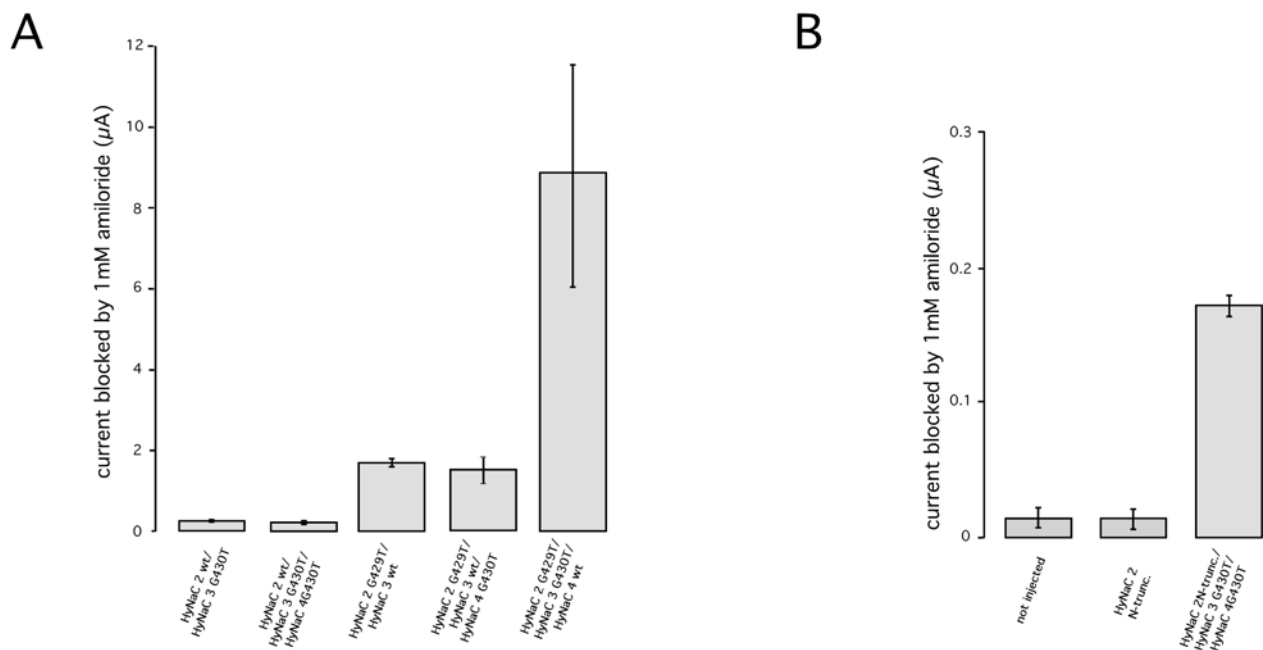


Fig. 19: Co-injection of HyNaC3 G430T evoked small currents in oocytes expressing HyNaC2 wildtype. N-terminal truncation of HyNaC2 did not increase amiloride-sensitive currents. (A) Mean current amplitudes blockable by 1 mM amiloride for heteromeric combinations between HyNaC wildtypes and DEG-mutations. (B) Mean current amplitudes blockable by 1 mM amiloride for a variant of HyNaC2 where the N-terminus is truncated (see text), with and without co-injection of the DEG-mutations of HyNaC3 and HyNaC4.

Similar to the pure DEG-mutant homo- and heteromers, currents showed variable onsets and offsets of the amiloride block (compare Fig. 18B). Often, the currents also did not return to their initial level after washout of amiloride and sometimes they partially declined upon amiloride washout as it is described for the DEG-combinations above (also compare Fig. 18B). As expected from the previous results, oocytes that co-expressed the HyNaC2 G429T and HyNaC3 G430T together with HyNaC4 wildtype exhibited large constitutive currents of several μA that were sensitive to amiloride (mean blocked current: $8.85 \pm 6.19 \mu\text{A}$; $n = 10$). These currents were six times larger than amiloride-sensitive currents from oocytes that co-expressed HyNaC2 G429T and HyNaC3 wildtype (mean: $1.68 \pm 0.23 \mu\text{A}$; $n = 5$), irrespective of additional HyNaC4 G430T co-injection (mean: $1.5 \pm 0.74 \mu\text{A}$; $n = 5$). Oocytes injected with HyNaC2 wildtype and HyNaC3 G430T cRNA displayed a further 7-fold reduction (mean: $0.24 \pm 0.06 \mu\text{A}$; $n = 5$) that was highly significant ($p \ll 0.001$) in comparison to HyNaC2 G429T/ HyNaC3 wildtype currents, which was also irrespective of HyNaC4 G430T co-expression (mean: $0.18 \pm 0.04 \mu\text{A}$; $n = 5$).

The fact that, in contrast to oocytes co-expressing HyNaC2 and HyNaC3 G430T, we could not detect amiloride-sensitive currents in oocytes expressing HyNaC3 G430T alone suggests that HyNaC3 did not reach the cell surface and that the HyNaC2 subunit may be important for the trafficking of HyNaC3 to the plasma membrane.

Similar to the above mentioned KKXX motifs, also di-arginine (RR) residues are known to serve as retention motifs (Schutze 1994; Michelsen 2005). Since the N-terminal starting sequence of HyNaC2 (MKARFARR) bears several arginines (R) that could serve as potential retention sites, we decided to generate a HyNaC2 variant lacking the N-terminal end up to the second methionine (see Appendix 1). The hope was to boost HyNaC2 surface expression resulting in detectable amiloride-sensitive currents. However, oocytes expressing the truncated HyNaC2 showed amiloride-sensitive currents that were comparable in size to amiloride sensitive currents of non-injected oocytes (see Fig. 19B). Co-injection with HyNaC3 and 4 DEG-mutants led to amiloride-sensitive currents (mean: $0.21 \pm 0.10 \mu\text{A}$; $n = 5$) that were comparable in size to amiloride-sensitive currents from HyNaC2 wildtype/HyNaC3 G430T/HyNaC4 G430T expressing oocytes (see above; $p = 0.6$). So, N-terminal truncation had no effect on the current amplitude of HyNaC2 wildtype alone or in combination with the DEG-mutants of HyNaC3 and 4, which indicates that the N-terminus of HyNaC2 does not contain a functional retention motif.

3.2.2 Co-injection of HyNaC3 G430T alters the properties of HyNaC2 G429T currents

Since HyNaC2 G429T generated robust constitutive currents and the co-expression of HyNaC3 G430T led to a multiplication of this current, we further characterized these two conditions to see whether the co-injection of the HyNaC3 DEG-mutant altered the properties of homomeric

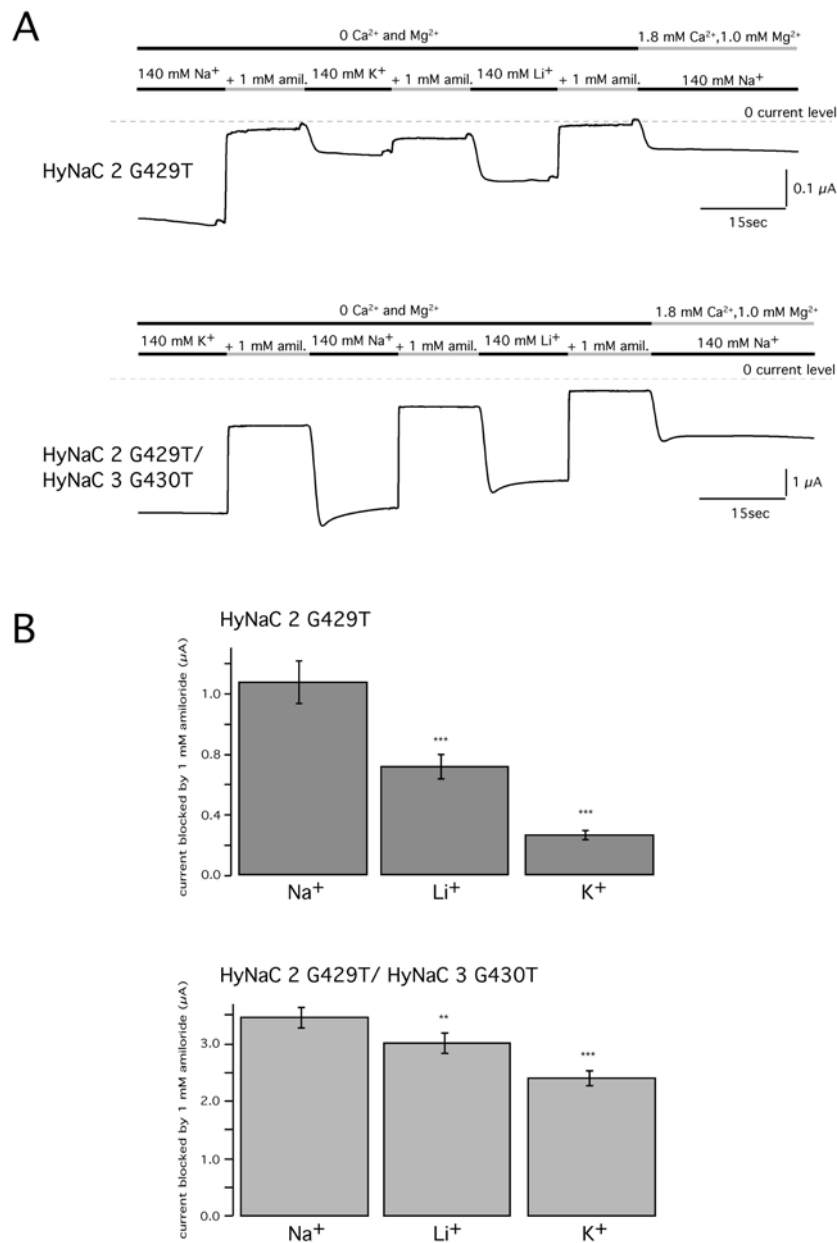


Fig. 20: Co-expression of HyNaC3 G430T changes ion selectivity of HyNaC2 G429T. (A) Example traces of selectivity measurements for HyNaC2 and HyNaC2/3 DEG mutations. (B) Statistical analysis of the ion substitution measurements. For details see text. **: $p \leq 0.005$; ***: $p \leq 0.001$.

HyNaC2 G429T currents. First, we compared the ion selectivity for homomeric HyNaC2 G429T and heteromeric HyNaC2 G429T/HyNaC3 G430T channels. For this purpose, we applied solutions containing only monovalent cations, either 140 mM Na⁺, K⁺ or Li⁺, but no divalent cations and looked for the amplitudes of currents that could be blocked with 1 mM amiloride. Robust currents sensitive to amiloride were evoked with all three cations, which is surprising, as the DEG/ENaC family members usually show a high selectivity for Na⁺ over K⁺. In Figure 20 example traces for HyNaC2 G429T and HyNaC2 G429T/HyNaC3 G430T are shown. As the recovery from amiloride block often was not complete, we varied the order of cation application. For each of the three cations the number of applications at the first, second and third position was the same. In addition, we performed a rather high number of measurements, 36 for the heteromeric condition and 21 for HyNaC2 G429T homomers. The bar graphs in Figure 20B summarize these measurements and show a rather pronounced selectivity of the HyNaC2 G429T homomeric channel for Na⁺ over Li⁺ and K⁺. When Na⁺ was replaced by Li⁺, mean current was reduced to 60% ($0.71 \pm 0.35 \mu\text{A}$; $p \ll 0.001$) compared to the Na⁺ currents ($1.27 \pm 0.62 \mu\text{A}$). The substitution of Na⁺ by K⁺ led to a reduction of the mean current by about 80% ($0.26 \pm 0.15 \mu\text{A}$; $p \ll 0.001$). Compared to HyNaC2 G429T homomers, currents of oocytes injected with both HyNaC2 G429T and HyNaC3 G430T showed a less pronounced selectivity for Na⁺. Reduction of the mean Li⁺ current was only 12% ($3.02 \pm 1.11 \mu\text{A}$; $p = 0.001$) and for K⁺ currents only 28% ($2.4 \pm 0.77 \mu\text{A}$; $p \ll 0.001$) compared to the Na⁺ mean current ($3.46 \pm 1.14 \mu\text{A}$). Statistical comparison of the percental Li⁺ and K⁺ current reductions between HyNaC2 G429T and HyNaC2 G429T/HyNaC3 G430T using the student's t-test revealed a high significance that was $p < 0.001$ for Li⁺ reduction and $p \ll 0.001$ for K⁺ reduction.

Next, we investigated whether co-expression of HyNaC3 G430T altered the amiloride affinity for HyNaC2 G429T. A concentration of 3 mM amiloride completely blocked both, HyNaC2 G429T and HyNaC2 G429T/HyNaC3 G430T constitutive currents. We thus applied a single amiloride concentration followed by the application of 3mM amiloride on HyNaC2 G429T and HyNaC2 G429T/ HyNaC3 G430T expressing oocytes and calculated the fractional inhibition for the different amiloride concentrations in comparison to the inhibition by 3 mM amiloride. In Figure 21 the measurements are summarized as amiloride dose-response-curves for both HyNaC2 G429T and HyNaC2 G429T/HyNaC 3 G430T. For each concentration between 7 and 19 measurements were done. The curve for HyNaC2 G429T is rather flat (Hill coefficient: 0.68), the concentration for half-maximal inhibition IC₅₀ was $0.01 \pm 0.002 \text{ mM}$. 1 μM amiloride, the lowest

concentration used, still inhibited about 20% of the HyNaC2 G429T homomeric currents. In contrast, the curve for HyNaC2 G429T/ HyNaC3 G430T is much steeper (Hill coefficient: 1.58) and the application of 10 μM amiloride inhibited only about 5% of the heteromeric currents. The curve is strongly shifted towards higher amiloride values, the IC_{50} is 0.08 ± 0.002 mM and thus 8 times higher than for the HyNaC2 DEG-mutant.

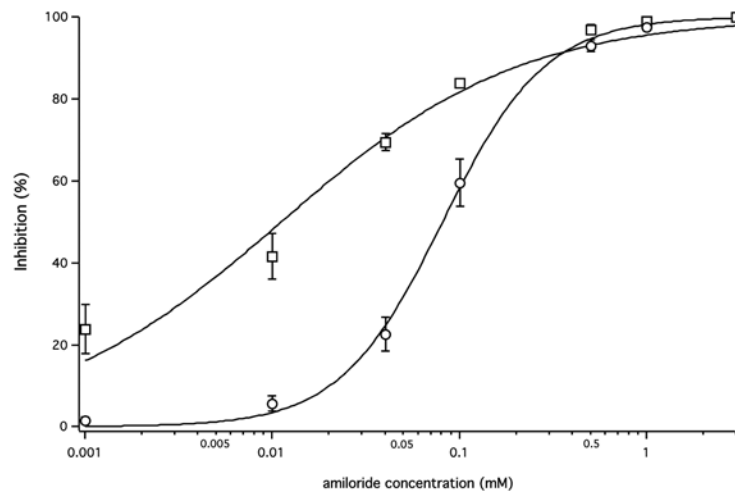


Fig. 21: Co-expression of HyNaC3 G430T altered the amiloride affinity for the HyNaC2 DEG-mutation. Squares represent mean values for HyNaC2 G429T and circles represent mean values for the HyNaC2/3 double DEG-mutation. $n = 7-19$. For details see text.

We found that Ca^{2+} had a blocking effect on HyNaC mutants since the removal of Ca^{2+} enhanced the currents for HyNaC2 G429T and HyNaC2 G429T/HyNaC3 G430T (see Fig. 22A). Thus, we investigated, whether co-expression of HyNaC3 G430T would also change the Ca^{2+} affinity of HyNaC2 G429T homomeric currents. For this purpose, we successively applied solutions with different Ca^{2+} concentrations to oocytes expressing HyNaC2 G429T or HyNaC2 G429T/HyNaC3 G430T. All Mg^{2+} was removed from the solutions and 0.1 mM flufenamic acid (FFA) was added to avoid opening of Cl^- channels at low Ca^{2+} concentrations (see Materials and methods). Figure 22A shows example traces of measurements for HyNaC2 G429T and HyNaC2 G429T/HyNaC3 G430T. Even with 10 mM Ca^{2+} , the highest concentration used, no complete block was achieved in both conditions, although the inhibition of homomeric channels was more complete. From the dose response curve in Figure 22B it seems that a complete block of the heteromeric channel by Ca^{2+} is not possible. Since nominal free Ca^{2+} solutions still contain some free Ca^{2+} , we applied an additional solution that was nominally free of Ca^{2+} and where 10 mM EDTA was added to

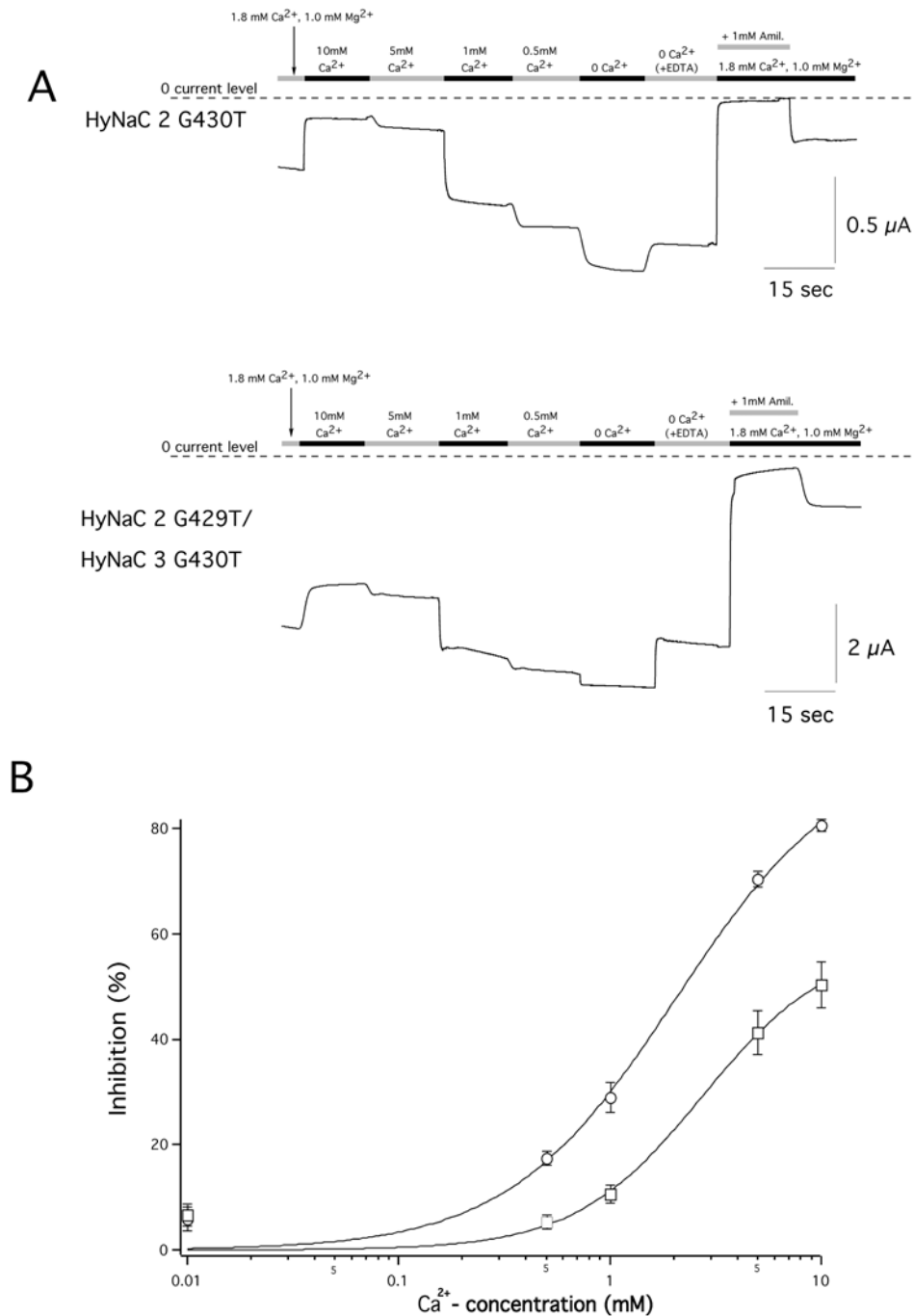


Fig. 22: HyNaC2 G429T was blocked by Ca^{2+} with lower efficacy when HyNaC3 G430T was co-expressed. (A) Examples of measurements made to determine Ca^{2+} affinity for HyNaC2 G429T homomers and HyNaC2 G429T/HyNaC3 G430T heteromers (see text). (B) Dose-response curves for Ca^{2+} block of amiloride-sensitive currents in oocytes injected either with cRNA for HyNaC2 G429T (circles) or HyNaC2 G429T/HyNaC3 G430T (squares). For details see text.

chelate any traces of Ca^{2+} . However, in most measurements the switch from nominally free Ca^{2+} solution to a Ca^{2+} free solution where EDTA was added led to an partial inhibition of the

constitutive current (see Fig. 22A). Thus, we assumed that maximal amplitude was already reached with the nominal Ca^{2+} free solution. The dose-response-curves in Figure 22B summarize the Ca^{2+} affinity measurements for HyNaC2 G429T and HyNaC2 G429T/HyNaC3 G430T. Although they were in the same range, the affinity for Ca^{2+} was slightly higher for HyNaC2 G429T with an IC_{50} of 2.06 ± 1.04 mM in comparison to an IC_{50} value of 2.74 ± 1.7 mM for the heteromeric condition. Hill coefficients for both curves were comparable: they were 1.09 for HyNaC2 G429T and 1.43 for HyNaC2 G429T/HyNaC3 G430T.

3.3 Electrophysiological analysis of HyNaC wild-type currents

3.3.1 Removal of Ca^{2+} and Mg^{2+} evokes large currents in oocytes co-expressing HyNaC2 and HyNaC3

Since constitutive currents of HyNaC2 G429T and HyNaC2 G429T/HyNaC3 G430T were inhibited by high Ca^{2+} concentrations, we next tried to evoke currents in oocytes injected with wildtype HyNaCs by removing Ca^{2+} . Indeed, we could elicit large, persistent currents in oocytes expressing HyNaC2 and 3, when we removed all the Ca^{2+} from the bath solution. The currents were in the range of several μA and the co-injection of HyNaC4 did not alter the current amplitudes (data not shown). We detected such currents only in oocytes expressing both subunits, HyNaC2 and 3, together. Next, we determined the Ca^{2+} affinity for the heteromeric HyNaC2/3 channel by applying successive solutions with different Ca^{2+} concentrations between 10 mM and 0 Ca^{2+} (see Fig. 23A). The concentration for inhibiting half of the maximum current (IC_{50}) was $827.84 \text{ nM} \pm 83.5 \text{ nM}$, and thus more than three thousand times lower than for the DEG-mutant heteromer (see Chapter 3.2.2). 1.8 mM Ca^{2+} , the concentration usually used in our standard bath solution, completely inhibited HyNaC2/3 wildtype current, whereas only about 10% of the heteromeric mutant current was blocked by this concentration.

With the same protocol we also determined the affinity for Mg^{2+} . In comparison to Ca^{2+} , the Mg^{2+} dose-response-curve was shifted towards higher concentrations (see Fig. 23B). IC_{50} was $65.24 \mu\text{M} \pm 2.82 \mu\text{M}$ and thus nearly 100 times higher than for Ca^{2+} (see above). Also, the Mg^{2+} curve was much steeper (Hill coefficient: 3.87) in comparison to the Ca^{2+} curve (Hill coefficient: 0.74).

Next, we wanted to see whether the HyNac2/3 current that were evoked by removing divalent

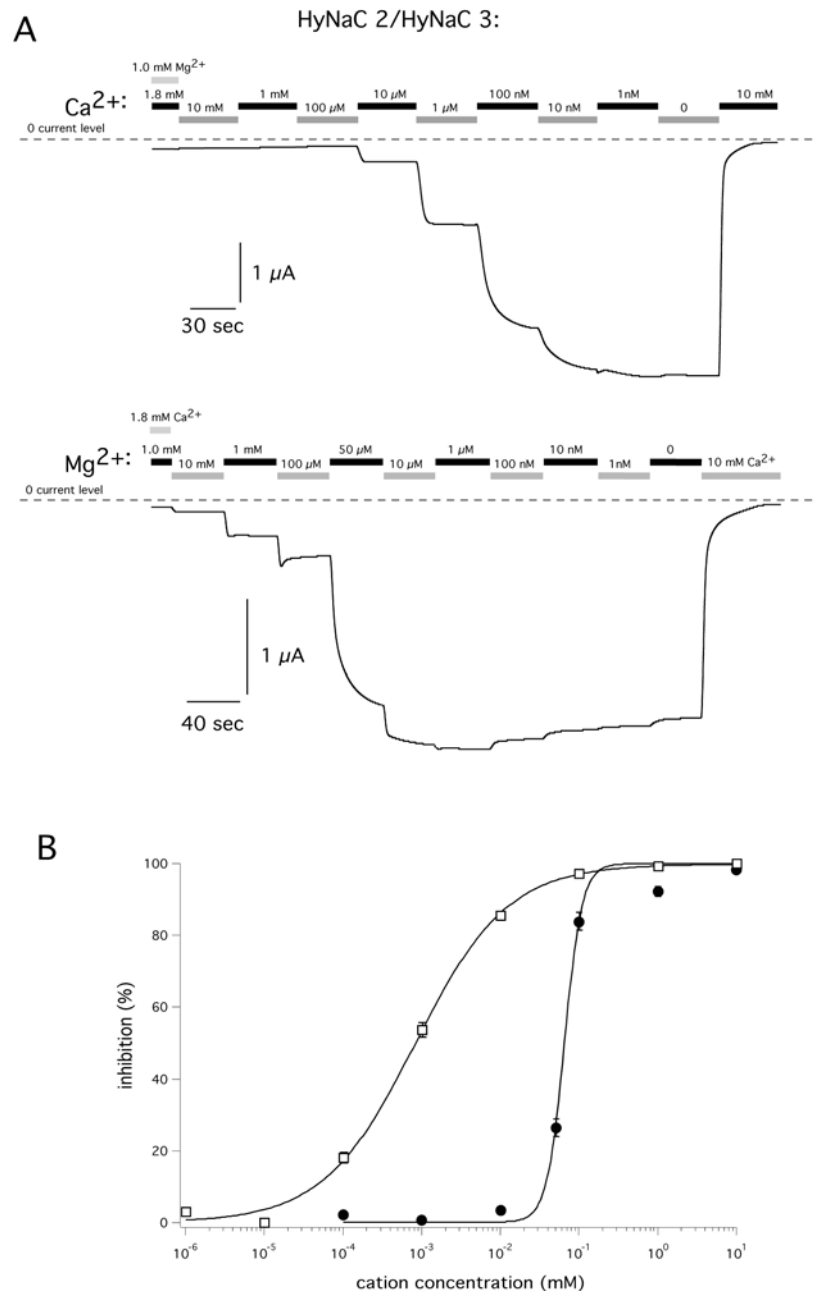


Fig. 23: HyNaC2/3 heteromeric channels were blocked by Ca^{2+} and Mg^{2+} . (A) Example current traces showing increasing currents by lowering the Ca^{2+} and Mg^{2+} concentrations (see text). (B) Dose response curves for the block of HyNaC2/3 currents by Ca^{2+} (open squares) and Mg^{2+} (filled circles). For details see text.

cations was carried by Na^+ ions. For this purpose, we applied successively solutions that were nominally free of divalent cations, containing increasing concentrations of Na^+ between 3 and 140 mM. As Figure 24A shows, currents became larger with increasing concentrations of Na^+ and did not saturate even with 140 mM Na^+ , the highest concentration used (Fig. 24B).

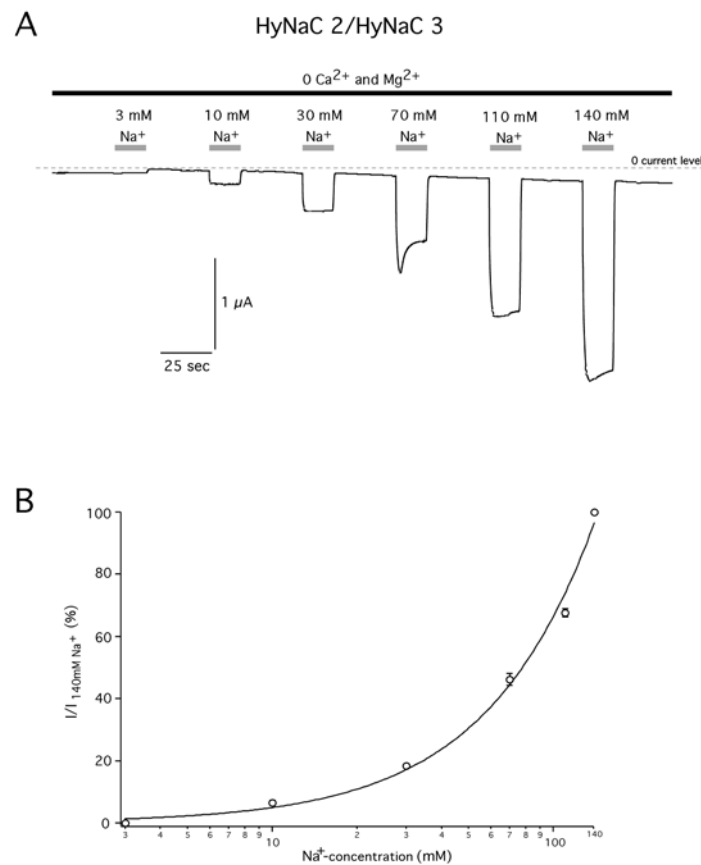


Fig. 24: Na⁺ passed through heteromeric HyNaC2/3 channels that were opened by removal of divalent cations. (A) Example current trace showing increasing currents when higher Na⁺-concentrations were applied (see text). (B) Statistical analysis of 4 measurements seen in (A). The dose-response curve was fitted to a Hill function (see Materials and methods).

Since for ASIC1a Ca²⁺ and amiloride compete for binding to the channel (Paukert 2004), we determined apparent amiloride affinity also in the absence of Ca²⁺. We used amiloride concentrations of 100 μM, 1 mM and 3 mM, which are doses sufficient to inhibit any known heterologously expressed DEG/ENaC channel. No divalent cations were added to the solutions that we used for these experiments. Under these conditions amiloride had unexpected effects. In most measurements application of 100 μM and more led to an increase of the persistent HyNaC2/3 currents that varied in amplitude (see Fig. 25). Usually, the current increase was constant over time or declined rather weakly, as can be seen in the example trace in Figure 25.

By application of 1 mM or 3 mM amiloride, we observed a fast, transient block before the current increased in most measurements. The extent of the transient inhibition was dose-dependent. However, washing off amiloride induced in most cases an off-current, which showed dose-dependent desensitization kinetics (see Fig. 25). Thus, under these experimental conditions

amiloride had a paradoxical potentiating effect. These observations suggest that amiloride has a dual effect on the HyNaC2/3 channel. On the one hand it inhibits the currents evoked by removal of divalent cations, which can be seen in Figure 25 in the fast transient current reductions upon application of 1 and 3 mM amiloride. On the other hand current increase upon application of 100 μ M amiloride and also the dose-dependent transient current increase upon washout of amiloride indicate that it also has an potentiating effect, which might be voltage and concentration dependent as it was already shown for ASIC2a (Adams 1999). The dual effect of amiloride on the HyNaC2/3 currents suggests that there might be two different interaction sites.

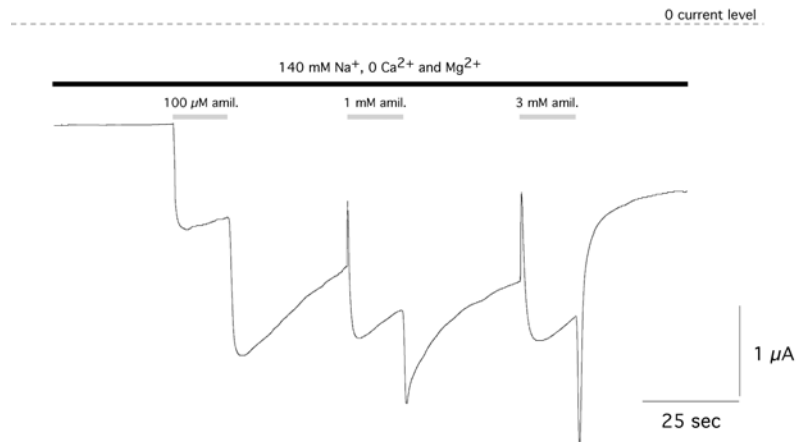


Fig. 25: Amiloride has a dual effect on HyNaC2/3 currents evoked by removal of divalent cations. Example current trace showing the paradoxical effect of amiloride. It blocked the channel as well as opened it concentration dependently. All solutions contained no Ca^{2+} and Mg^{2+} .

3.3.2 HyNaC2/3 currents evoked by removal of divalent cations are inhibited by acidic pH

Interestingly, we found that the HyNaC2/3 currents evoked by removal of divalent cations could be inhibited by acidification (see Fig. 26A). However, the amplitudes in solutions free of divalent cations were increased after washout of acidic solutions. Figure 26A shows an example for such a measurement. Increasing acidification of the conditioning solutions led to larger currents evoked by removal of divalent cations, which reached a maximum at pre-application of pH 4.5. Note that with increasing acidification a pronounced transient current developed. The pre-applied proton concentration needed to activate half-maximal current (EC_{50}) was $\text{pH } 6.33 \pm 0.06$ ($n = 6$). By pre-applying pH 4.0, we could increase currents about 10-fold compared to pre-application of pH 7.4 (see Fig. 26). Similar to amiloride (see previous chapter), such a behavior can be explained by a

dual effect of protons. The dose-dependent inhibition of the current evoked by removal of divalent cations during acidification suggests a blocking effect of protons. On the other hand, the dose-dependent current increase upon washout of protons and also the slow current increase after the initial block at moderate acidification (see Fig. 26A) indicates also an stimulating effect of protons on HyNaC2/3 channels. Thus, like for amiloride (see previous chapter), the dual effect might indicate two interaction sites also for protons.

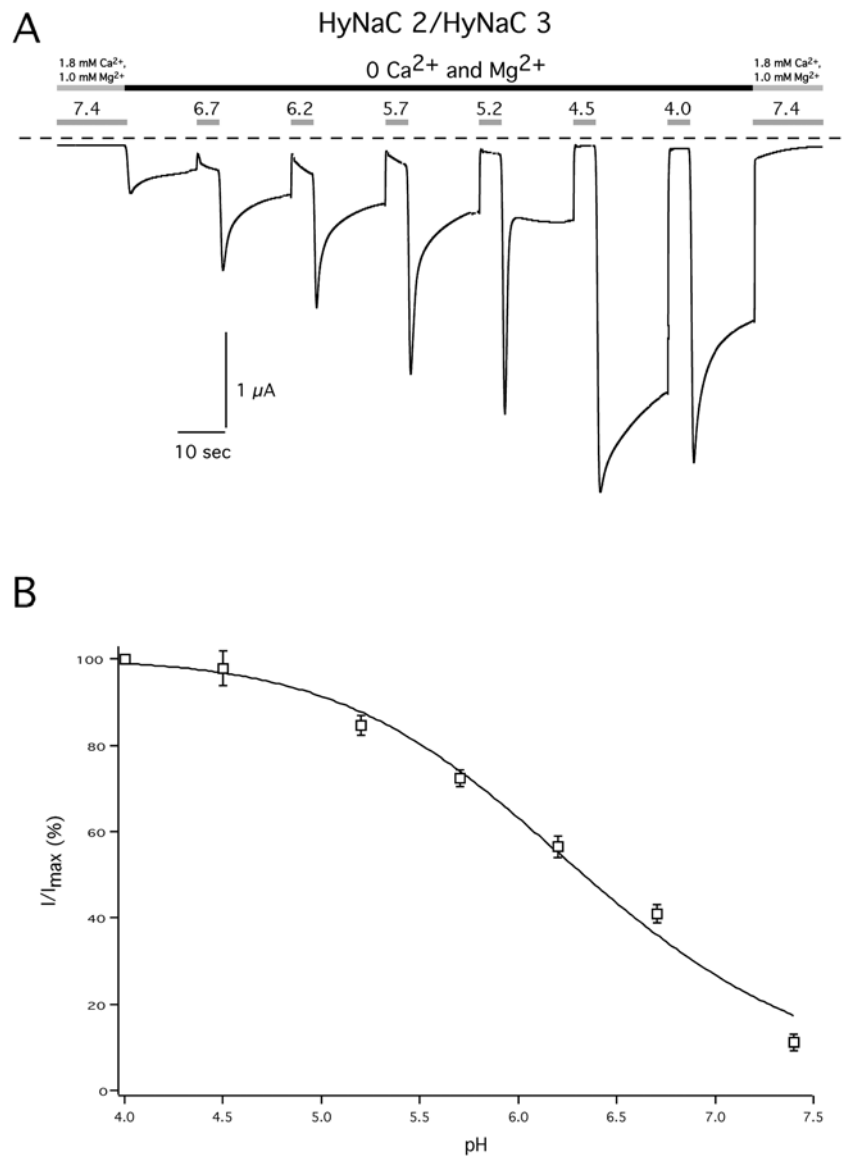


Fig. 26: Acid inhibits HyNaC2/3 currents evoked by removal of Ca²⁺. (A) Example current trace showing block of HyNaC2/3 current by acid as well as the potentiation of the current upon acid wash-out. Both effects were dose-dependent. The dashed line indicates the 0 current level. (B) Statistical analysis of the current potentiation after acid removal for HyNaC2/3. Pre-applied proton concentration is plotted against the size of the wash-off currents. For details see text.

3.3.3 Neuropeptides from *Hydra* evoke currents in oocytes co-expressing HyNaC2 and HyNaC3

FaNaCs are activated by FMRFamide in neurons of snails and there is a multitude of similar neuropeptides in cnidarians, including *Hydra* (see Introduction). Thus, we tested some of these peptides on HyNaCs. Dr. Cornelius Grimmelikhuijzen, who identified these peptides in *Hydra*, provided small amounts of HydraRFamides I-IV (see Introduction). We injected oocytes with cRNA for the three subunits, HyNaC2, HyNaC3 and HyNaC4 in all possible combinations and applied 50 μM of each peptide. Application of HydraRFamides I and II elicited currents of several μA in oocytes that expressed HyNaC2 and HyNaC3 (see Fig. 27A). Co-injection of HyNaC4 did not alter the amplitudes and kinetics of the currents (data not shown).

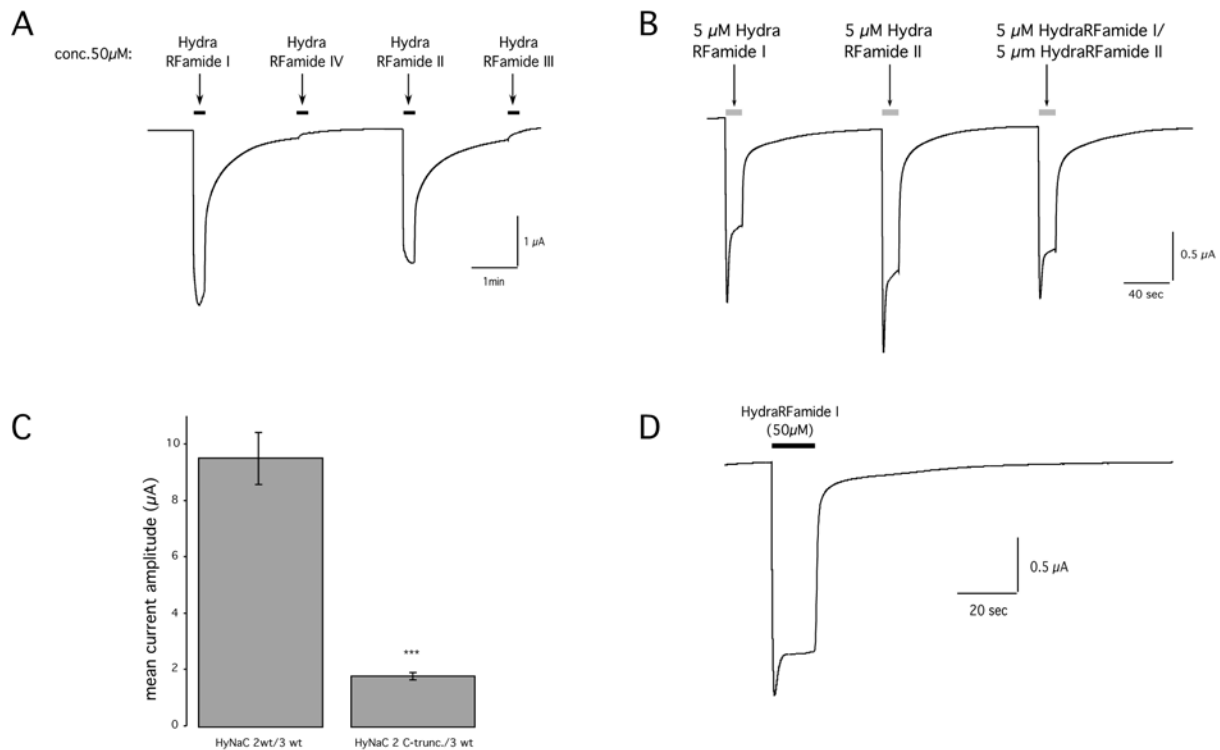


Fig. 27: Peptides from *Hydra* activated heteromeric HyNaC2/3 channels. (A) Example current trace showing that only HydraRFamide I and II elicit currents in oocytes co-expressing HyNaC2 and 3. (B) Co-application of HydraRFamide I and II had no potentiating effect. Notice that the current evoked by HydraRFamide II is larger compared to HydraRFamide I and co-application of both peptides. (C) C-terminal truncation of HyNaC2 (see Text) significantly decreased currents evoked by 50 μM HydraRFamide I. ***: $p \leq 0.001$. (D) Example trace showing typical activation and desensitization kinetics of peptide-evoked HyNaC2/3 currents. For details see text.

Co-application of both activating peptides together, HydraRFamide I and II, did not potentiate

the current (see Figure 27B). Application of 50 μM HydraRFamide III and IV did not lead to any activation at all. Co-injection of a truncated HyNaC2 construct, where the potential C-terminal KKKS-retention motif had been deleted (see Chapter 3.2.1) together with HyNaC3 wildtype led to a strong reduction of the mean current amplitude evoked by 50 μM HydraRFamide I from $9.56 \pm 2.07 \mu\text{A}$ ($n = 5$) in oocytes co-injected with HyNaC2 and 3 to $1.82 \pm 0.29 \mu\text{A}$ ($n = 5$; $p < 0.001$; see Fig. 27C).

After this finding, we synthesized more peptide in collaboration with Dr. Hubert Kalbacher and further characterized the properties of the HyNaC2/3 channel. Most of our measurements were done with HydraRFamide I.

First, we characterized the currents that were activated by the peptides. Figure 27D shows a typical current elicited by 50 μM HydraRFamide I, although we saw strong variations in the kinetics of desensitization. Usually, the currents were activated very fast, but sometimes activation was more gradual in the last third as it is seen in Figure 27A. Currents desensitized partially in the presence of the peptide, the fraction of current that desensitized varied strongly from almost no desensitization to up to 50%. Washout of the peptide proceeded in a biphasic way, with a fast initial component and a very slow second component (see Fig. 27D), both could be fit with a double-exponential equation (see Materials and methods).

We determined the average desensitization time constants for washout, τ_1 and τ_2 , for seven HyNaC2/3 injected oocytes from the same batch. The faster component had a time constant τ_1 of 2.91 ± 0.47 ms and the slower component a time constant τ_2 of 678.98 ± 246.66 ms. Washout kinetics varied strongly between different batches of oocytes. Often, after peptide washout the current baseline did not reach the initial level before peptide application (see Fig. 28A). The amplitude of the remaining current was variable and could make up to about 15 % of the peptide activated current.

3.3.4 Peptide-activated HyNaC currents exhibit tachyphylaxis, which is suppressed by pre-application of acidic pH

Repeated application of *Hydra* peptides led to a successive decrease of the activated current, a phenomenon called tachyphylaxis (Chen 2007). We activated oocytes that were expressing HyNaC2/3 for 15 sec with 50 μM HydraRFamide I. Subsequently, we washed the peptide out and waited for another 30 sec to activate the channel again, and repeated this procedure one more

time. One representative current trace is shown in Figure 28A.

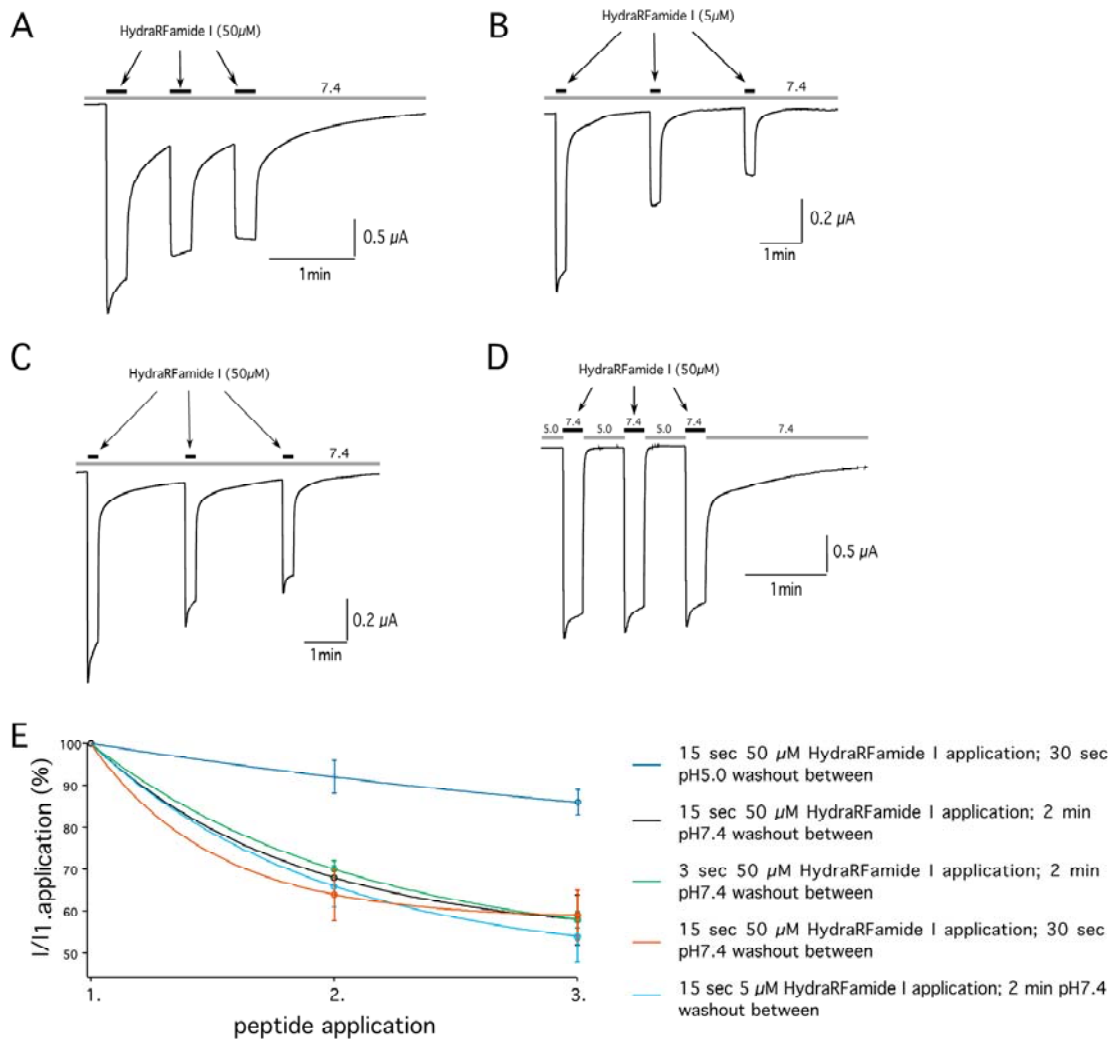


Fig 28: Peptide activated currents in oocytes co-expressing HyNaC2 and 3 showed tachyphylaxis that could be suppressed by pre-application of acid. (A) – (C) Example current traces showing tachyphylaxis of peptide activated HyNaC2/3 currents with variable peptide concentrations and application times. (D) Example current trace showing that pre-application of pH 5.0 suppressed tachyphylaxis. (E) Statistical analysis of the tachyphylaxis measurements seen in (A)-(D). Current amplitudes of the second and third peptide application were normalized to the first one. Data points were fitted to a simple exponential equation.

The current got smaller with each peptide application, whereby the current reduction between the first and second peptide application was always larger than the reduction between the second and third peptide-activated current. This tachyphylaxis effect was always seen, although it varied in its degree. It was not dependent from parameters like duration of peptide application, peptide concentration or duration of peptide washout, since we could still see tachyphylaxis when we

reduced the application time to 3 sec (see fits Fig. 28E) or when we applied only 5 μM HydraRFamide I (see Fig. 28B,E) and prolonged the washout phases up to 2 min (see Fig. 28C,E).

Similar to proton-modulation of currents elicited by removal of Ca^{2+} , peptide-activated HyNaC2/3 currents were also strongly modulated by acidic solutions. By lowering the pH of the conditioning solutions to 5.0 the slow phase of the desensitization upon peptide washout disappeared and current baseline returned very fast to the initial level (see Fig. 28D). The tachyphylaxis effect was strongly decreased when the channels were repeatedly activated under these conditions (see Fig. 28E). Figure 28E summarizes the experiments investigating tachyphylaxis.

3.3.5 Peptide-activated HyNaC currents are blocked by low pH

In addition to releasing tachyphylaxis, protons also blocked peptide-activated currents: When 50 μM peptide was applied in solutions with a pH of 5.0, the current amplitudes were suppressed to about 14% (mean: $0.46 \pm 0.25 \mu\text{A}$; $n = 4$) compared to activation in pH 7.4 (mean: $3.25 \pm 0.87 \mu\text{A}$; $n = 4$; $p = 0.001$).

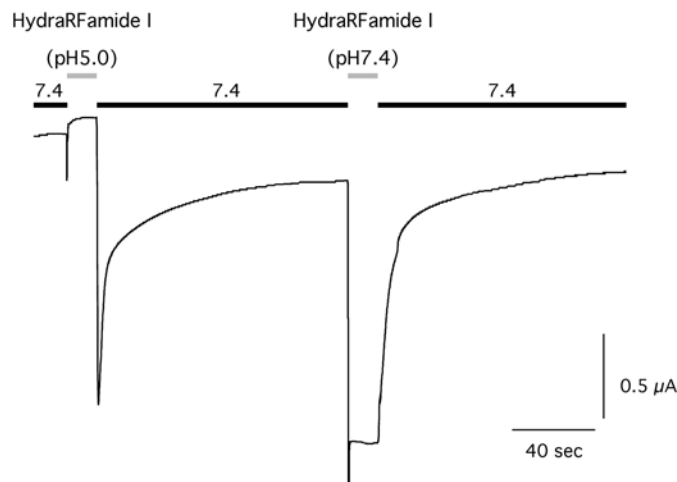


Fig. 29: Co-application of protons inhibited peptide-activated currents in oocytes co-expressing HyNaC2 and 3. Example current trace showing inhibition of HyNaC2/3 currents and the potentiated transient current upon washout of peptide and protons. For details see text.

However, washout of both, peptide and protons, evoked transient off-currents that were more than 2.5 times smaller (mean: $1.26 \pm 0.46 \mu\text{A}$; $n = 4$) than the peptide-activated current in

pH 7.4 solution (see above; also see Fig. 29). These off-currents did not desensitize to the initial current base line, as it is seen in the example trace of Figure 29. However, the experiment confirms previous observations that protons block the peptide-activated currents in HyNaC2/3 expressing oocytes.

3.3.6 HydraRFamide I and II activate heteromeric HyNaC2/3 currents with similar potency, which is enhanced by removal of Ca^{2+}

Next, we determined the apparent affinity for both peptides, HydraRFamide I and II, for HyNaC2/3.

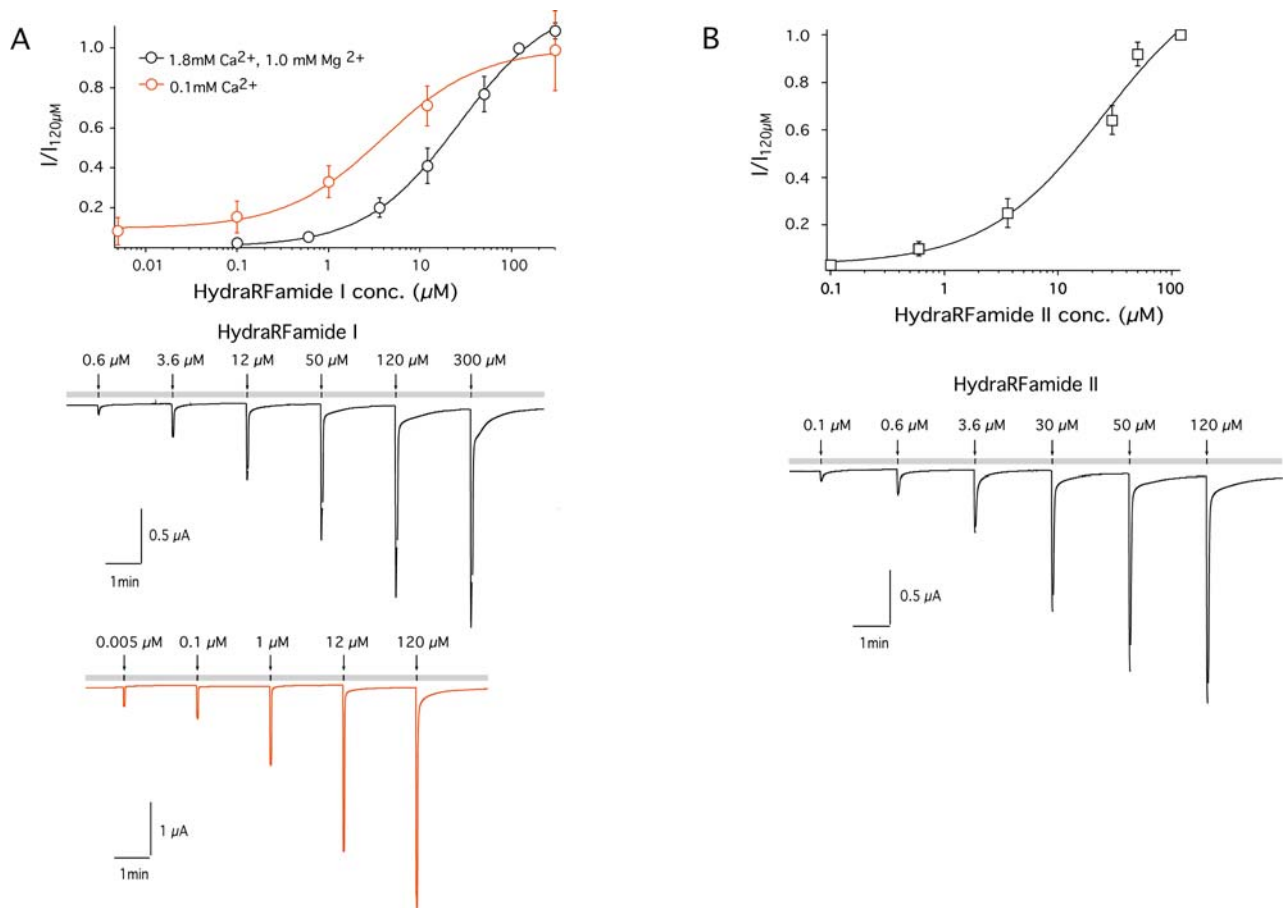


Fig. 30: HydraRFamides I and II activated the HyNaC2/3 channel with the same potency that could be enhanced by removal of Ca^{2+} . (A) Top: Dose-response curves for activation with HydraRFamide I using standard Ca^{2+} and Mg^{2+} concentrations (black) or just 0.1 mM Ca^{2+} (red). Bottom: Example measurements used for the statistical analysis at the top. (B) Top: Dose-response curve for activation with HydraRFamide II using standard ion concentrations. Bottom: Example measurement used for the statistical analysis at the top. For details see text.

For this purpose, we successively applied different peptide concentrations of HydraRFamide I (0.1 μM - 300 μM) and of HydraRFamide II (0.1 μM - 120 μM), respectively, on oocytes co-injected with HyNaC2 and 3. We waited 2 min between the 3 seconds lasting peptide applications, as it is shown in the example traces in Figure 30A and B. Concentrations for half-maximal activation (EC_{50}) of HyNaC2/3 under standard conditions (see Materials and Methods) was $27.06 \pm 3.37 \mu\text{M}$ ($n = 3-6$) for HydraRFamide I and $25.33 \mu\text{M} \pm 22.6 \mu\text{M}$ ($n = 6-8$) for HydraRFamide II, respectively (see dose-response curves Fig. 30A and B).

Since we knew that HyNaC2/3 could be opened by removing divalent cations, we performed similar measurements for HydraRFamide I under conditions, in which we removed all the Mg^{2+} and lowered Ca^{2+} concentration to 0.1 mM in the peptide containing solutions. Under these conditions the affinity of HyNaC2/3 for HydraRFamide I was increased by a factor of almost 7. EC_{50} for the peptide was shifted from 27 μM to $3.9 \pm 0.9 \mu\text{M}$ ($n = 3-9$; see dose-response curves in Fig. 30A). Note that due to the removal of divalent cations the dose-response curve did not reach the zero current level (Fig. 30A).

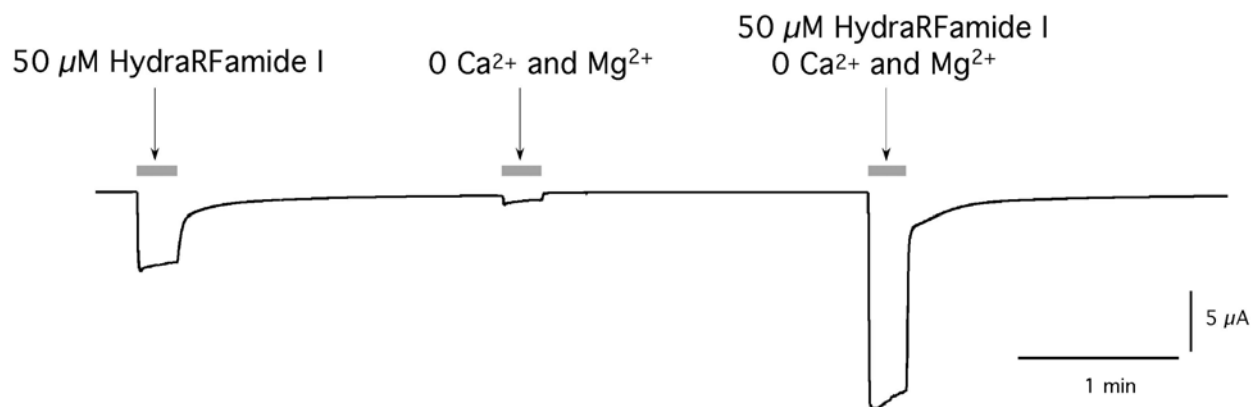


Fig. 31: Peptide-activated currents in oocytes expressing HyNaC2 and 3 were blocked by Ca^{2+} . Example traces showing that currents evoked by HydraRFamide I was inhibited by Ca^{2+} . For details see text.

We investigated whether Ca^{2+} , in addition to lowering the peptide affinity, had also a blocking effect on peptide-activated HyNaC2/3 currents. To test this, HyNaC2/3 was activated by 50 μM HydraRFamide I for 15 sec. After 2 min, the same oocyte was activated by removal of all Ca^{2+} and Mg^{2+} for 15 sec. Another 2 min later, 50 μM HydraRFamide I was applied in a solution nominally free of Ca^{2+} and Mg^{2+} for 15 sec. Figure 31 shows an example trace for this experiment. If peptide was applied without Ca^{2+} and Mg^{2+} , the peak current amplitude ($16.10 \pm$

1.45 μA ; $n = 3$) was strongly increased compared to both, the peptide-evoked amplitude under standard conditions ($5.74 \pm 0.81 \mu\text{A}$; $n = 3$; $p = 0.002$) and the current evoked by removal of the divalent cations ($1.03 \pm 0.89 \mu\text{A}$; $n = 3$; $p = 0.004$). According to the peptide dose-response curves in Figure 30A, 50 μM HydraRFamide I should activate about 60 % of the maximal current in standard bath solutions containing 1.8 mM Ca^{2+} and 1.0 mM Mg^{2+} . In solutions free of divalent cations activation should be almost maximal. Thus, one would expect that the peptide-activated current amplitude in solutions nominally free of Ca^{2+} and Mg^{2+} should be at most twice as large as the current amplitude under standard conditions. However, mean current amplitude under standard conditions was only about 35% (see values above) of the mean amplitude in solutions nominally free Ca^{2+} and Mg^{2+} , which suggests that divalent cations block HyNaC2/3 channels in addition to lowering their apparent affinity for the *Hydra* peptides.

3.3.7 Peptide-activated HyNaC currents are unselective and can be blocked by amiloride with low affinity

As Na^+ selectivity and block by amiloride are two major characteristics of ion channels within the DEG/ENaC family, we next investigated these features for the HyNaC2/3 heteromer. Currents evoked by 50 μM HydraRFamide I were blocked by amiloride with a rather low affinity. Amiloride concentration necessary for inhibition of 50% of the maximal current (IC_{50}) was $508 \pm 70 \mu\text{M}$ (see Figure 32; $n = 3-5$).

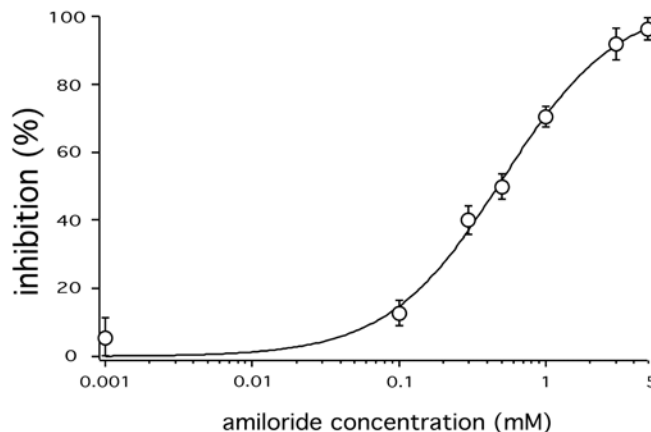


Fig. 32: Amiloride blocked peptide-activated HyNaC2/3 currents with low affinity. Currents were evoked with 50 μM HydraRFamide I and inhibited by successive application of different amiloride concentrations between 1 μM and 3 mM; $n = 5$. Mean value for inhibition by 5 mM amiloride is the average of 3 single measurements done independently from the previous mentioned measurements. Inhibited currents were normalized to maximal current.

Thus, the affinity of wildtype HyNaC2/3 is about 50-fold lower than amiloride affinity of HyNaC2 G429T (IC_{50} : $10 \pm 2 \mu\text{M}$;) and still 6 times lower than amiloride affinity of HyNaC2 G429T/HyNaC3 G430T (IC_{50} : $80 \pm 2 \mu\text{M}$; see Chapter 3.2.2). These results suggest an important role for the DEG-position, as the replacement of short-chain amino acids by amino acids with longer side chains increases the affinity of HyNaC2/3 for amiloride. Furthermore it confirms previous observations made for the DEG-mutants that co-expression of the HyNaC3 subunit decreases amiloride affinity.

For investigating the ion selectivity, we used ion substitution protocols and voltage ramps. For ion substitution experiments, we applied three times $30 \mu\text{M}$ HydraRFamide I under standard conditions on oocytes co-expressing HyNaC2 and 3, where Na^+ was substituted by K^+ or Li^+ , respectively. The duration of peptide application was 3 seconds and bath solutions that were applied for 2 min between the peptide applications contained the monovalent cation that was also present in the following peptide solution. Figure 33B shows an example trace for this protocol. The order of application was changed between single experiments to balance the tachyphylaxis effect. The mean current amplitude ($n = 6$) was nearly unaltered when Na^+ ($1.70 \pm 0.98 \mu\text{M}$) was replaced by either K^+ ($1.47 \pm 0.96 \mu\text{M}$; $p = 0.65$) or Li^+ ($1.23 \pm 0.89 \mu\text{M}$; $p = 0.35$), because of the tachyphylaxis the SD and SEM values were rather high. The bar graph in Figure 33A summarizes the measurements showing the results as normalized values. This result confirms the unselective current found with HyNaC2 and 3 DEG-mutants.

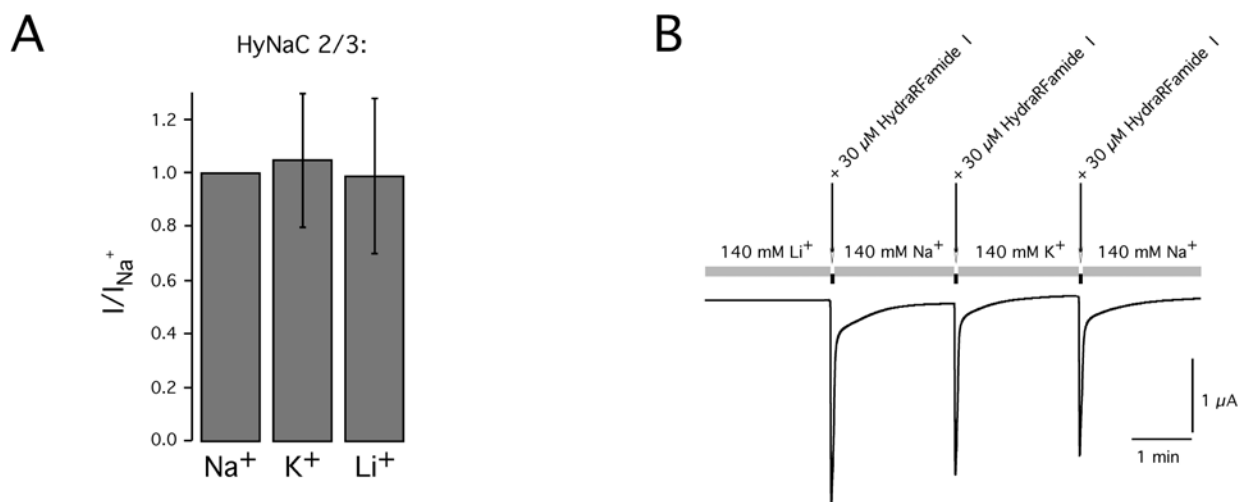


Fig. 33: Peptide-activated currents from oocytes co-expressing HyNaC2 and 3 were unselective. (A) Bar graph showing normalized mean current amplitudes from oocytes expressing HyNaC2/3, where Na^+ was replaced by K^+ and Li^+ during peptide activation. For details see text. (B) Representative current trace for measurements summarized in (A).

Besides the permeability for monovalent cations, we also investigated whether HyNaC2/3 is permeable for Ca^{2+} ions. For this purpose, we used solutions containing 40 mM CaCl_2 as only cation and performed 6 seconds lasting voltage ramps from -150 mV to $+50$ mV with and without $50 \mu\text{M}$ HydraRFamide I. Under these conditions, the driving force for Ca^{2+} at voltages more negative than -80 mV is so large that macroscopic inward currents should be detectable for Ca^{2+} -permeable ion channels (Kellenberger 1999). 3-5 hours before measurement, oocytes were injected with 50 nl of 40 mM BAPTA and 10 mM Hepes (pH 7.2) containing solution to prevent an increase of intracellular Ca^{2+} levels and activation of endogenous Ca^{2+} -activated Cl^- channels. In Figure 34 an I-V curve representing the mean for 6 oocytes injected with HyNaC2/3 is shown. The procedure for calculation of the curve is described in the legend of Figure 34.

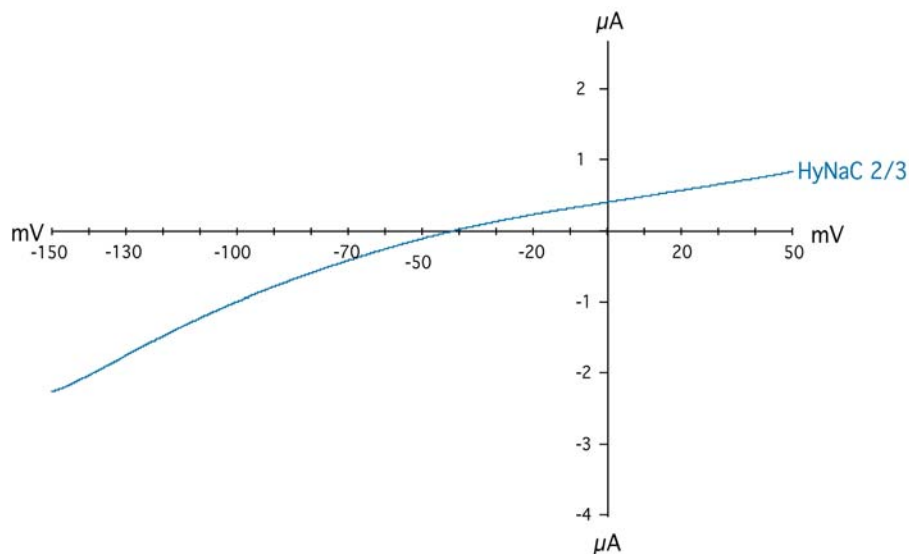


Fig. 34: Peptide-activated HyNaC2/3 showed robust inward currents in the highly negative voltage range when Na^+ was replaced by Ca^{2+} . Two voltage ramps were performed from -150 mV to $+50$ mV for six oocytes expressing HyNaC2/3, one before peptide application and one during application of $50 \mu\text{M}$ HydraRFamide I. Both ramps were subtracted from each other and the blue line represents the resulting average I-V relationship for the six measured oocytes. Solutions contained only 40 mM CaCl_2 and 10 mM Hepes. Oocytes were injected with 10 mM BAPTA to prevent activation of Ca^{2+} -activated Cl^- currents.

The determination of Ca^{2+} permeability for ion channels with the TEVC method is rather difficult and this ramp can give only an indication. Nevertheless, peptide-activated currents of HyNaC2/3 were rather large in the strongly hyperpolarized voltage range between -100 and -150 mV, which should not be the case for Ca^{2+} -impermeable ion channels. Furthermore the I-V-curve shows a tendency towards inward rectification, which is another indication for a Ca^{2+} -permeability, since the voltage ramps of Ca^{2+} -impermeable ion channels like ENaC display a

horizontal course in the hyperpolarized voltage range (Kellenberger 1999).

3.3.8 Unselective currents activated by HydraRFamides are not evoked by the opening of hemi gap junctions

The unselectivity of peptide-activated currents in oocytes co-expressing HyNaC2 and 3 and its rather low affinity for amiloride are untypical features for members of the DEG/ENaC ion channel family. Furthermore, the block by increasing Ca^{2+} concentrations and by lowering the pH are additional features that are shared with hemi gap junctional channels (Ripps 2002 and 2004; Ebihara 2003). Recently, Pelegrin et al. have shown that activation of ATP-gated P2X_7 cation channels opened the unselective large pore hemi gap junctional channel pannexin-1 (Pelegrin 2006). Theoretically, a similar coupling with hemi gap junctions could also be the case for HyNaC2/3.

As we knew from previous experiments, co-expression of HyNaC3 G430T altered the ion selectivity of HyNaC2 G429T (see Fig. 20). So, we introduced a point mutation into the selectivity filter (see Introduction) of HyNaC3 and replaced the glycine (G) at position 444 by a serine (S). If the currents activated by HydraRFamides would flow through the HyNaC2/3 channel pore, one would expect a difference in the selectivity between HyNaC2/3 wildtype and HyNaC2/3 G444S.

We did the same ion substitution experiments as described in Chapter 3.3.7. The concentration of HydraRFamide I was 50 μM and application time for the peptide was 15 seconds. Since divalent cations affected the peptide-activated currents (see Fig. 31), we removed all Ca^{2+} and Mg^{2+} from the peptide containing solutions. The K^+ permeability was robustly reduced for the mutated heteromer in comparison to the wildtype. At -70 mV the mean current in K^+ containing solution was lowered from 100% for the wildtype heteromer ($7.52 \pm 2.16 \mu\text{A}$; $n = 12$) to 54% for the mutated HyNaC channel ($6.63 \pm 1.92 \mu\text{A}$) compared to the mean currents in Na^+ containing solutions (wildtype: $8.09 \pm 2.55 \mu\text{A}$; mutant: $12.89 \pm 4.74 \mu\text{A}$; $n = 12$). Nevertheless, compared to currents in Na^+ containing solutions permeability for Li^+ was in the same range for both wildtype ($9.43 \pm 3.11 \mu\text{A}$; $n = 12$) and mutated heteromer ($12.88 \pm 3.92 \mu\text{A}$; $n = 12$). The peptide-activated mean current in Li^+ containing solution was not significantly increased in comparison to the mean current in Na^+ containing solution for the wildtype heteromer (124%) and the mutated HyNaC2/3 G444S (104%; see Fig. 35A).

In addition, we performed voltage ramps from -90mV to $+95\text{mV}$ within 6 seconds in solutions where divalent cations were removed to determine the reversal potential of the current evoked by $50\ \mu\text{M}$ HydraRFamide I in oocytes expressing HyNaC2/3 and HyNaC2/3 G444S. For each condition we measured 5 oocytes. Two ramps were performed, one before peptide application and one during application of $50\ \mu\text{M}$ HydraRFamide I. Afterwards, both ramps were subtracted from each other and the resulting ramps for all 5 oocytes were averaged. Figure 35B shows the resulting I-V curves representing the mean for both wildtype and mutated heteromer.

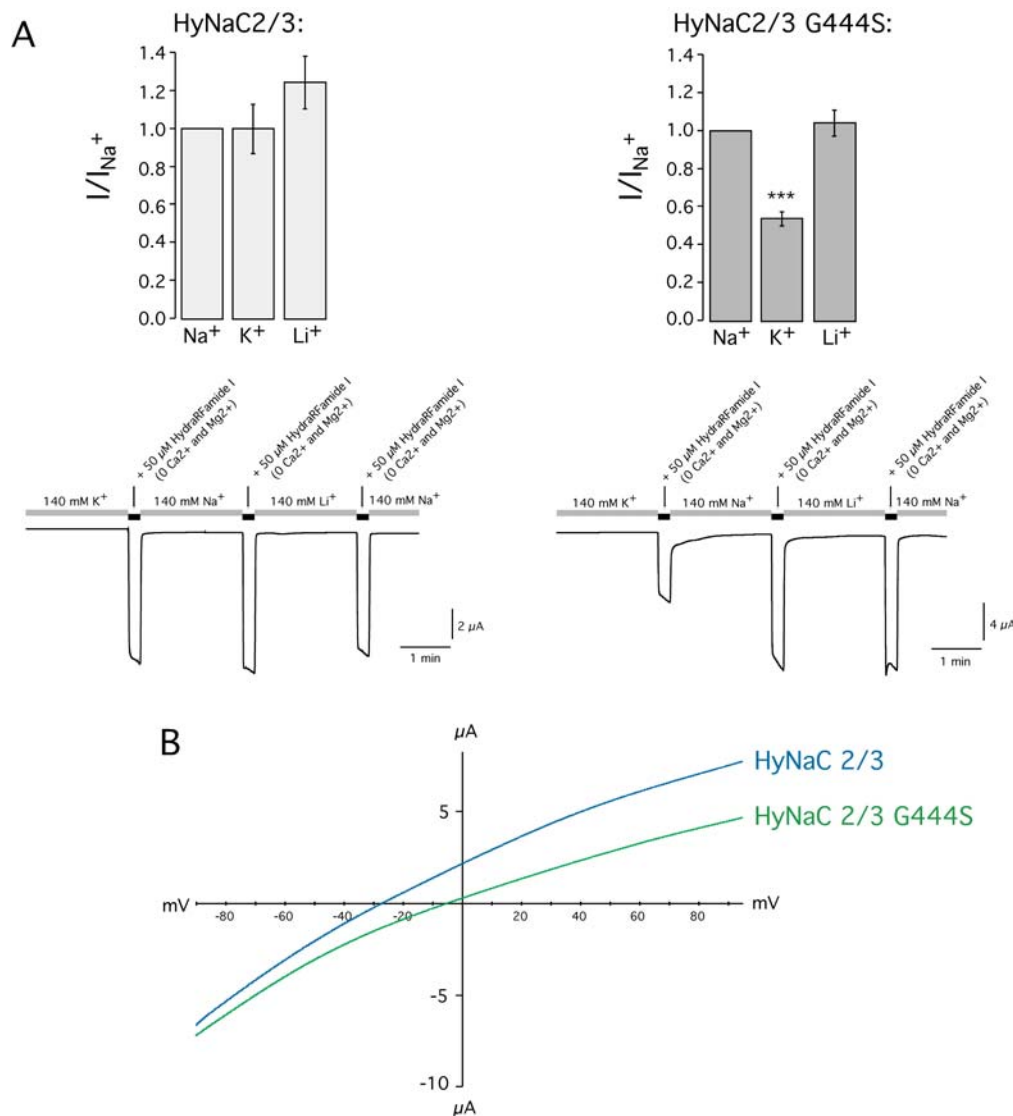


Fig. 35: Mutation of the glycine (G) at position 444 in HyNaC3 resulted in altered ion selectivity of the HyNaC2/3 heteromer. (A) Top: Bar graphs summarizing the ion substitution experiments for HyNaC2/3 (left) and HyNaC2/3 G444S (right). Bottom: Example current traces showing measurements summarized in the bar graphs at the top. Mg^{2+} and Ca^{2+} were removed from peptide containing solutions. (B) Mean I-V relationships ($n = 5$) for HyNaC2/3 wildtype heteromer and HyNaC2/3 G444S. For details see text.

The voltage ramps indicate that the reversal potential for HyNaC2/HyNaC3 G444S was shifted towards more positive values, from about -25 mV for the HyNaC2/3 wildtype to -5 mV (see Figure 35B). The shift of the reversal potential confirms the lower permeability of HyNaC2/HyNaC3 G444S for K^+ showed in the ion substitution experiments and strongly suggests that peptide-activated currents in HyNaC2/3 expressing oocytes flow through the HyNaC pore.

To further verify that currents elicited by HydraRFamide application in oocytes expressing HyNaC2/3 were not a product of activation of hemi gap junctional channels we cloned the hemi gap junction subunit innexin-1 from *Hydra magnipapillata* and co-injected the cRNA together with HyNaC2 and 3 to see whether additional expression of hemi gap junctional channels from *Hydra* would influence the amplitude of peptide activated currents. After activation with 50 μ M HydraRFamide I, mean current amplitude for oocytes co-injected with innexin-1 was not significantly altered (1.05 ± 0.40 μ A; $n = 5$; $p = 0.49$) compared to currents from oocytes where only HyNaC2 and 3 were expressed (1.27 ± 0.56 μ A; $n = 5$; Fig. 36A).

In addition, we injected an anti-sense oligonucleotide directed against the first 30 nucleotides at the 5'-end of *Xenopus laevis* pannexin-1. Injection of this oligonucleotide should inhibit, at least partially, the expression of the endogenous hemi gap junctional channel pannexin-1 in oocytes, and thus clearly reduce the peptide-activated current if pannexin-1 was involved. However, the co-injection of the pannexin-1 oligonucleotide also had no significant effect on current amplitudes evoked by 50 μ M HydraRFamide I. The mean current amplitude was only slightly decreased (1.14 ± 0.69 μ A; $n = 5$; $p = 0.75$; Fig. 36A).

As a negative control for these experiments we co-expressed stomatin, a completely different protein, from which we knew that it has no effect on peptide-activated currents (data not shown), with HyNaC2 and 3. The reduction of the mean current after co-injection of *Hydra* innexin-1 or anti sense oligos against *Xenopus* pannexin-1 was in the same range as for co-injection of stomatin (1.18 ± 0.61 μ A; $n = 5$; $p = 0.82$; see Figure 36A), which suggests that expression level of hemi gap junctions had no influence on peptide-activated HyNaC2/3 currents.

Since the pores of hemi gap junctions are rather large and allow the transit of molecules up to 1-2 kDa, we tried to exchange the Na^+ by $NMDG^+$, which is a cation that is much larger than Na^+ and K^+ and usually does not permeate through DEG/ENaC channels. The Na^+ -replacement by 140 mM $NMDG^+$ reduced the current activated by 30 μ M HydraRFamide I dramatically. The decrease was reversible when $NMDG^+$ was replaced by Na^+ again. In 5 measured oocytes,

replacement of Na^+ by NMDG^+ for 1 minute led to a reduction of the peptide activated current to a level that was identical with the current level reached after wash-out of the peptide in Na^+ containing solutions (see Fig. 36B). Thus, the dramatic reduction of the current suggests that NMDG^+ can not pass through the pore opened by *Hydra* peptides, which would exclude an involvement of hemi gap junctions in peptide-activated currents in oocytes expressing HyNaC2 and 3.

In summary, the facts that the ion selectivity changes after introducing a selectivity mutation in HyNaC3 and the current amplitude is unchanged when the expression of hemi gap channels is altered, but also that the peptide-evoked current is dramatically reduced when Na^+ is replaced by NMDG^+ all suggest that hemi gap junctions are not involved in the activation of peptide-evoked currents in oocytes expressing HyNaC2/3.

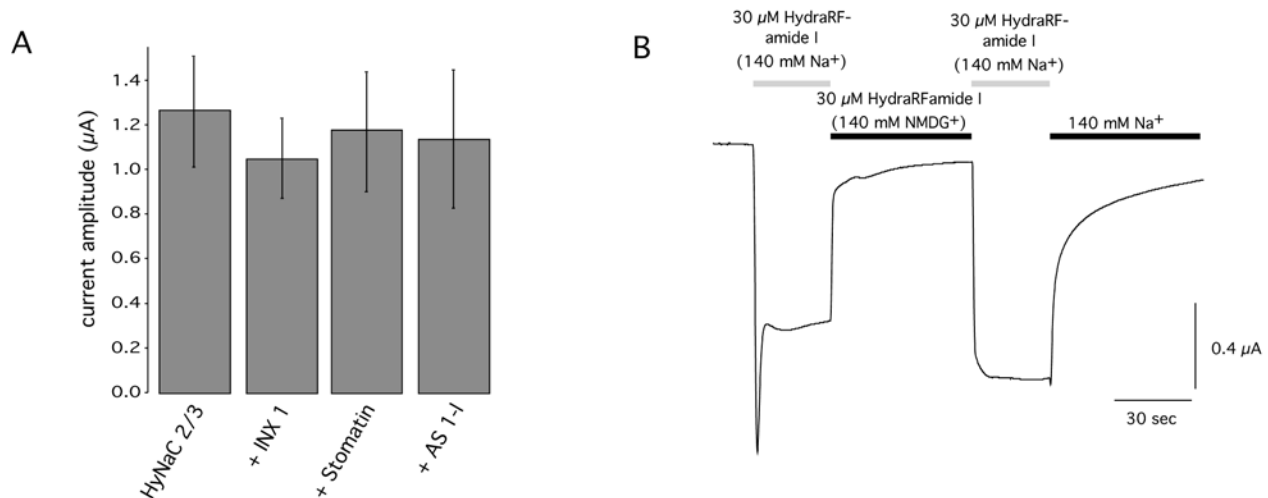


Fig. 36: Altering the expression of hemi gap channels in oocytes did not change amplitudes of peptide-activated HyNaC2/3 currents. (A) Bar graph showing mean current amplitudes evoked by application of 50 µM HydraRFamide I in oocytes expressing only HyNaC2/3, oocytes co-injected with cRNA for innexin-1 from *Hydra magnipapillata* (INX 1) and with antisense oligonucleotide against pannexin-1 from *Xenopus laevis* (AS 1-1). As a control we used HyNaC2/3 expressing oocytes co-injected with stomatin. For details see text. (B) Example trace showing complete reduction of the peptide activated current when Na^+ was replaced by NMDG^+ .

3.3.9 HyNaC2/3 heteromers form ion channels that are directly activated by the *Hydra* neuropeptides

The next important question was whether the current elicited by HydraRFamides in HyNaC2/3 injected oocytes was directly gated by the peptides or indirectly by second messengers, which is

typical for peptide effects on ion channels (see Introduction). For this purpose, we first investigated the activation kinetics, since channel opening via second messenger cascades is much slower compared to direct activation by ligands. So, we activated 5 oocytes expressing HyNaC2 and 3 with 150 μM HydraRFamide II, which is a nearly maximal concentration (see Fig. 30) and determined the activation time constant τ and in addition the time elapsed between activation of 10% to 90% of the maximal current. As a control, we injected some oocytes with IRK-1, a voltage gated potassium channel that was activated by replacement of 70 mM Na^+ by K^+ (see Figure 37A). IRK-1 is constantly open at -70 mV and activation should be immediate and without any delay by ligand binding or second messenger cascades. So, we determined the above mentioned parameters for IRK-1 and compared it with the activation kinetics of peptide-gated HyNaC currents. For both, IRK-1 and HyNaC2/3, the activation time constant τ was 0.17 sec ($n = 5$). Also the time that elapsed between activation of 10% and 90% of maximal current was in a similar range for both channels. It was 475.60 ± 156.62 ms for IRK-1 and 440.60 ± 87.33 ms for HyNaC2/3, which suggests that activation of HyNaC2/3 channels by *Hydra* peptides is direct and just limited by the speed of solution exchange.

To further verify this finding, we injected oocytes expressing HyNaC2/3 with GDP- β -S, an unspecific inhibitor of G-proteins, prior to activation by 50 μM HydraRFamide I. GDP- β -S is a non-hydrolyzable GDP analogue blocking the formation of G-protein heterotrimers. So, if peptide-activated HyNaC currents were mediated by G-proteins, the pre-injection of GDP- β -S should have strongly reduced them. We injected 23 nl of 50 mM GDP- β -S solution into HyNaC2/3 expressing oocytes directly before activation with 50 μM HydraRFamide I and compared the amplitudes with oocytes expressing HyNaC2 and 3 that were not treated with GDP- β -S. The mean peak current amplitude for 10 oocytes was not significantly reduced from 3.45 ± 2.18 μA without GDP- β -S treatment to 3.02 ± 1.25 μA ($n = 10$; $p = 0.38$) after GDP- β -S injection (see Figure 37B). As a control, we used the same protocol for non-injected oocytes that were stimulated by 10 $\mu\text{g/ml}$ trypsin. Oocytes have an endogenous trypsin receptor that is coupled to internal Ca^{2+} stores via G_i -proteins. The receptor activation by external trypsin raises internal Ca^{2+} and thereby opens Ca^{2+} -activated Cl^- channels leading to transient inward currents of several μA (Schultheiss 1997). These trypsin-activated currents in non-injected oocytes were significantly reduced by pre-injection of GDP- β -S from 2.06 ± 1.54 μA ($n = 10$) without GDP- β -S treatment to $1.16 \mu\text{A} \pm 1.08 \mu\text{A}$ ($n = 10$; $p = 0.01$) after injection of the GDP analogue (see Fig.

37B).

We also stimulated oocytes expressing HyNaC2 and 3 with 100 $\mu\text{g/ml}$ trypsin to see whether stimulation of the G_i -protein pathway would evoke any additional currents besides the above mentioned in non-injected oocytes. However, we could not observe any differences in trypsin-activated currents between non-injected oocytes and oocytes expressing HyNaC2 and 3 (see Fig. 37C). Mean current amplitude for non-injected oocytes was $1.88 \pm 0.49 \mu\text{A}$ in comparison to $1.88 \pm 0.16 \mu\text{A}$ in oocytes expressing HyNaC2 and 3 ($n = 5$; $p = 0.97$).

cAMP is the most important intracellular mediator in G-protein coupled second messenger processes. It is synthesized from ATP by the plasma-membrane-bound enzyme adenylate cyclase and is rapidly and continuously destroyed by one or more cyclic AMP phosphodiesterases, which hydrolyze cAMP to adenosine 5'-monophosphate (5'AMP). So, we next investigated, if it is possible to evoke currents in oocytes expressing HyNaC2/3 just by raising the intracellular cAMP level. For this purpose, we used two different substances. One of them was forskolin, which is a labdane diterpene that is produced by the Indian *Coleus* plant (*Plecthranthus barbatus*). Forskolin resensitizes cell receptors by activating the enzyme adenylyl cyclase and increasing the intracellular levels of cAMP. The other substance was IBMX (3-isobutyl-1-methyl-xanthin), which is an unspecific inhibitor of phosphodiesterase activity. Both agents are permeating the plasma membrane of oocytes and thus we could apply them from the extracellular side. Application of a mixture of 50 μM forskolin and 1 mM IBMX for 3 minutes did not evoke any currents, neither in oocytes expressing HyNaC2/3 ($n = 6$; data not shown) nor in non-injected oocytes ($n = 5$). In summary, the fast activation kinetics, as well as the fact that altering the activity of G-proteins did not significantly change currents both suggest that the HydraRFamides directly activate HyNaC2/3 channels in oocytes.

Furthermore, we wanted to exclude that activation of currents in HyNaC expressing oocytes was mediated by G-protein coupled opiate receptors, which are usually activated by opioide peptides like morphine. One could imagine that heteromeric channels composed of HyNaC2 and 3 subunits were coupled to endogenous opiate receptors via G-protein coupled signaling cascades. To verify whether opiate receptors were involved in the opening of HyNaC2/3 channels, we used naloxone, which is an antagonist of opiate receptors. If such receptors would participate in HyNaC activation, the currents evoked by HydraRFamides should be strongly reduced by the application of naloxone. Since currents evoked by *Hydra* peptides in oocytes expressing HyNaC2 and 3 showed pronounced tachyphylaxis, particularly between the first and second application,

we applied 30 μM HydraRFamide II 3 times for 5 seconds ($n = 5$) adding 500 μM naloxone before and during the third application. As a control, we performed the same protocol without naloxone for direct comparison of the third current, in respect to the mean peak amplitude and the degree of tachyphylaxis. The mean peak current amplitudes after the third activation by HydraRFamide II were comparable in size as it can be seen from the bar graph in Figure 37D. It was slightly reduced for the naloxone treated oocytes ($2.45 \pm 0.79 \mu\text{A}$) in comparison to the control oocytes ($2.83 \pm 0.65 \mu\text{A}$), but the reduction was not significant ($p = 0.44$). Also the course of tachyphylaxis was in a similar range for both groups (see curves Fig. 37D). The current elicited by the third application of *Hydra* peptide was reduced to 60% compared to the first activation ($4.94 \pm 1.51 \mu\text{A}$) for the control oocytes and to 53% ($4.59 \pm 1.04 \mu\text{A}$) for the naloxone treated oocytes .

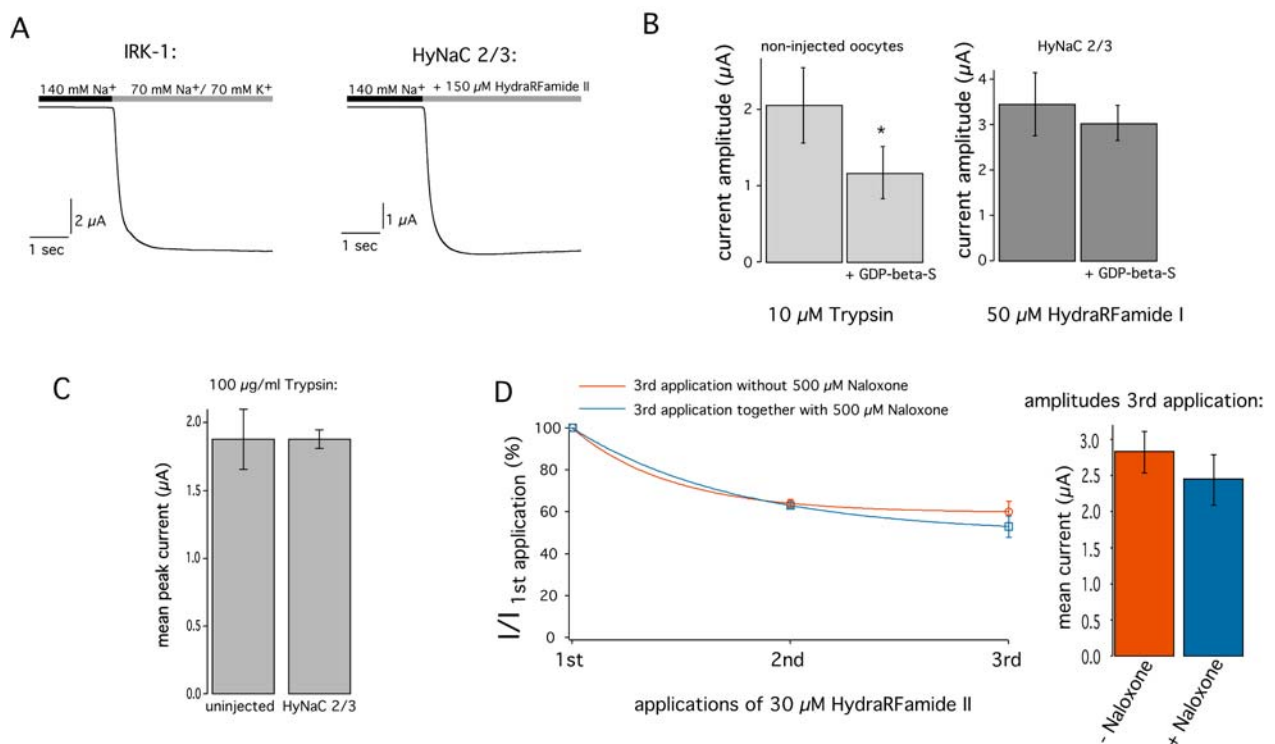


Fig. 37: Peptide-activated currents in oocytes injected with HyNaC2/3 were directly gated. (A) Example current traces for activation of IRK-1 channels by replacement of 70 mM Na⁺ with K⁺ (left) and HyNaC2/3 by application of 150 μM HydraRFamide II (right). (B) Left: Bar graph summarizing measurements ($n = 10$), where Ca²⁺-activated Cl⁻ currents were activated by application of 10 $\mu\text{g/ml}$ trypsin in uninjected oocytes and in oocytes where GDP- β -S was injected before trypsin application. Right: Bar graph showing mean current amplitudes for oocytes expressing HyNaC2/3 activated by 50 μM HydraRFamide I with and without prior injection of GDP- β -S. (C) Mean Ca²⁺-activated Cl⁻ currents for uninjected oocytes and oocytes expressing HyNaC2/3 activated by 100 $\mu\text{g/ml}$ trypsin. (D) Left: Curves showing mean tachyphylaxis for oocytes expressing HyNaC2/3. In the blue curve third peptide application was in the presence of 500 μM naloxone. $n = 5$ for both curves. Right: Bar graph showing mean current amplitudes for the third peptide application. Colors correspond to the curves on the left side.

Thus, the naloxone treatment did not influence peptide-activated current in HyNaC2/3 expressing oocytes, which is another indication that HyNaC2/3 channels are not gated by G-proteins.

3.4 Modulation of ASIC currents by HydraRFamides

It was already known that currents of some ASIC subunits are modulated by FMRFamide and Neuropeptide FF (see Introduction). We investigated whether HydraRFamides could also alter the amplitudes and desensitization kinetics of ASIC currents. For this purpose, we injected oocytes with cRNA for ASIC1a, 1b, 2a and 3, and pre-applied the HydraRFamides I-IV before we stimulated the channels with proton concentrations sufficient for maximal activation. For ASIC 1a, 1b, and 3 pH 5.5 was used, whereas ASIC2a was activated by pH 3.5. In total, we tested 3-7 oocytes for each ASIC subunit and activated them successively 5 times for 15 seconds: one activation without any peptide and four activations each together with 50 μ M of one of the peptides. Between the applications we waited 40 sec. For ASIC2a homomeric currents ($n = 8$) amplitudes and desensitization kinetic were not significantly changed by application of the HydraRFamides I-IV (data not shown).

For ASIC1a we observed a significant reduction of the mean peak amplitude by HydraRFamides. Mean peak current amplitude was reduced from $5.36 \pm 2.71 \mu$ A ($n = 6$) to $2.61 \pm 0.74 \mu$ A by pre-application HydraRFamide II ($n = 6$; $p = 0.04$; data not shown), to $3.45 \pm 1.50 \mu$ A ($n = 6$; $p = 0.16$) by HydraRFamide I, to $3.31 \pm 0.90 \mu$ A ($n = 6$; $p = 0.11$) by HydraRFamide III and to $4.48 \pm 1.77 \mu$ A ($n = 6$; $p = 0.52$) by HydraRFamide IV. However, ASIC1a shows pronounced tachyphylaxis, which probably accounts for this reduction.

Furthermore, pre-application of HydraRFamide I fastened the desensitization of proton-activated ASIC1b currents significantly. Desensitization constant τ was reduced from 0.73 ± 0.02 seconds ($n = 3$) to 0.69 ± 0.01 seconds after pre-application of HydraRFamide I ($n = 3$; $p = 0.05$). Notice the small number of measured oocytes and the rather small difference between both τ values, since τ for the other peptides was in a similar range (HydraRFamide II: $\tau = 0.72 \pm 0.03$ sec., $n = 3$, $p = 0.65$; HydraRFamide III: $\tau = 0.71 \pm 0.03$ sec., $n = 3$, $p = 0.40$; HydraRFamide IV: $\tau = 0.74 \pm 0.04$ sec., $n = 3$, $p = 0.53$).

Pre-application of HydraRFamides III and IV exerted the most dramatic effects on the desensitization of proton-activated ASIC3 currents (see Fig. 38). Desensitization constant τ was

increased from 0.54 ± 0.09 seconds to 2.05 ± 0.37 seconds by pre-application of HydraRFamide III ($n = 7$; $p \ll 0.001$) and even to 3.21 ± 0.20 seconds by pre-application of HydraRFamide IV ($n = 4$; $p \ll 0.001$). Desensitization constant τ was also significantly raised when HydraRFamide II was pre-applied ($\tau = 0.64 \pm 0.07$ sec., $n = 7$; $p = 0.03$), whereas the slight increase of τ after pre-application of HydraRFamide I was not significant ($\tau = 0.60 \pm 0.07$ sec., $n = 9$; $p = 0.15$). Furthermore, we observed a tendency, although not significant, for reduced peak amplitudes of homomeric ASIC3 currents after pre-application of HydraRFamide III. They were decreased from $6.54 \pm 2.98 \mu\text{A}$ ($n = 7$) when the peptide was not pre-applied to $4.68 \pm 1.88 \mu\text{A}$ ($n = 7$; $p = 0.19$). The mean peak current amplitude after pre-application of the other three peptides was similar to the control amplitude (HydraRFamide I: $6.35 \pm 3.03 \mu\text{A}$, $n = 7$, $p = 0.91$; HydraRFamide II: $6.26 \pm 2.95 \mu\text{A}$, $n = 7$, $p = 0.86$; HydraRFamide IV: $7.13 \pm 2.75 \mu\text{A}$, $n = 7$, $p = 0.70$). Thus, the modulation of proton-evoked ASIC currents by HydraRFamides and other RFamides is another indication that ASICs have a conserved interaction site for RFamides, similar to HyNaCs and FaNaCs, which probably was already present in the precursor channel of the DEG/ENaC family.

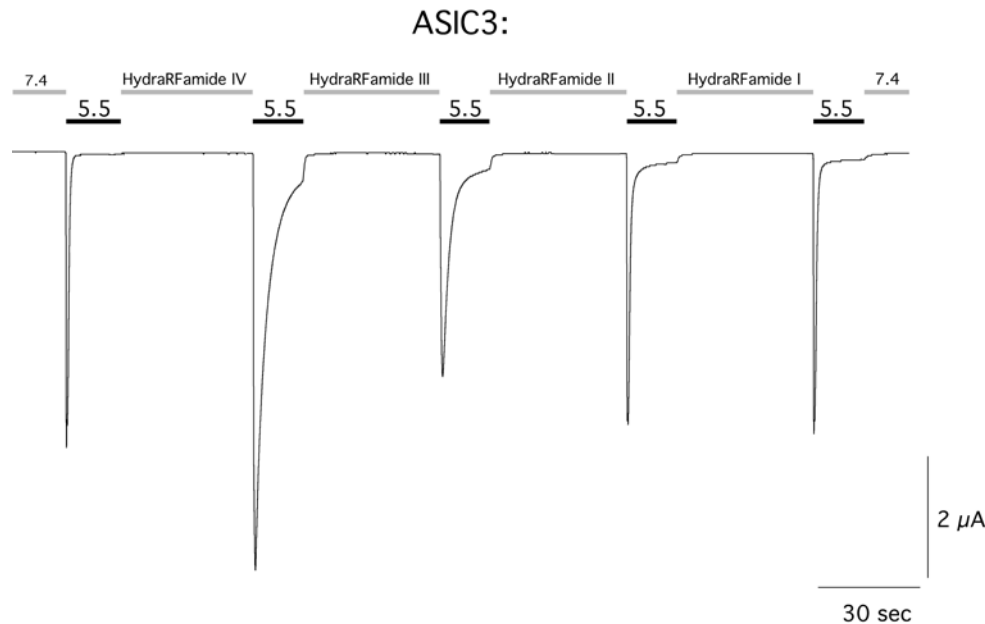


Fig. 38: HydraRFamides III and IV alter desensitization kinetics of acid-evoked ASIC3 currents. Example current trace showing that pre-applications of HydraRFamides III and IV slowed down desensitization of ASIC3 currents. For details see text.

CHAPTER IV

Discussion

4.1 HyNaCs are members of the DEG/ENaC family with ASICs and BLINaC/INaC as closest relatives

Comparison of the HyNaC sequences with DEG/ENaC proteins revealed that the newly cloned subunits from *Hydra magnipapillata* are real members of this ion channel superfamily. In HyNaC2, 3, and 4, we found all the conserved regions and residues that are characteristic for DEG/ENaC ion channels like 2 transmembrane domains, a large cyteine-rich extracellular loop and short N- and C-termini. The highly conserved HG-motif preceding the first transmembrane domain that is essential for gating of DEG/ENaC channels (Gründer 1997), is missing in HyNaC1. Moreover, cDNA coding for HyNaC1 did not contain a methionine (M) to initiate protein translation upstream of the predicted first transmembrane domain but it did contain a stop codon there. The absence of an initiator methionine was confirmed by ESTs from the public database. Therefore, we conclude that *hynac1* is an inactive pseudogene.

Our phylogenetic analysis has shown that the newly cloned HyNaC subunits are closely related to ASICs and BLINaC/INaC. All methods used (see Materials and Methods) have put HyNaCs, ASICs and BLINaC/INaC together on a common branch of the phylogenetic tree, which means that these three subgroups are forming a monophyletic assemblage within the DEG/ENaC superfamily. We included 82 proteins into the analysis, as far as we know, there are no other such detailed phylogenetic analysis existing for the DEG/ENaC family. This makes it rather difficult to compare our results with the published phylogenetic trees from other groups, since the composition of the members included into the analysis can influence the calculated tree. We tried to find a balanced composition and included a similar number of members of the different DEG/ENaC subgroups and also a comparable number of vertebrate and invertebrate proteins. Another point that has to be considered when comparing different phylogenetic trees are the alignments that serve as basis for calculation. "...attempting to improve the alignment.....is probably the single most

important thing you can do to ensure a high-quality alignment and make a high-quality phylogeny possible.” (Hall 2004). Thus, we spend a lot of time to trim the aligned full sequences to get a good fundament for the phylogenetic calculations. A third point concerning the quality of a phylogenetic analysis is the software used for calculation. We used 3 different approaches in combination with three different programs to calculate phylogenetic relationships within the DEG/ENaC superfamily (see Materials and Methods). All the applied programs and methods calculated phylogenetic trees that corresponded almost completely. The classification of the major subgroups was identical for all calculated trees: ASICs, BLINaC/INaC and HyNaCs were put together on a branch, as well as ENaCs, DEGs and FaNaCs. The accordance of the different trees verifies the quality of our alignment.

Comparison of our results with already existing phylogenetic trees in the literature shows a general accordance concerning the classification of the major DEG/ENaC subgroups. The work of Kellenberger and Schild from 2002 that includes more than 30 DEG/ENaC proteins confirms our results (Kellenberger 2002). There are older works with fewer sequences analyzed, where the emphasis was put on the invertebrate members of the DEG/ENaC family (Mano 1999; Tavernarakis 2001). In these phylogenetic trees, contradictory to our results, FaNaCs or ENaCs, respectively, are placed in close proximity to the ASICs, whereas BLINaCs/INaC are not included. However, due to the low number of sequences used for the analysis and the unbalanced choice of the proteins, one should look rather carefully on such incomplete analyses.

In contrast to channels that appeared at an early stage of evolution such as potassium, chloride, or water channels, DEG/ENaC genes are only present in multicellular animals (Metazoa) (Kellenberger 2002). Thus, it is likely that the first DEG/ENaC ion channels evolved in the course of intercellular communication. Since cnidarians, including *Hydra*, are one of the simplest metazoans concerning their body plan and life style, one should assume that also ion channels in *Hydra* are primitive and ancient. Unfortunately, there are no means to proof this definitely. Assuming that HyNaCs are rather simple DEG/ENaC ion channels that did not change very much during evolution would mean that they should highly resemble the common ancestor of the DEG/ENaC ion channels that existed about 700 million years ago. The close relationship of ASICs and BLINaC/INaC to the *Hydra* subunits would mean that these two vertebrate DEG/ENaC subgroups evolved more slowly

than for example the invertebrate FaNaCs, DEGs or PPKs. It is indeed known that the rate of divergence in the model invertebrates *Caenorhabditis elegans* and *Drosophila melanogaster* is much higher than in vertebrates (Aguinaldo 1997; de Rosa 1999), which means that the appearance of genes and proteins, respectively, changes faster in protostomian invertebrates. This finding would also explain the diverse distribution and the many isolated proteins from *C.elegans* and *Drosophila* in our phylogenetic trees. Many genes expressed in mammals are not found in flies or worms and for a long time it was believed that most of these genes are vertebrate innovations. By comparison with ESTs from the anthozoan cnidarian *Acropora millepora* Kortschak and colleagues could, however, show that many of these genes were already present in the common metazoan ancestor (Kortschak 2003). Gene loss has thus been much more extensive in the model invertebrate lineages than previously assumed and could mean that ASICs or BLINaC were present in flies and worms in early evolution but had been lost during their long separate development.

4.2 HyNaCs are directly activated by *Hydra* neuropeptides

We could show in our work that HydraRFamides I and II could activate heteromeric HyNaC2/3 ion channels heterologously expressed in *Xenopus* oocytes. After the finding that FaNaC was activated by FMRFamide (Lingueglia 1995), this is the second heterologously expressed ion channel that is directly activated by peptides. The EC₅₀ for activation of HyNaC2/3 by HydraRFamides I and II is 25-30 μ M and thus in a similar range as FaNaC activation by FMRFamide (Lingueglia 1995; Jeziorski 2000; Furukawa 2006). The relatively low affinity of HyNaCs and FaNaCs for their activating peptides could be explained with a relative slow removal of neuropeptides. Thus, the low affinity prevents a constant depolarization by low concentrations of diffusing neuropeptides.

In several control experiments, we could exclude indirect activation by second messenger cascades. First of all, the rapid activation in the sub-second range speaks against an involvement of second messengers. Furthermore, the unspecific G-protein inhibition by GDP- β -S and also the inhibition of opioide-receptors by naloxone did not influence peptide-activated HyNaC2/3 currents.

HydraRFamide I and II, both arise from preprohormones A and B, whereas HydraRFamide

I is also synthesized from preprohormone C. Recently, Hansen and colleagues did whole-mount in situ hybridization of *Hydra*, using cRNA probes coding for the different preprohormones. For preprohormone A in situ hybridization showed intensively stained, distinct neurons in the ectoderm of the tentacles, hypostome, upper gastric region and peduncle. In developing buds, staining was first seen in the neurons of the hypostome region (see Appendix 6; Hansen 2000). However, staining pattern for preprohormone B was confined to discrete neurons in the ectoderm of the hypostome and upper gastric region, whereas in situ hybridization with a probe specific for preprohormone C stained only neurons in the tentacles of *Hydra* (see Appendix 6).

In situ hybridization with cRNA probes coding for HyNaC2, 3 or 4, showed intense staining in the hypostome region at the bases of the tentacles (see Appendix 6). Unfortunately, HyNaC probes did not precisely stain distinct cells. Nevertheless, it is clear that in the hypostome region cells expressing HyNaCs lie in close proximity to neurons that express HydraRFamides.

Already in 1985, before discovery of HydraRFamides, Grimmelikhuijzen reported the visualization of the three-dimensional structure of the ectodermal nervous system in the hypostome, tentacles, gastric region and peduncle by whole-mount incubation of different *Hydras* with antisera to RFamides (Grimmelikhuijzen 1985). He described the occurrence of “...a ganglion-like structure ...consisting of numerous sensory cells located in the region around the mouth opening and a dense plexus of processes which project mostly radially towards the bases of the tentacles...” This observation fits very well to the expression pattern of HyNaCs and suggests that HydraRFamide containing neurons, which project towards the bases of the tentacles, make synaptic junctions to epitheliomuscular cells expressing HyNaCs. It is already known that in Cnidaria such synaptic junctions generally have dense-cored vesicles that contain HydraRFamides among other neuropeptides. It is therefore likely that HydraRFamides are released onto cells expressing HyNaCs. Unfortunately, to date no data are published about the physiological function of RFamides in *Hydra*. The expression pattern of HyNaCs at the bases of the tentacles would suggest a role in the movement and control of the tentacles, but this is just speculation and thus functional *in vivo* studies are necessary to uncover the physiological role of HyNaCs and RFamides in *Hydra*.

4.3 Properties of peptide-evoked HyNaC2/3 currents and their evolutionary implications

In contrast to other DEG/ENaC channels (Kellenberger 2002), HyNaC2/3 is not selective for Na⁺ over K⁺ ions, and moreover, our results indicate a permeability also for Ca²⁺. Mutation of the glycine 444 to serine in the selectivity filter of HyNaC3 reduces permeability for K⁺ strongly and makes the heteromeric channel more selective for Na⁺. A serine is present in all the other Na⁺ selective members of the DEG/ENaC family, which confirms the important role of this amino acid for Na⁺ selectivity (Kellenberger 1999; Sheng 2000; Snyder 1999). However, Na⁺ selectivity varies between different subgroups of the DEG/ENaC family. The Na⁺/K⁺ selectivity for native ENaC from toad bladder and frog skin was estimated to be >500 (Benos 1996; Palmer 1982), whereas this ratio is ≤10 for ASICs and FaNaC (Lingueglia 1995; Zhainazarov 1998). Moreover, ASICs show some permeability to Ca²⁺, which is highest in ASIC1a with Na⁺/Ca²⁺ permeability ratio between 2.5 (Waldmann 1997) and ~17 (Bässler 2001; Sutherland 2001). Recently, Bianchi et al. could also show Ca²⁺ permeability for the neurotoxic DEG-mutant of MEC-4 in *Xenopus* oocytes (Bianchi 2004).

In addition to permeating through the channel, divalent cations also block peptide-activated HyNaC2/3 currents. Amplitudes in the presence of Ca²⁺ and Mg²⁺ were decreased and also the peptide affinity was reduced by higher Ca²⁺ concentrations. Furthermore, HyNaC2/3 channels could be opened just by removal of Ca²⁺ and Mg²⁺. Regulation by extracellular divalent cations is a common characteristic of DEG/ENaC channels, since a dual inhibitory and stimulatory effect was also observed for ASICs (Babini 2002; Berdiev 2001; de Weille 2001; Paukert 2004; Sutherland 2001; Zhang 2001 and 2002). Ca²⁺ inhibits Na⁺ currents in several different ASIC multimers with an apparent IC₅₀ in the millimolar range. Also for the peptide-gated FaNaCs sensitivity to blockade by divalent cations is described, as well as for the UNC-105 A692V mutant from *C.elegans* (Furukawa 2006; Jeziorski 2000; Hamill 1996). However, affinity for Ca²⁺ in the above mentioned subgroups is in the millimolar range, whereas Ca²⁺ blocks HyNaC2/3 with an IC₅₀ of 800 nM. However, Immke et al. could show an even higher Ca²⁺ affinity for ASIC3. The IC₅₀ for Ca²⁺ was 150 nM and thus about 5-fold higher than for HyNaC2/3 (Immke 2003).

For FaNaC cloned from *Aplysia kurodai*, even a potentiation of the current evoked by

FMRFamide was observed when extracellular Mg^{2+} was increased (Furukawa 2006). Thus, although there are variations in the affinity, the influence by extracellular divalent cations and the binding site for Ca^{2+} and Mg^{2+} seem to be general characteristics for DEG/ENaC channels, which were likely already present in the common ancestor of this ion channel family.

Amiloride inhibits HyNaC2/3 currents activated by HydraRFamides with a rather low affinity. IC_{50} is about 500 μM and thus much higher than for other members of the DEG/ENaC family, where half of the maximal current is blocked with low-micromolar concentrations (Kellenberger 2002). However, a reason for this low amiloride affinity is not obvious, since the amiloride binding site preceding the second transmembrane domain is a glycine in HyNaCs, as it is the case for almost all other DEG/ENaC channel subunits. Moreover, experiments where HyNaC2/3 channels were opened by removal of extracellular divalent cations revealed that amiloride not only has an inhibitory effect on HyNaC2/3 channels, but also stimulates the channel. This paradoxical influence of amiloride was also described for other DEG/ENaC channels like ASIC2a (Adams 1999), ASIC3 (Yagi 2006) and FaNaCs (Furukawa 2006; Green 2002; Jeziorski 2000) that's why Adams and colleagues postulated two binding sites for amiloride, one inhibiting and one stimulating (Adams 1999). However, to date interaction of amiloride with DEG/ENaC channels is poorly understood and depends on many different factors like extracellular pH and voltage, but it seems rather clear that amiloride binding sites are ancient features of DEG/ENaC channels.

HyNaC2/3 channels exhibit rapid current decrease in response to repeated HydraRFamide application, a phenomenon called tachyphylaxis. Within the DEG/ENaC ion channel family, ASIC1a (Paukert 2004; Gitterman 2005; Neaga 2005; Chen 2007) and FaNaC (Perry 2001; Lingueglia 1995) also exhibit tachyphylaxis. However, the physiological relevance and the precise mechanism are not well understood. Chen et al. showed that tachyphylaxis of ASIC 1a is dependent on extracellular Ca^{2+} . They suggested that it is probably linked to Ca^{2+} permeability of the channel (Chen 2007). Since HyNaC2/3 seems to be also permeable for Ca^{2+} , this could be a reason for tachyphylaxis of peptide activated HyNaC currents. On the other hand FaNaC, which is not permeable for Ca^{2+} also exhibits tachyphylaxis, a fact that speaks against a general involvement of permeating Ca^{2+} ions. However, Chen et al. also showed that the impact of tachyphylaxis on ASIC1a activity

depends on many other parameters that we have not examined for HyNaC2/3, like extra- and intracellular pH, duration of the open state and number of stimulations.

We could observe an inhibitory influence of protons on HyNaC2/3. Low pH decreased HyNaC currents activated by peptides. However, high proton concentrations also accelerated the desensitization upon washout of the peptide and prevented tachyphylaxis. Protons also influence other members of the DEG/ENaC family. Similar to the effect on HyNaC2/3, an inhibitory effect of low pH is also reported for FaNaCs. Acidification of the bath solution has two effects on FMRFamide activated FaNaC currents in cultured neurons from the snail *Lymnea stagnalis*: it reduces the amplitude of the currents and it prevents tachyphylaxis (Perry 2001). ASICs are activated by a drop of extracellular pH and protons seem to be the physiological ligand for this subgroup (Bevan 1991; Grantyn 1988; Krishtal 1981; Varming 1999; Waldmann 1998). Recently, it was shown that heterologously expressed silent δ ENaC can be activated by lowering the pH (Yamamura 2004). Furthermore, protons enhance the constitutive current seen in $\delta\beta\gamma$ ENaC expressing oocytes (Ji 2004). Thus, interaction with protons seems to be an ancient feature of DEG/ENaC channels since FaNaC/ENaCs and ASICs/HyNaCs share a proton binding site although both groups diverged rather early in history.

Most of the above mentioned properties of peptide-activated HyNaC2/3 currents are characteristic for large pore hemi gap junctional channels, like unselectivity for cations or inhibition by Ca^{2+} and H^+ . Recently, Pelegrin et al. showed that activation of the P_2X_7 receptor in oocytes opens linked pannexin-1, which is responsible for the unselective current (Pelegrin 2006). Although peptide activated HyNaC2/3 current was inhibited by the known blockers of hemi gap junctions, carbenoxolone and flufenamic acid (data not shown), we could clearly show with the aid of a mutation in the selectivity filter of HyNaC3 that the current flew through the heteromeric HyNaC2/3 pore.

The above mentioned properties of peptide-activated HyNaC2/3 currents, display a mixture of new characteristics and already known features from other DEG/ENaC channels. The unselectivity for cations is untypical. In terms of parsimony, it is likely that the Na^+ selectivity got lost during the long separate evolution of HyNaCs, which diverged about 700 millions years ago from the bilaterian members. On the other hand, assuming that HyNaCs are highly similar to the common DEG/ENaC ancestor, it is not excluded that this unselectivity is a rather ancient characteristic and Na^+ selectivity derived in the bilaterian

lineage. It is conceivable that during evolution a few rather common amino acid changes in the pore region of DEG/ENaC channels were able to make them selective for Na⁺ in bilaterians, which became necessary due to changed life-styles. Furthermore, the conserved appearance and life-style of cnidarians make it rather unlikely that the properties of their ion channels changed to a greater extent during evolution.

Many structural features in HyNaCs seem to be rather conserved within the DEG/ENaC family. Although affinity varies, the binding of amiloride and its modulatory effect on currents is a common characteristic in the DEG/ENaC ion channel family. Thus, we assume that at least one binding site for amiloride was present in the common ancestor of DEG/ENaC channels. However, also a binding site for divalent cations seem to be an ancient structural characteristic within the ion channel family, since currents of distantly related subgroups like ASICs/HyNaCs on the one side and FaNaCs/DEGs on the other side are influenced by extracellular Ca²⁺ and Mg²⁺.

Furthermore, our functional results for HyNaC together with the phylogenetic analysis implicate that a proton binding site and the modulation by protons is no unique feature of ASICs but seems to have evolved rather early in DEG/ENaC evolution. The proton effect on HyNaCs and FaNaCs together with the observation that protons can activate δ ENaC and enhance $\delta\beta\gamma$ ENaC currents suggests that at least one proton binding site was present in the precursor channel of the DEG/ENaC ion channel family.

4.4 Neuropeptides and DEG/ENaC ion channels

In the present work we could show that newly cloned DEG/ENaC subunits from *Hydra* are directly gated by FMRFamide related *Hydra* peptides. Since we assume that HyNaCs strongly resemble the common DEG/ENaC precursor channel, which existed about 700 million years ago, and did not change their properties during their long isolated evolution, it is likely that the ancestral DEG/ENaC channel was already gated or at least modulated by RFamide-like neuropeptides. FMRFamides and other peptides usually exert their action through G-protein coupled receptors. However, in the DEG/ENaC family FaNaC is another member that is directly activated by FMRFamide (Lingueglia 1995) and FLRFamide, which is significantly less potent (Cottrell 1997). A look on the phylogenetic tree reveals that HyNaCs and FaNaCs are on two different branches, which confirms the hypothesis

that interaction with peptides is probably an ancient characteristic of DEG/ENaC channels. We could also show that HyNaC-activating HydraRFamides modulated proton-evoked ASIC currents. The most striking effect was seen for proton-evoked ASIC3 currents, where co-application of HydraRFamide III and IV led to a strong deceleration of the desensitization in the presence of protons. Similar observations were already made in the past by co-application of FMRFamide, FLRFamide and neuropeptide FF, respectively (Askwith 2000). These peptides are not able to activate ASICs on their own but potentiate proton-gated currents and slow down desensitization of heterologously expressed ASIC1 and ASIC3, whereas FMRFamide is more potent than FLRFamide. The Met-enkephalin-RF (YGGFMRF), which is structurally related to FMRFamide but lacks the amide group did not affect ASIC currents. However, synthetic Met-enkephalin-RFamide (YGGFMRFamide) with a C-terminal amide, is as potent as FMRFamide on ASIC3 currents (Askwith 2000), which shows that, similar to activation of FaNaCs, the effects of RFamides are specific and the amide group seems to be important for the modulation of ASIC currents.

Our results suggest that HyNaC2/3 channels also display a rather high specificity for HydraRFamides I and II, since application of HydraRFamides III and IV or FMRFamide did not evoke any current at all. In contrast to HydraRFamides III and IV, HydraRFamides I and II have a pyro-Glu (glutamic acid) that could be crucial for activation of HyNaC2/3. On the other hand, it is possible that such a pyro-Glu prevents interaction with ASICs, since HydraRFamides I and II do not have any clear effect on proton-activated ASIC currents.

Nevertheless, the close relationship of mammalian ASICs and BLINaC/INaC to HyNaCs make them strong candidates for channels directly gated by RFamides. Especially for channels with unknown activation mechanism, like ASIC4 and BLINaC/INaC, a ligand is likely to be found within the overwhelming number of neuropeptides. However, until today no peptide is known that evokes currents on its own in ASICs or BLINaC/INaC expressing cells, but it is likely that many unknown RFamide containing neuropeptides exist in the mammalian nervous system (Espinoza 2000) and that at least one of them has the potency to activate mammalian DEG/ENaC channels.

Since the function of ASICs and FaNaC in the nervous system remains poorly understood, also the physiological role of the impact of RFamides on these DEG/ENaC subgroups is just a matter of speculation. It seems clear that FMRFamide is the natural ligand of FaNaC,

but its participation in neuronal pathways as well as their involvement in synaptic transmission still has to be investigated.

For ASICs, protons are the only known ligands. ASICs are suggested to function as extracellular pH sensors in processes where protons play a signaling role in the CNS and during tissue acidification induced in pathophysiological conditions like ischemia and inflammation. The influence of endogenous RFamide neuropeptides on mammalian ASICs has been proposed to play a role in the response to noxious acidosis in the peripheral and central nervous system. However, since there is a multitude of different FMRFamides and also several ASICs forming heteromeric assemblies the modulation by neuropeptides is likely to be rather complex.

We could show in this work that HydraRFamides are likely to be the physiological ligands for HyNaC channels. Besides HyNaC4, which seems to be not necessary for heteromeric HyNaC2/3 channels, there are still other HyNaC subunits that we did not clone and which are probably also able to participate in functional ion channels that can be activated by one of the many *Hydra* neuropeptides. In situ hybridizations for HydraRFamide precursor peptides (Hansen 2000) and HyNaC2-4 suggest that HydraRFamides function as transmitters in neuromuscular synapses since they are expressed in neurons in the hypostome region that project to the bases of the tentacles where HyNaCs are expressed.

CHAPTER V

References

- Adams, C.M., Anderson, M.G., Motto, D.G., Price, M.P., Johnson, W.A. and Welsh, M.J.** (1998) Ripped pocket and pickpocket, novel *Drosophila* DEG/ENaC subunits expressed in early development and in mechanosensory neurons. *J Cell Biol*, **140**, 143-52.
- Adams, C.M., Snyder, P.M. and Welsh, M.J.** (1999) Paradoxical stimulation of a DEG/ENaC channel by amiloride. *J Biol Chem*, **274**, 15500-4.
- Aguinaldo, A.M., Turbeville, J.M., Linford, L.S., Rivera, M.C., Garey, J.R., Raff, R.A. and Lake, J.A.** (1997) Evidence for a clade of nematodes, arthropods and other moulting animals. *Nature*, **387**, 489-93.
- Ainsley, J.A., Pettus, J.M., Bosenko, D., Gerstein, C.E., Zinkevich, N., Anderson, M.G., Adams, C.M., Welsh, M.J. and Johnson, W.A.** (2003) Enhanced locomotion caused by loss of the *Drosophila* DEG/ENaC protein Pickpocket1. *Curr Biol*, **13**, 1557-63.
- Allard, M., Geoffre, S., Legendre, P., Vincent, J.D. and Simonnet, G.** (1989) Characterization of rat spinal cord receptors to FLFQPQRamide, a mammalian morphine modulating peptide: a binding study. *Brain Res*, **500**, 169-76.
- Anctil, M.** (1987) Bioactivity of FMRamide and related peptides on a contractile system in the coelenterate *Renilla koellikeri*. *J Comp Physiol*, **157**, 31-38.
- Askwith, C.C., Cheng, C., Ikuma, M., Benson, C., Price, M.P. and Welsh, M.J.** (2000) Neuropeptide FF and FMRamide potentiate acid-evoked currents from sensory neurons and proton-gated DEG/ENaC channels. *Neuron*, **26**, 133-41.
- Babini, E., Paukert, M., Geisler, H.S. and Gründer, S.** (2002) Alternative splicing and interaction with di- and polyvalent cations control the dynamic range of acid-sensing ion channel 1 (ASIC1). *J Biol*, **277**, 41597-603.
- Babini, E., Geisler, H.S., Siba, M. and Gründer, S.** (2003) A new subunit of the epithelial Na⁺ channel identifies regions involved in Na⁺ self-inhibition. *J Biol Chem*, **278**, 28418-26.
- Babinski, K., Le, K.T. and Seguela, P.** (1999) Molecular cloning and regional distribution of a human proton receptor subunit with biphasic functional properties. *J Neurochem*, **72**, 51-7.

- Barnard, E.A., Miledi, R. and Sumikawa, K.** (1982) Translation of exogenous messenger RNA coding for nicotinic acetylcholine receptors produces functional receptors in *Xenopus* oocytes. *Proc R Soc Lond B Biol Sci*, **215**, 241-6.
- Bässler, E.L., Ngo-Anh, T.J., Geisler, H.S., Ruppertsberg, J.P. and Gründer, S.** (2001) Molecular and functional characterization of acid-sensing ion channel (ASIC) 1b. *J Biol Chem*, **276**, 33782-7.
- Benos, D.J., Fuller, C.M., Shlyonsky, V.G., Berdiev, B.K., and Ismailov, I.I.** (1997) Amiloride-sensitive Na⁺ channels: insights and outlooks. *News Physiol Sci*, **12**, 55-61.
- Benson, C.J., Eckert, S.P. and McCleskey, E.W.** (1999) Acid-evoked currents in cardiac sensory neurons: A possible mediator of myocardial ischemic sensation. *Circ Res*, **84**, 921-8.
- Berdiev, B.K., Mapstone, T.B., Markert, J.M., Gillespie, G.Y., Lockhart, J., Fuller, C.M. and Benos, D.J.** (2001) pH alterations "reset" Ca²⁺ sensitivity of brain Na⁺ channel 2, a degenerin/epithelial Na⁺ ion channel, in planar lipid bilayers. *J Biol Chem*, **276**, 38755-61.
- Bevan, S. and Yeats, J.** (1991) Protons activate a cation conductance in a sub-population of rat dorsal root ganglion neurones. *J Physiol*, **433**, 145-61.
- Bianchi, L., Gerstbrein, B., Frokjaer-Jensen, C., Royal, D.C., Mukherjee, G., Royal, M.A., Xue, J., Schäfer, W.R. and Driscoll, M.** (2004) The neurotoxic MEC-4(d) DEG/ENaC sodium channel conducts calcium: implications for necrosis initiation. *Nat Neurosci*, **7**, 1337-44.
- Canessa, C.M., Horisberger, J.D. and Rossier, B.C.** (1993) Epithelial sodium channel related to proteins involved in neurodegeneration. *Nature*, **361**, 467-70.
- Canessa, C.M., Schild, L., Buell, G., Thorens, B., Gautschi, I., Horisberger, J.D., Rossier, B.C.** (1994) Amiloride-sensitive epithelial Na⁺ channel is made of three homologous subunits. *Nature*, **367**, 463-7.
- Carlberg, M., Mons, N., Geffard, M., Nassel, D.R.** (1989) L-DOPA and FMRFamide immunoreactivity in the tentacular nerve plexus of the sea anemone *Metridium senile*. *Comp Biochem Physiol*, **94**, 435-440.
- Carlberg, M.** (1992) Localization of dopamine in the freshwater hydrozoan *Hydra attenuata*. *Cell Tissue Res*, **270**, 601-607.
- Catarsi, S., Babinski, K. and Seguela, P.** (2001) Selective modulation of heteromeric ASIC proton-gated channels by neuropeptide FF. *Neuropharmacology*, **41**, 592-600.
- Chalfie, M and Wolinsky, E.** (1990) The identification and suppression of inherited neurodegeneration in *Caenorhabditis elegans*. *Nature*, **345**, 410-6.

- Chang, S.S., Gründer, S., Hanukoglu, A., Rosler, A., Mathew, P.M., Schild, L., Lu, Y., Shimkets, R.A., Nelson-Williams, C., Rossier, B.C., Lifton, R.P.** (1996) Mutations in subunits of the epithelial sodium channel cause salt wasting with hyperkalaemic acidosis, pseudohypoaldosteronism type 1. *Nat Genet*, **12**, 248-53.
- Chelur, D.S., Ernstrom, G.G., Goodman, M.B., Yao, C.A., Chen, L., O' Hagan, R. and Chalfie, M.** (2002) The mechanosensory protein MEC-6 is a subunit of the *C. elegans* touch-cell degenerin channel. *Nature*, **420**, 669-73.
- Chen, C.C., England, S., Akopian, A.N. and Wood, J.N.** (1998) A sensory neuron-specific, proton-gated ion channel. *Proc Natl Acad Sci U S A*, **95**, 10240-5.
- Chen, C.C., Zimmer, A., Sun, W.H., Hall, J., Brownstein, M.J. and Zimmer, A.** (2002) A role for ASIC3 in the modulation of high-intensity pain stimuli. *Proc Natl Acad Sci U S A*, **99**, 8992-7.
- Chen, X. Paukert, M., Kadurin, I., Pusch, M. and Gründer, S.** (2006) Strong modulation by RFamide neuropeptides of the ASIC1b/3 heteromer in competition with extracellular calcium. *Neuropharmacology*, **50**, 964-74.
- Chen, X. and Gründer, S.** (2007) Permeating protons contribute to tachyphylaxis of the acid-sensing ion channel (ASIC) 1a. *J Physiol*, **579**, 657-70.
- Cho, K. and McFarlane, I.D.** (1996) The anthozoan neuropeptide Antho-RWamide I modulates Ca^{2+} current in sea anemone myoepithelial cells. *Neurosci Lett*, **209**, 53-6.
- Cho, K. and McFarlane, I.D.** (1996) Physiological actions of the neuropeptide Antho-RNamide on antagonistic muscle systems in sea anemones. *Neurosci Lett*, **219**, 171-4.
- Colasanti, M., Venturini, G., Merante, A., Musci, G. and Lauro, G.M.** (1997) Nitric oxide involvement in *Hydra vulgaris* very primitive olfactory-like system. *J Neurosci*, **17**, 493-9.
- Coric, T., Zheng, D., Gerstein, M. and Canessa, C.M.** (2005) Proton sensitivity of ASIC1 appeared with the rise of fishes by changes of residues in the region that follows TM1 in the ectodomain of the channel. *J Physiol*, **568**, 725-35.
- Coscoy, S., Lingueglia, E., Lazdunski, M. and Barbry P.** (1998) The Phe-Met-Arg-Phe-amide-activated sodium channel is a tetramer. *J Biol Chem*, **273**, 8317-22.
- Cottrell, G.A., Green, K.A. and Davies, N.W.** (1990) The neuropeptide Phe-Met-Arg-Phe-NH₂ (FMRFamide) can activate a ligand-gated ion channel in *Helix* neurones. *Pflugers Arch*, **416**, 612-4.
- Cottrell, G.A.** (1997) The first peptide-gated ion channel. *J Exp Biol*, **200**, 2377-86.
- Darboux, I., Lingueglia, E., Champigny, G., Coscoy, S., Barbry, P. and Lazdunski, M.** (1998) dGNaC1, a gonad-specific amiloride-sensitive Na⁺ channel. *J Biol Chem*, **273**, 9424-9.

- Darboux, I., Lingueglia, E., Pauron, D., Barbry, P. and Lazdunski, M.** (1998) A new member of the amiloride-sensitive sodium channel family in *Drosophila melanogaster* peripheral nervous system. *Biochem Biophys Res Commun*, **246**, 210-6.
- Davey, F., Harris, S.J. and Cottrell, G.A.** (2001) Histochemical localisation of FMRamide-gated Na⁺ channels in *Helisoma trivolvis* and *Helix aspersa* neurones. *J Neurocytol*, **30**, 877-84.
- De Rosa, R., Grenier, J.K., Andreeva, T., Cook, C.E., Adoutte, A., Akam, M., Carroll, S.B. and Balavoine, G.** (1999) Hox genes in brachiopods and priapulids and protostome evolution. *Nature*, **399**, 772-6.
- De Weille, J. and Bassilana, F.** (2001) Dependence of the acid-sensitive ion channel, ASIC1a, on extracellular Ca²⁺ ions. *Brain*, **900**, 277-81.
- Deval, E., Baron, A., Lingueglia, E., Mazarguil, H., Zajac, J.M. and Lazdunski, M.** (2003) Effects of neuropeptide SF and related peptides on acid sensing ion channel 3 and sensory neuron excitability. *Neuropharmacology*, **44**, 662-71.
- Dijkink, L., Hartog, A., van Os, C.H. and Bindels, R.J.** (2002) The epithelial sodium channel (ENaC) is intracellularly located as a tetramer. *Pflugers Arch*, **444**, 549-55.
- Driscoll, M. and Chalfie, M.** (1991) The *mec-4* gene is a member of a family of *Caenorhabditis elegans* genes that can mutate to induce neuronal degeneration. *Nature*, **349**, 588-93.
- Ebihara L.** (2003) Physiology and biophysics of hemi-gap-junctional channels expressed in *Xenopus* oocytes. *Acta Physiol Scand*, **179**, 5-8.
- Emtage, L., Gu, G., Hartweg, E. and Chalfie, M.** (2004) Extracellular proteins organize the mechanosensory channel complex in *C. elegans* touch receptor neurons. *Neuron*, **44**, 795-807.
- Espinoza, E., Carrigan, M., Thomas, S.G., Shaw, G. and Edison, A.S.** (2000) A statistical view of FMRamide neuropeptide diversity. *Mol Neurobiol*, **21**, 35-56.
- Firsov, D., Gautschi, I., Merillat, A.M., Rossier, B.C. and Schild, L.** (1998) The heterotetrameric architecture of the epithelial sodium channel (ENaC). *EMBO J*, **17**, 344-52.
- Firsov, D., Robert-Nicoud, M., Gruender, S., Schild, L. and Rossier, B.C.** (1999) Mutational analysis of cysteine-rich domains of the epithelium sodium channel (ENaC). Identification of cysteines essential for channel expression at the cell surface. *J Biol Chem*, **274**, 2743-9.
- Fuller, C.M., Berdiev, B.K., Shlyonsky, V.G., Ismailov, I.I. and Benos, D.J.** (1997) Point mutations in alpha ENaC regulate channel gating, ion selectivity, and sensitivity to amiloride. *Biophys J*, **72**, 1622-32.

- Furukawa, Y., Miyawaki, Y. and Abe, G.** (2006) Molecular cloning and functional characterization of the *Aplysia* FMRFamide-gated Na⁺ channel. *Pflugers Arch*, **451**, 646-56.
- Gao, J., Duan, B., Wang, D.G., Deng, X.H., Zhang, G.Y., Xu, L. and Xu, T.L.** (2005) Coupling between NMDA receptor and acid-sensing ion channel contributes to ischemic neuronal death. *Neuron*, **48**, 635-46.
- Garcia-Anoveros, J., Derfler, B., Neville-Golden, J., Hyman, B.T. and Corey, D.P.** (1997) BNaC1 and BNaC2 constitute a new family of human neuronal sodium channels related to degenerins and epithelial sodium channels. *Proc Natl Acad Sci U S A*, **94**, 1459-64.
- Garcia-Anoveros, J., Garcia, J.A., Liu, J.D. and Corey, D.P.** (1998) The nematode degenerin UNC-105 forms ion channels that are activated by degeneration- or hypercontraction-causing mutations. *Neuron*, **20**, 1231-41.
- Gayton, R.J.** (1982) Mammalian neuronal actions of FMRFamide and the structurally related opioid Met-enkephalin-Arg6-Phe7. *Nature*, **298**, 275-6.
- Gitterman, D.P., Wilson, J. and Randall, A.D.** (2005) Functional properties and pharmacological inhibition of ASIC channels in the human SJ-RH30 skeletal muscle cell line. *J Physiol*, **562**, 759-69.
- Goldin, A.L.** (1992) Maintenance of *Xenopus laevis* and oocyte injection. *Methods Enzymol*, **207**, 266-79.
- Goodman, M.B., Ernstrom, G.G., Chelur, D.S., O'Hagan, R., Yao, C.A. and Chalfie, M.** (2002) MEC-2 regulates *C. elegans* DEG/ENaC channels needed for mechanosensation. *Nature*, **415**, 1039-42.
- Gouarderes, C., Sutak, M., Zajac, J.M. and Jhamandas, K.** (1993) Antinociceptive effects of intrathecally administered F8Famide and FMRFamide in the rat. *Eur J Pharmacol*, **237**, 73-81.
- Grantyn, R. and Lux, H.D.** (1988) Similarity and mutual exclusion of NMDA- and proton-activated transient Na⁺-currents in rat tectal neurons. *Neurosci Lett*, **89**, 198-203.
- Green, K.A., Falconer, S.W. and Cottrell, G.A.** (1994) The neuropeptide Phe-Met-Arg-Phe-NH₂ (FMRFamide) directly gates two ion channels in an identified *Helix* neurone. *Pflugers Arch*, **428**, 232-40.
- Green, K.A. and Cottrell, G.A.** (2002) Activity modes and modulation of the peptide-gated Na⁺ channel of *Helix* neurones. *Pflugers Arch*, **443**, 813-21.
- Grimmelikhuijzen, C.J., Dockray, G.J. and Schot, L.P.** (1982) FMRFamide-like immunoreactivity in the nervous system of *Hydra*. *Histochemistry*, **73**, 499-508.

- Grimmelikhuijzen, C.J.P.** (1985) Antisera to the sequence Arg-Phe-amide visualize neuronal centralization in hydroid polyps. *Cell Tissue Res*, **241**, 171-182.
- Gründer, S., Firsov, D., Chang, S.S., Jaeger, N.F., Gautschi, I., Schild, L., Lifton, R.P. and Rossier, B.C.** (1997) A mutation causing pseudohypoaldosteronism type 1 identifies a conserved glycine that is involved in the gating of the epithelial sodium channel. *EMBO J*, **16**, 899-907.
- Gründer, S., Geissler, H.S., Bässler, E.L. and Ruppertsberg, J.P.** (2000) A new member of acid-sensing ion channels from pituitary gland. *Neuroreport*, **11**, 1607-11.
- Gurdon, J.B., Lane, C.D., Woodland, H.R. and Marbaix, G.** (1971) Use of frog eggs and oocytes for the study of messenger RNA and its translation in living cells. *Nature*, **233**, 177-82.
- Hall, B.G.** (2004) *Phylogenetic Trees Made Easy*. Sinauer Associates, Inc., **2nd** edition.
- Hamill, O.P. and McBride, D.W. Jr.** (1996) The pharmacology of mechanogated membrane ion channels. *Pharmacol Rev*, **48**, 231-252.
- Hansen, G.N., Williamson, M. and Grimmelikhuijzen, C.J.** (2000) Two-color double-labeling in situ hybridization of whole-mount *Hydra* using RNA probes for five different *Hydra* neuropeptide preprohormones: evidence for colocalization. *Cell Tissue Res*, **301**, 245-53.
- Hansen, G.N., Williamson, M. and Grimmelikhuijzen, C.J.** (2002) A new case of neuropeptide coexpression (RGamide and LWamides) in *Hydra*, found by whole-mount, two-color double-labeling in situ hybridization. *Cell Tissue Res*, **308**, 157-65.
- Hansson, J.H., Nelson-Williams, C., Suzuki, H., Schild, L., Shimkets, R., Lu, Y., Canessa, C., Iwasaki, T., Rossier, B. and Lifton, R.P.** (1995) Hypertension caused by a truncated epithelial sodium channel gamma subunit: genetic heterogeneity of Liddle syndrome. *Nat Genet*, **11**, 76-82.
- Hansson, J.H., Schild, L., Lu, Y., Wilson, T.A., Gautschi, I., Shimkets, R., Nelson-Williams, C., Rossier, B.C. and Lifton, R.P.** (1995) A de novo missense mutation of the beta subunit of the epithelial sodium channel causes hypertension and Liddle syndrome, identifying a proline-rich segment critical for regulation of channel activity. *Proc Natl Acad Sci U S A*, **92**, 11495-9.
- Harris, L.L., Lesser, W. and Ono, J.K.** (1995) FMRFamide is endogenous to the *Aplysia* heart. *Cell Tissue Res*, **282**, 331-41.
- Hong, K. and Driscoll, M.** (1994) A transmembrane domain of the putative channel subunit MEC-4 influences mechanotransduction and neurodegeneration in *C. elegans*. *Nature*, **367**, 470-3.

- Huang, M. and Chalfie, M.** (1994) Gene interactions affecting mechanosensory transduction in *Caenorhabditis elegans*. *Nature*, **367**, 467-70.
- Huang, M., Gu, G., Ferguson, E.L. and Chalfie, M.** (1995) A stomatin-like protein necessary for mechanosensation in *C. elegans*. *Nature*, **378**, 292-5.
- Immke, D.C., McCleskey, E.W.** (2001) Lactate enhances the acid-sensing Na⁺ channel on ischemia-sensing neurons. *Nat Neurosci*, **4**, 869-70.
- Immke, D.C., McCleskey, E.W.** (2003) Protons open acid-sensing ion channels by catalyzing relief of Ca²⁺ blockade. *Neuron*, **37**, 75-84.
- Immke, D.C., McCleskey, E.W.** (2003) ASIC3: a lactic acid sensor for cardiac pain. *Scientific World Journal*, **1**, 510-2.
- Inoue, T., Okauchi, Y., Matsuzaki, Y., Kuwajima, K., Kondo, H., Horiuchi, N., Nakao, K., Iwata, M., Yokogoshi, Y., Shintani, Y., Bando, H. and Saito, S.** (1998) Identification of a single cytosine base insertion mutation at Arg-597 of the beta subunit of the human epithelial sodium channel in a family with Liddle's disease. *Eur J Endocrinol*, **138**, 691-7.
- Ishibashi, K. and Marumo, F.** (1998) Molecular cloning of a DEG/ENaC sodium channel cDNA from human testis. *Biochem Biophys Res Commun*, **245**, 589-93.
- Iwasaki, K., Liu, D.W. and Thomas, J.H.** (1995) Genes that control a temperature-compensated ultradian clock in *Caenorhabditis elegans*. *Proc Natl Acad Sci U S A*, **92**, 10317-21.
- Jahr, H., van Driel, M., van Osch, G.J., Weinans, H. and van Leeuwen, J.P.** (2005) Identification of acid-sensing ion channels in bone. *Biochem Biophys Res Commun*, **337**, 349-54.
- Jeziorski, M.C., Green, K.A., Sommerville, J. and Cottrell, G.A.** (2000) Cloning and expression of a FMRamide-gated Na⁺ channel from *Helisoma trivolvis* and comparison with the native neuronal channel. *J Physiol*, **526**, 13-25.
- Ji, H.L. and Benos, D.J.** (2004) Degenerin sites mediate proton activation of deltatetagamma-epithelial sodium channel. *J Biol Chem*, **279**, 26939-47.
- Jones, N.G., Slater, R., Cadiou, H., McNaughton, P. and McMahon, S.B.** (2004) Acid-induced pain and its modulation in humans. *J Neurosci*, **24**, 10974-9.
- Jones, R.C. 3rd, Xu, L. and Gebhart, G.F.** (2005) The mechanosensitivity of mouse colon afferent fibers and their sensitization by inflammatory mediators require transient receptor potential vanilloid 1 and acid-sensing ion channel 3. *J Neurosci*, **25**, 10981-9
- Kass-Simon, G. and Pierobon, P.** (2007) Cnidarian chemical neurotransmission, an updated overview. *Comp Biochem Physiol A Mol Integr Physiol*, **146**, 9-25.

- Katsura, I., Kondo, K., Amano, T., Ishihara, T. and Kawakami, M.** (1994) Isolation, characterization and epistasis of fluoride-resistant mutants of *Caenorhabditis elegans*. *Genetics*, **136**, 145-54.
- Kavaliers, M. and Hirst, M.** (1985) The influence of opiate agonists on day-night feeding rhythms in young and old mice. *Brain Res*, **326**, 160-7.
- Kavaliers, M.** (1987) Calcium channel blockers inhibit the antagonistic effects of Phe-Met-Arg-Phe-amide (FMRFamide) on morphine- and stress-induced analgesia in mice. *Brain Res*, **415**, 380-4.
- Kellenberger, S., Gautschi, I., Rossier, B.C. and Schild, L.** (1998) Mutations causing Liddle syndrome reduce sodium-dependent downregulation of the epithelial sodium channel in the *Xenopus* oocyte expression system. *J Clin Invest*, **101**, 2741-50.
- Kellenberger, S., Gautschi, I. and Schild, L.** (1999) A single point mutation in the pore region of the epithelial Na⁺ channel changes ion selectivity by modifying molecular sieving. *Proc Natl Acad Sci U S A*, **96**, 170-5.
- Kellenberger, S., Auberson, M., Gautschi, I., Schneeberger, E. and Schild L.** (2001) Permeability properties of ENaC selectivity filter mutants. *J Gen Physiol*, **118**, 679-92.
- Kellenberger, S. and Schild, L.** (2002) Epithelial sodium channel/degenerin family of ion channels: a variety of functions for a shared structure. *Physiol Rev*, **82**, 735-67.
- Kellenberger, S., Gautschi, I. and Schild, L.** (2003) Mutations in the epithelial Na⁺ channel ENaC outer pore disrupt amiloride block by increasing its dissociation rate. *Mol Pharmacol*, **64**, 848-56.
- Koizumi, O., Wilson, J.D., Grimmelikhuijzen, C.J., and Westfall, J.A.** (1989) Ultrastructural localization of RFamide-like peptides in neuronal dense-cored vesicles in the peduncle of *Hydra*. *J Exp Zool*, **249**, 17-22.
- Kortschak, R.D., Samuel, G., Saint, R. and Miller, D.J.** (2003) EST analysis of the cnidarian *Acropora millepora* reveals extensive gene loss and rapid sequence divergence in the model invertebrates. *Curr Biol*, **13**, 2190-5.
- Kosari, F., Sheng, S., Li, J., Mak, D.O., Foskett, J.K. and Kleyman, T.R.** (1998) Subunit stoichiometry of the epithelial sodium channel. *J Biol Chem*, **273**, 13469-74.
- Krishtal, O.A., and Pidoplichko, V.I.** (1981) A receptor for protons in the membrane of sensory neurons may participate in nociception. *Neuroscience*, **6**, 2599-601.
- Lentz, T.L. and Barnett, R.J.** (1961) Enzyme histochemistry of *Hydra*. *J Exp Zool*, **147**, 125-49.
- Lentz, T.L. and Barnett, R.J.** (1962) Changes in the distribution of enzyme activity in the regenerating *Hydra*. *J Exp Zool*, **150**, 103-17.

- Lentz, T.L. and Barnett, R.J.** (1963) The role of the nervous system in regenerating *Hydra*: the effect of neuropharmacological agents. *J Exp Zool*, **154**, 305-27.
- Lentz, T.L.** (1966) Intramitochondrial glycogen granules in digestive cells of *Hydra*. *J Cell Biol*, **29**, 162-7.
- Lifton, R.P.** (1995) Genetic determinants of human hypertension. *Proc Natl Acad Sci U S A*, **92**, 8545-51
- Lingueglia, E., Champigny, G., Lazdunski, M. and Barbry, P.** (1995) Cloning of the amiloride-sensitive FMRFamide peptide-gated sodium channel. *Nature*, **378**, 730-3.
- Lingueglia, E., de Weille, J.R., Bassilana, F., Heurteaux, C., Sakai, H., Waldmann, R. and Lazdunski, M.** (1997) A modulatory subunit of acid sensing ion channels in brain and dorsal root ganglion cells. *J Biol Chem*, **272**, 29778-83.
- Lingueglia, E., Deval, E. and Lazdunski, M.** (2006) FMRFamide-gated sodium channel and ASIC channels: a new class of ionotropic receptors for FMRFamide and related peptides. *Peptides*, **27**, 1138-52.
- Liu, J., Schrank, B. and Waterston, R.H.** (1996) Interaction between a putative mechanosensory membrane channel and a collagen. *Science*, **273**, 361-4.
- Liu, L., Johnson, W.A. and Welsh, M.J.** (2003) *Drosophila* DEG/ENaC pickpocket genes are expressed in the tracheal system, where they may be involved in liquid clearance. *Proc Natl Acad Sci U S A*, **100**, 2128-33.
- Liu, L., Leonard, A.S., Motto, D.G., Feller, M.A., Price, M.P., Johnson, W.A. and Welsh, M.J.** (2003) Contribution of *Drosophila* DEG/ENaC genes to salt taste. *Neuron*, **39**, 133-46.
- Madeja, M., Musshoff, U. and Speckmann, E.J.** (1995) Improvement and testing of a concentration-clamp system for oocytes of *Xenopus laevis*. *Journal of Neuroscience Methods*, **63**, 211-213.
- Mano, I. and Driscoll, M.** (1999) DEG/ENaC channels: a touchy superfamily that watches its salt. *Bioessays*, **21**, 568-78.
- McFarlane, I.D., Graff, D. and Grimmelikhuijzen, C.J.P.** (1987) Excitatory actions of Antho-RWamide, an anthozoan neuropeptide, on muscle and conducting systems in the sea anemone *Calliactis parasitica*. *J Exp Biol*, **133**, 157-168.
- McFarlane, I.D., Anderson, P.A. and Grimmelikhuijzen, C.J.P.** (1991) Effects of three anthozoan neuropeptides, Antho-RWamide I, Antho-RWamide II and Antho-RFamide, on slow muscles from sea anemones. *J Exp Biol*, **156**, 419-31.
- McFarlane, I.D. and Grimmelikhuijzen, C.J.P.** (1991) Three anthozoan neuropeptides, Antho-RFamide and Antho-RWamides I and II, modulate spontaneous tentacle contractions in sea anemones. *J Exp Biol*, **155**, 669-673.

- McFarlane, I.D., Reinscheid, R.K. and Grimmelikhuijzen, C.J.P.** (1992) Opposite actions of the anthozoan neuropeptide Antho-RNamide on antagonistic muscle groups in sea anemones. *J Exp Biol*, **164**, 295-299.
- McFarlane, I.D., Hudman, D., Nothacker, H.P. and Grimmelikhuijzen, C.J.P.** (1993) The expansion behaviour of sea anemones may be coordinated by two inhibitory neuropeptides, Antho-KAamide and Antho-RIamide. *Proc Biol Sci*, **253**, 183-8.
- Michelsen, K., Yuan, H. and Schwappach, B.** (2005) Hide and run. Arginine-based endoplasmic-reticulum-sorting motifs in the assembly of heteromultimeric membrane proteins. *EMBO Rep*, **6**, 717-22.
- Moroz, L.L., Meech, R.W., Sweedler, J.V. and Mackie, G.O.** (2004) Nitric oxide regulates swimming in the jellyfish *Aglantha digitale*. *J Comp Neurol*, **471**, 26-36.
- Neaga, E., Amuzescu, B., Dinu, C., Macri, B., Pena, F. and Flonta, M.L.** (2005) Extracellular trypsin increases ASIC1a selectivity for monovalent versus divalent cations. *J Neurosci Methods*, **144**, 241-8.
- Nilsson, T., Jackson, M. and Peterson, P.A.** (1989) Short cytoplasmic sequences serve as retention signals for transmembrane proteins in the endoplasmic reticulum. *Cell*, **58**, 707-18.
- Page, A.J., Brierley, S.M., Martin, C.M., Martinez-Salgado, C., Wemmie, J.A., Brennan, T.J., Symonds, E., Lewin, G.R., Welsh, M.J. and Blackshaw, L.A.** (2004) The ion channel ASIC1 contributes to visceral but not cutaneous mechanoreceptor function. *Gastroenterology*, **127**, 1739-47.
- Page, A.J., Brierley, S.M., Martin, C.M., Price, M.P., Symonds, E., Butler, R., Wemmie, J.A. and Blackshaw, L.A.** (2005) Different contributions of ASIC channels 1a, 2, and 3 in gastrointestinal mechanosensory function. *Gut*, **54**, 1408-15.
- Palmer, L.G.** (1982) Ion selectivity of the apical membrane Na channel in the toad urinary bladder. *J Membr Biol*, **67**, 91-98.
- Park, E.C. and Horvitz, H.R.** (1986) *C. elegans* unc-105 mutations affect muscle and are suppressed by other mutations that affect muscle. *Genetics*, **113**, 853-67.
- Paukert, M., Babini, E., Pusch, M. and Gründer, S.** (2004) Identification of the Ca²⁺ blocking site of acid-sensing ion channel (ASIC) 1: implications for channel gating. *J Gen Physiol*, **124**, 383-94.
- Pelegrin, P. and Surprenant, A.** (2006) Pannexin-1 mediates large pore formation and interleukin-1beta release by the ATP-gated P2X7 receptor. *EMBO J*, **25**, 5071-82.
- Perry, S.J., Straub, V.A., Schofield, M.G., Burke, J.F. and Benjamin, P.R.** (2001) Neuronal expression of an FMRFamide-gated Na⁺ channel and its modulation by acid pH. *J Neurosci*, **21**, 5559-67.

- Pierobon, P., Kemali, M. and Milici, N.** (1989) Substance P and *Hydra*: an immunohistochemical and physiological study. *Comp Biochem Physiol C*, **92**, 217-21.
- Price, D.A. and Greenberg, M.J.** (1977) Structure of a molluscan cardioexcitatory neuropeptide. *Science*, **197**, 670-671.
- Price, M.P., Snyder, P.M. and Welsh, M.J.** (1996) Cloning and expression of a novel human brain Na⁺ channel. *J Biol Chem*, **271**, 7879-82.
- Price, M.P., Lewin, G.R., McIlwrath, S.L., Cheng, C., Xie, J., Heppenstall, P.A., Mannsfeldt, A.G., Brennan, T.J., Drummond, H.A., Qiao, J., Benson, C.J., Tarr, D.E., Hrstka, R.F., Yang, B., Williamson, R.A. and Welsh, M.J.** (2000) The mammalian sodium channel BNC1 is required for normal touch sensation. *Nature*, **407**, 1007-11.
- Price, M.P., McIlwrath, S.L., Xie, J., Cheng, C., Qiao, J., Tarr, D.E., Sluka, K.A., Brennan, T.J., Lewin, G.R. and Welsh, M.J.** (2001) The DRASIC cation channel contributes to the detection of cutaneous touch and acid stimuli in mice. *Neuron*, **32**, 1071-83.
- Raffa, R.B., Heyman, J. and Porreca, F.** (1986) Intrathecal FMRFamide (Phe-Met-Arg-Phe-NH₂) induces excessive grooming behavior in mice. *Neurosci Lett*, **65**, 94-8.
- Raffa, R.B.** (1988) The action of FMRFamide (Phe-Met-Arg-Phe-NH₂) and related peptides on mammals. *Peptides*, **9**, 915-22.
- Raffa, R.B.** (1988) Supraspinal FMRFamide antagonizes morphine-induced horizontal, but not vertical, locomotor activity. *Peptides*, **10**, 403-6.
- Ripps, H., Qian, H. and Zakevicius, J.** (2002) Pharmacological enhancement of hemigap-junctional currents in *Xenopus* oocytes. *J Neurosci Methods*, **121**, 81-92.
- Ripps, H., Qian, H. and Zakevicius, J.** (2004) Properties of connexin26 hemichannels expressed in *Xenopus* oocytes. *Cell Mol Neurobiol*, **24**, 647-65.
- Roumy, M. and Zajac, J.M.** (1998) Neuropeptide FF, pain and analgesia. *Eur J Pharmacol*, **345**, 1-11.
- Sakai, H., Lingueglia, E., Champigny, G., Mattei, M.G. and Lazdunski, M.** (1999) Cloning and functional expression of a novel degenerin-like Na⁺ channel gene in mammals. *J Physiol*, **519**, 323-33.
- Salleo, A., Musci, G., Barra, P. and Calabrese, L.** (1996) The discharge mechanism of acontial nematocytes involves the release of nitric oxide. *J Exp Biol*, **199**, 1261-7.
- Sanetra, M., Begemann, G., Becker, M.B. and Meyer, A.** (2005) Conservation and co-option in developmental programmes: the importance of homology relationships. *Front Zool*, 2-15.

- Schaefer, L., Sakai, H., Mattei, M., Lazdunski, M. and Lingueglia, E.** (2000) Molecular cloning, functional expression and chromosomal localization of an amiloride-sensitive Na⁺ channel from human small intestine. *FEBS Lett*, **471**, 205-10.
- Schild L.** (1996) The ENaC channel as the primary determinant of two human diseases: Liddle syndrome and pseudohypoaldosteronism. *Nephrologie*, **17**, 395-400.
- Schild, L., Schneeberger, E., Gautschi, I. and Firsov, D.** (1997) Identification of amino acid residues in the alpha, beta, and gamma subunits of the epithelial sodium channel (ENaC) involved in amiloride block and ion permeation. *J Gen Physiol*, **109**, 15-26.
- Schultheiss, M., Neumcke, B. and Richter, H.P.** (1997) Endogenous trypsin receptors in *Xenopus* oocytes: linkage to internal calcium stores. *Cell Mol Life Sci*, **53**, 842-9.
- Schutze, M.P., Peterson, P.A. and Jackson, M.R.** (1994) An N-terminal double-arginine motif maintains type II membrane proteins in the endoplasmic reticulum. *EMBO J*, **13**, 1696-705.
- Sheng, S., Li, J., McNulty, K.A., Avery, D. and Kleyman, T.R.** (2000) Characterization of the selectivity filter of the epithelial sodium channel. *J Biol Chem*, **275**, 8572-81.
- Singer, R.H.** (1964) The effect of neuropharmacological drugs on the light response of *Hydra pirardi*. *Anat Rec*, **148**, 402-403.
- Snyder, P.M., Cheng, C., Prince, L.S., Rogers, J.C. and Welsh, M.J.** (1998) Electrophysiological and biochemical evidence that DEG/ENaC cation channels are composed of nine subunits. *J Biol Chem*, **273**, 681-4.
- Snyder, P.M., Olson, D.R. and Bucher, D.B.** (1999) A pore segment in DEG/ENaC Na⁺ channels. *J Biol Chem*, **274**, 28484-90.
- Spencer, A.N.** (1991) Peptides in the Hydrozoa: are they transmitters? *Hydrobiologia*, **216/217**, 565-571.
- Storch, V. and Welsch, U.** (1996) *Kükenthal: Zoologisches Praktikum*. Gustav Fischer Verlag, **22**. Aufl.
- Stühmer, W.** (1998) Electrophysiologic recordings from *Xenopus* oocytes. *Methods Enzymol*, **293**, 280-300.
- Sutherland, S.P., Cook, S.P. and McCleskey, E.W.** (2000) Chemical mediators of pain due to tissue damage and ischemia. *Prog Brain Res*, **129**, 21-38.
- Sutherland, S.P., Benson, C.J., Adelman, J.P. and McCleskey, E.W.** (2001) Acid-sensing ion channel 3 matches the acid-gated current in cardiac ischemia-sensing neurons. *Proc Natl Acad Sci USA*, **98**, 711-716.

- Syntichaki, P. and Tavernarakis, N.** (2004) Genetic models of mechanotransduction: the nematode *Caenorhabditis elegans*. *Physiol Rev*, **84**, 1097-153.
- Take-Uchi, M., Kawakami, M., Ishihara, T., Amano, T., Kondo, K. and Katsura, I.** (1998) An ion channel of the degenerin/epithelial sodium channel superfamily controls the defecation rhythm in *Caenorhabditis elegans*. *Proc Natl Acad Sci U S A*, **95**, 11775-80.
- Tavernarakis, N., Shreffler, W., Wang, S. and Driscoll, M.** (1997) *unc-8*, a DEG/ENaC family member, encodes a subunit of a candidate mechanically gated channel that modulates *C. elegans* locomotion. *Neuron*, **18**, 107-19.
- Tavernarakis, N. and Driscoll, M.** (1997) Molecular modeling of mechanotransduction in the nematode *Caenorhabditis elegans*. *Annu Rev Physiol*, **59**, 659-89.
- Tavernarakis, N. and Driscoll, M.** (1997) Degenerins. At the core of the metazoan mechanotransducer? *Ann N Y Acad Sci*, **940**, 28-41.
- Teasdale, R.D. and Jackson, M.R.** (1996) Signal-mediated sorting of membrane proteins between the endoplasmic reticulum and the golgi apparatus. *Annu Rev Cell Dev Biol*, **12**, 27-54.
- Ugawa, S., Ueda, T., Ishida, Y., Nishigaki, M., Shibata, Y., Shimada, S.** (2002) Amiloride-blockable acid-sensing ion channels are leading acid sensors expressed in human nociceptors. *J Clin Invest*, **110**, 1185-90.
- Varming, T.** (1999) Proton-gated ion channels in cultured mouse cortical neurons. *Neuropharmacology*, **38**, 1875-81.
- Waldmann, R., Champigny, G., Voilley, N., Lauritzen, I. and Lazdunski, M.** (1996) The mammalian degenerin MDEG, an amiloride-sensitive cation channel activated by mutations causing neurodegeneration in *Caenorhabditis elegans*. *J Biol Chem*, **271**, 10433-6.
- Waldmann, R., Champigny, G., Bassilana, F., Heurteaux, C. and Lazdunski, M.** (1997) A proton-gated cation channel involved in acid-sensing. *Nature*, **386**, 173-7.
- Waldmann, R. and Lazdunski, M.** (1998) H⁺-gated cation channels: neuronal acid sensors in the NaC/DEG family of ion channels. *Curr Opin Neurobiol*, **8**, 418-24.
- Wemmie, J.A., Askwith, C.C., Lamani, E., Cassell, M.D., Freeman, J.H. Jr. and Welsh, M.J.** (2003) Acid-sensing ion channel 1 is localized in brain regions with high synaptic density and contributes to fear conditioning. *J Neurosci*, **23**, 5496-502.
- Wemmie, J.A., Chen, J., Askwith, C.C., Hruska-Hageman, A.M., Price, M.P., Nolan, B.C., Yoder, P.G., Lamani, E., Hoshi, T., Freeman, J.H. Jr. and Welsh, M.J.** (2002) The acid-activated ion channel ASIC contributes to synaptic plasticity, learning, and memory. *Neuron*, **34**, 463-77.

- Westfall, J.A.** (1970) Ultrastructure of synapses in a primitive coelenterate. *J Ultrastruct Res*, **32**, 237-46.
- Westfall, J.A., Yamataka, S. and Enos, P.D.** (1971) Ultrastructural evidence of polarized synapses in the nerve net of *Hydra*. *J Cell Biol*, **51**, 318-23.
- Westfall, J.A.** (1973) Ultrastructural evidence for a granule-containing sensory-motor-interneuron in *Hydra littoralis*. *J Ultrastruct Res*, **42**, 268-82.
- Westfall, J.A. and Grimmelikhuijzen, C.J.P.** (1993) Antho-RFamide immunoreactivity in neuronal synaptic and nonsynaptic vesicles of sea anemones. *Biol Bull*, **185**, 109-114.
- Westfall, J.A., Sayyar, K.L., Elliott, C.F., Grimmelikhuijzen, C.J.P.** (1995) Ultrastructural localization of Antho-RWamides I and II at neuromuscular synapses in the gastrodermis and oral sphincter muscle of the sea anemone *Calliactis parasitica*. *Biol Bull*, **189**, 280-287.
- Westfall, J.A., Elliott, S.R., MonhanKumar, P.S and Carlin, R.W.** (2000) Immunocytochemical evidence for biogenic amines and immunogold labeling of serotonergic synapses in tentacles of *Aiptasia pallida* (Cnidaria, Anthozoa). *Invert Biol*, **119**, 370-378.
- Wetzel, C., Hu, J., Riethmacher, D., Benckendorff, A., Harder, L., Eilers, A., Moshourab, R., Kozlenkov, A., Labuz, D., Caspani, O., Erdmann, B., Machelkska, H., Heppenstall, P.A. and Lewin, G.R.** (2006) A stomatin-domain protein essential for touch sensation in the mouse. *Nature*, **445**, 206-9.
- Wood, J.G.** (1963) Identification of and observations on epinephrine and norepinephrine containing cells in the adrenal medulla. *Am J Anat*, **112**, 285-303.
- Wood, J.G. and Lentz, T.L.** (1964) Histochemical localization of amines in *Hydra* and the sea anemone. *Nature*, **201**, 88-90.
- Wood, J.G. and Barnett, R.J.** (1965) Histochemical demonstration of norepinephrine at a fine structural level. *J Histochem*, **12**, 197-209.
- Xie, J., Price, M.P., Wemmie, J.A., Askwith, C.C. and Welsh, M.J.** (2003) ASIC3 and ASIC1 mediate FMRamide-related peptide enhancement of H⁺-gated currents in cultured dorsal root ganglion neurons. *J Neurophysiol*, **89**, 2459-65.
- Xiong, Z.G., Zhu, X.M., Chu, X.P., Minami, M., Hey, J., Wie, W.L., MacDonald, J.F., Wemmie, J.A., Price, M.P., Welsh, M.J. and Simon, R.P.** (2004) Neuroprotection in ischemia: blocking calcium-permeable acid-sensing ion channels. *Cell*, **118**, 687-98.
- Yagi, J., Wenk, H.N., Naves, L.A. and McCleskey, E.W.** (2006) Sustained currents through ASIC3 ion channels at the modest pH changes that occur during myocardial ischemia. *Circ Res*, **99**, 501-9.

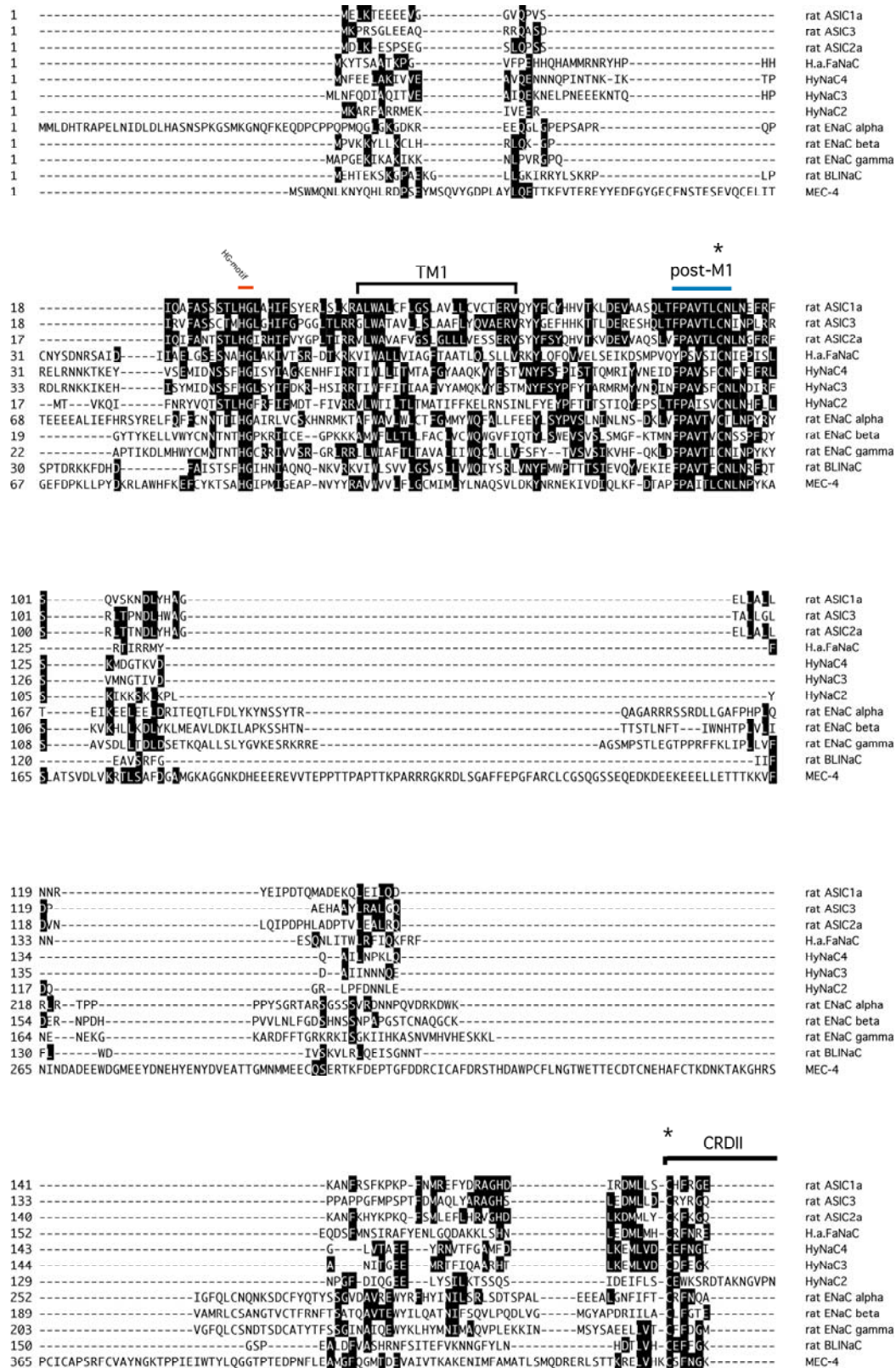
Yamamura, H., Ugawa, S., Ueda, T., Nagao, M. and Shimada, S. (2004) Protons activate the delta-subunit of the epithelial Na⁺ channel in humans. *J Biol Chem*, **279**, 12529-34.

Zhainazarov, A.B. and Cottrell, G.A. (1998) Single-channel currents of a peptide-gated sodium channel expressed in *Xenopus* oocytes. *J Physiol*, **513**, 19-31.

Zhang, P. and Canessa, C.M. (2001) Single-channel properties of recombinant acid-sensitive ion channels formed by the subunits ASIC2 and ASIC3 from dorsal root ganglion neurons expressed in *Xenopus* oocytes. *J Gen Physiol*, **117**, 563-72.

Zhang, P. and Canessa, C.M. (2002) Single channel properties of rat acid-sensitive ion channel-1alpha, -2a, and -3 expressed in *Xenopus* oocytes. *J Gen Physiol*, **120**, 553-66.

VI. APPENDIX



Appendix 1: Complete alignment of HyNaC2-4 together with selected members of the DEG/ENaC ion channel superfamily. Identical amino acids are shown in white letters on black ground. Important conserved regions are labeled. TM 1 and 2 stand for transmembrane domain 1 and 2, respectively. CRD is an abbreviation for cysteine rich domain. Conserved cysteines (C) are labeled with an asterisk, for conserved cysteine residues not present in HyNaCs the asterisk is in red color, blue asterisks indicate conservatively substituted cysteines in HyNaCs.

(The alignment is continued on the next page.)

* CRDII *

```

178 ACSAE--KAVFTRVQ-KCYTFNSQDGRRLKTKGGTGNGLIEMLDVQOQY---LPV---WGTEDTTSEAGLVDIHSQDEPPFDLGFQVA
171 PGCPEN--FTVIFTRM-QCYTFNSQHGAEELLTPKGAANGLEIMLDVQOQY---LPI---WKDMEITPFEVGIHVQIHSQDEPPFDLGFQVA
177 EGHQD--FTVIFTRVQ-KCYTFNSQDGRPLLTIVKGGTGNGLIEMLDVQOQY---LPI---WGTEITTEAGVVDIHSQDEPPFDLGFQVA
191 LHVSN--FSTFDGMI--NCFNFSGQ--RLQMH--ATSPENGLSITFSVEKDDP---LPGTYGVYFNDNHLHSAGRVWVAPGSMSPVVDHGDIP
174 PCSDEN--FTMFSWQBERCFNFSQKFPHKLLKVGAGINRSRLTINVIHYSY---Y---KDEMDAIIHMVHGDDTP-LKMRGPTLS
175 KSYEN--FTESWQBERCFNFSQKPPHTLLKVGAGINRSRLTINVIHYSY---Y---RDKMDAGIHLILHGDDTP-VKMRGHLIP
172 PGCPNN--FTVYSGLYQOQCYTFNPGVSGYLLLSLSTGVNMGKLELDLQSKDS---L---OGIQTGALIVIHGDDTP-VLQAGFVVS
316 PNQAN--YSKFHHPMYG-NCYTFNPKNN-SNVMSSMPVNVNGLSITLRTQNDP---TP---LSTVIGARVWVHGDEPAPVDDGGFNLR
253 CSHRN--FTPIYDPYG-NCYTFNPKMT-EKALPSANPRTFGLKLLDITQOEDY---VP---FASTAGARMLHRTYPFREEQIYAM
267 SCDARN--FTLHHPMYG-NCYTFNPKSN-ATLISAGSEYGLDVLLYINEDEY---NP---FVSSITGAKVTHQDNEPPEIDVQHELE
191 TDDKD--KHMVTRVQ-NCFNFSYGE--NVQSNKVSVSRGLKLLDVIHDEFTDNPVYG---FADAGVIFVHSPKKEPFDLGFQSSP
456 ADIEADFLTIDPAF--SCFTFNHR--TVNLTISRAQPMYGLRMLVYNASDY---MPT---TEATGVRLLTHKEDFPDFGFYSIP

```

rat ASIC1a
rat ASIC3
rat ASIC2a
H.a.FaNaC
HyNaC4
HyNaC3
HyNaC2
rat ENaC alpha
rat ENaC beta
rat ENaC gamma
rat BLiNaC
MEC-4

* CRDIII * * * *

```

267 PGFQT VSCQDQKLYLPSPIGTENAVIMSDFFD-----SYSLIACRIDETRYLVENNORM--VHMPG--DAPYCTPEQYK---
260 PGFQT VSCQDQDLSFPPWGDNTASLDPDFPEPSDPLGSPRPRPSPYSLIGRLAESRYVARKCGGRM--MHMPG--NSVCSPOQYK---
266 PGFQT VATEQDRITYLPPWGERSRSEMGDFEP-----VYSIACRIDETRYLIVENNORM--VHMPG--DAPYCTPEQYK---
281 PGYSSVGLKAILHTRPYPYGNITDMLNGKQYK-----YIFFACLQLEKRLIQRGCKSSALPEVPSYNATFCVTKWQIENR
256 PGFTIYIQLEKMIINLEAPYKTKGSKKYDF-----SYSLDTEIQLTDHHSVAKCKD--FFVPG--DIPICSLDAMS
257 PGFTSYIQIEKTIENLEAPYKTKGSSVEKYDF-----SYSMHITQLEQLTDHHSVAKCKD--VFPVPG--DIPICSLDAMN
254 PGFQT VWEIKVQTEMLPPYATKGGSKPKNYQ-----ITRQSSCFLEQLGDIETKCKCS--SPVAGR--NIPYCSLROIVT---
399 PGVETISMRKEALDLSGGNYGDCETENGSDVPVKNLY-----PSKYIDVGLHSCFQENMIKCGGAYIFYPKPK--GVFECDYRQSS
336 AGTETSIGMLDKLQKGEPSPTMNGSDVAIQNLYSDY-----NTTYSIACLHSCFDHMIHNSGHYLYPLPA--GEKYCNDRFPD---
350 TAMSTIGMLHTESEKSEPSYQCTEDGSDVPVTNLY-----NAAYSLOQCLYSCFQTKMVEKCGGAQYSQPLPP--AAVNCYQDHPN---
275 VHMARVTIROLNTHOEPYGEINPDIKLRNFT-----YTYGLCKEKAKHQRLLGGLP--FLLPG--NGVECSLKYNN
538 TQVYSFGRLRMSRIPAPYGDQVDFGKTSIYYSN-----YEYSVEGYSRQFQLLKEKRGDPRFVPE--NARHDAADPIARK--

```

rat ASIC1a
rat ASIC3
rat ASIC2a
H.a.FaNaC
HyNaC4
HyNaC3
HyNaC2
rat ENaC alpha
rat ENaC beta
rat ENaC gamma
rat BLiNaC
MEC-4

CRDIII * * *

```

343 -CAFPALDELVEKDEY-----CVCEMPCNLTTRNKELSVWITP-----
352 -CASPALDAMLKDDT-----CVCPNCAITRNKELSWRITP-----
342 -CAFPALGLLAEKDSNY-----CARTPCNLTTRNKELSVWITP-----
365 NHSNEDHQSEEDRAFIPTPYLAEEREQKLNLDNDRTY---ELSGEIPDCSEISYLSVLSYMPLEFYQLSAVERFFKQERQAGQNHFMKTAYEYLEK
331 -CMWPEWARLDQLKMQ-----NCPVQVIDSYKLSLSRALFP-----
332 -CMWQWETDQLKTY-----HCPVQVIDSYVAVLSRALFP-----
330 -CLMPTIYDPRKFINN-----NCPVDETIQVLSLSVAFIT-----
481 -WGYQYKLGQASLSDS-----CFSKRKECNSVINKLSAGYSRWP-----
421 -WAYYLSLQMSWORET-----CLSMKESNDIQKWTISMDADP-----
432 -WMYQYQLYQAFVREE-----CQSYKQKQSSFKEWITLTSADMP-----
350 -CVSPHLDHTEKRGCTMGTNHSSEVPCSEEETPATIAYSTFP-----
621 -SLDARMNDLG-GH--GSFRERDOPCRQSIQSVTYSPAKWP-----

```

rat ASIC1a
rat ASIC3
rat ASIC2a
H.a.FaNaC
HyNaC4
HyNaC3
HyNaC2
rat ENaC alpha
rat ENaC beta
rat ENaC gamma
rat BLiNaC
MEC-4

pre-TM2 TM2

```

381 -KASAKYLAKRFNKS-----DYTGSENLVLDIIFEMLYNETIEQKAYEITAGLDGIGGQGLGFIGASLITVLEFDY----Y
388 -BRASARYLAKRYNRS-----EYITENYVLDIIFEMLYNAYEAVQKAYEYSELDGIGGQGLGFIGASLITVLEFDY----Y
380 -KTSARYLAKRFNKS-----EYITSENLVLDIIFEMLYNETIEQKAYEVAALDGIIGGQGLGFIGASLITVLEFDY----C
462 LAHPSDHLARNDHMDILSKSYSLSEKEMAKEASDLRQNRNRYLFDLSDVVEYRQPAYGLADFADGGTGLMMGTSVLTIVETV----F
367 -PQYQDSINSDQPHIINSIKNISD---K--VQFARDNLRVYIYDLSYELIEQKPSYDITLVMLGDVGGQGLGFIGASMSYFEFDCL---A
368 -TARYASSANEARKHQHVAMNLSKNTD---E--LAFMRENLLRVIYIYDLSYELIEQKPNYDITLVMLGDVGGQGLGFIGASMSYFEFDCL---A
366 -SN--VTYSSNAEESYIRKLNKSMSP---KKLQSYTENIVAVQFYDEMCKRQKQEPSYDFYKLTEDVGGQGLGLTASVLTLEVFDFL---I
523 -SVLSQDWIFEMSLQNN--Y-----TINNARN--GVAKNIEFKELNYITNSESPTVMVSLSNLGGQSLWFGSSVLSVVEAEITFDLL
462 -SEASDWLHVSDQRD--Q-----SSNITLRSKGLVKNIYFOEYNYITLESANVWVLLSNLGGQGLWFGSSVLSVVEAEITFDLL
474 -SEASDWLHVSDQDS--Q-----QINKLNKTDIAKLTIFYDLNRSIMESPAANSIEMLSNFGGQGLWMSCSVVCVIEITVEVFFIDFF
393 -QRATKFAKLN-----QSQEYIRENLVIEINYSNLNYKITQDKAVSVEPLADVGGQGLGFIGASLITVLEFDY----F
660 -SLSLQIQVGCNGTA-----VECNHYKENAMVEVEYEQLNFMLTSESAVGFVNLADVFGGQGLWFIGASLITVCEVFF----L

```

rat ASIC1a
rat ASIC3
rat ASIC2a
H.a.FaNaC
HyNaC4
HyNaC3
HyNaC2
rat ENaC alpha
rat ENaC beta
rat ENaC gamma
rat BLiNaC
MEC-4

TM2

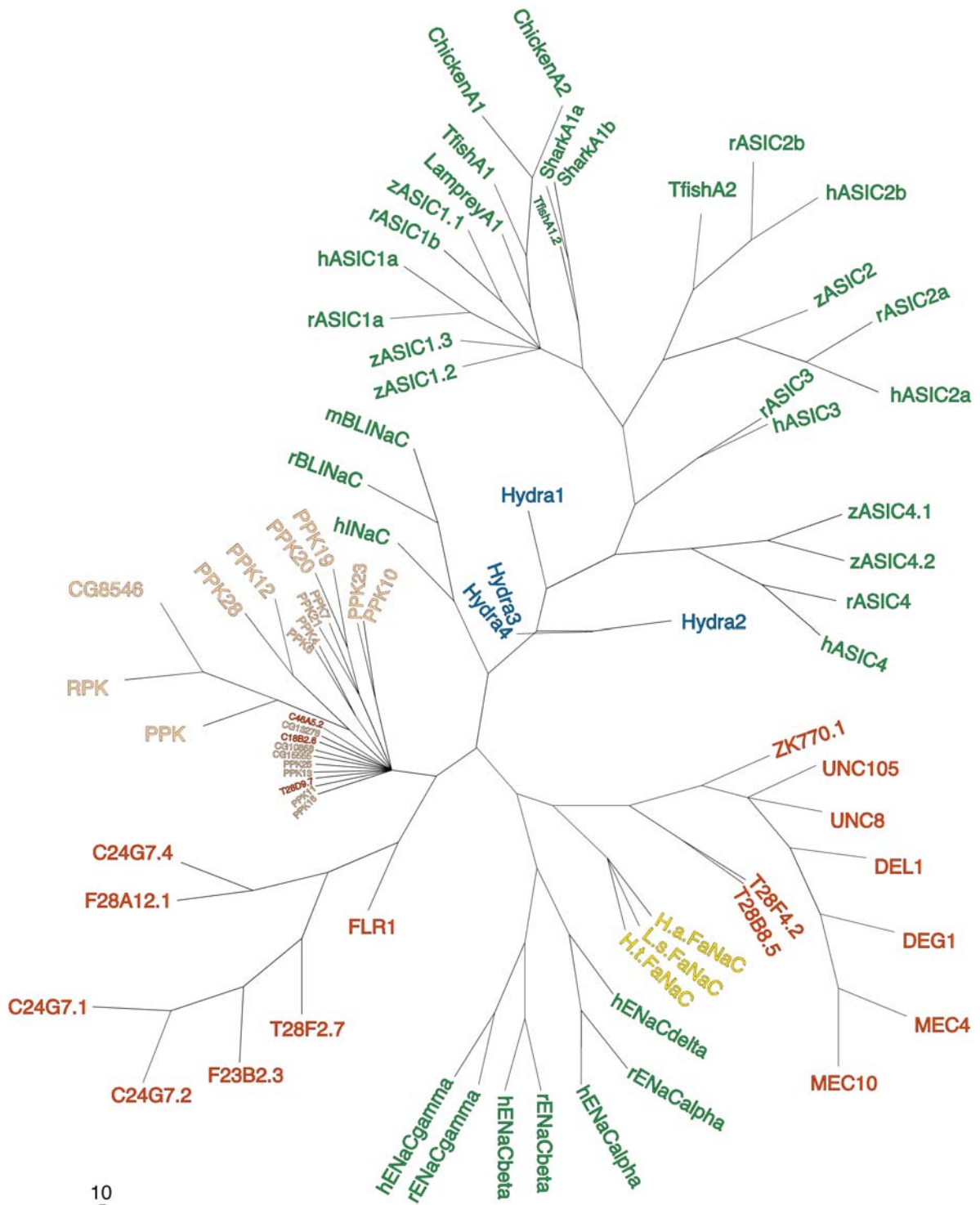
```

457 -LTKHLRGRGKQKFA-----KRSADKGVALSLDVKKRNPCESSRGIPAGMTYANILPHHPARGTFEDFTC.
464 -EFDQMLGYFNRRSA-----QKRSNTLLQEELNGHRTVPHLSGPRPPTTPCAVT-KTLSASHRTCYLVTRL.
456 -LTKELD--LLGKSE-----EEGSHDENMST-----CDTMAPNSETSHSTVNV-VPQLQALGTLEEIAC.
458 RLTLGLVFNSEKGLPRGP-----TIVNNNGSNHNSQSTSDILYNGYMDIHSYSDSSGASVDFRRGVEPSV.
456 LVIYNQFFK-----TY-----R.
457 MLVYTRFE-----KF-----TK.
455 FTLHQLR-----LS-----KKS.
606 VITLMLRFRFRYSWS-PGRGARGAR-EVASTPASSFSPSRFCPIPTSPPPSLPQOQMTPLALT-APPPAVATLGPSPAPLDSAAPDCSACALAL.
547 WITVIVASCKGLRRRRPQRYTPPTVAELVEAHTNCVFOPTSCRPAEYVPOOTLPIPGTAPPYVDSLRLQ--PLDTMESDSEVAI.
560 SILTARVNHKAKDWWARRQTPPSTETP--SRQGDNPALDITDILPTFTSAMRPPAPGSTVPGTPPPRINTLRLDR-AFSSQLTDQTLNEL.
469 TSPVW-----VTFIFLLKILEMQRTSPPQTV.
739 TATMSAE-----HINYSLYKKKAKKAKKIASG5F.

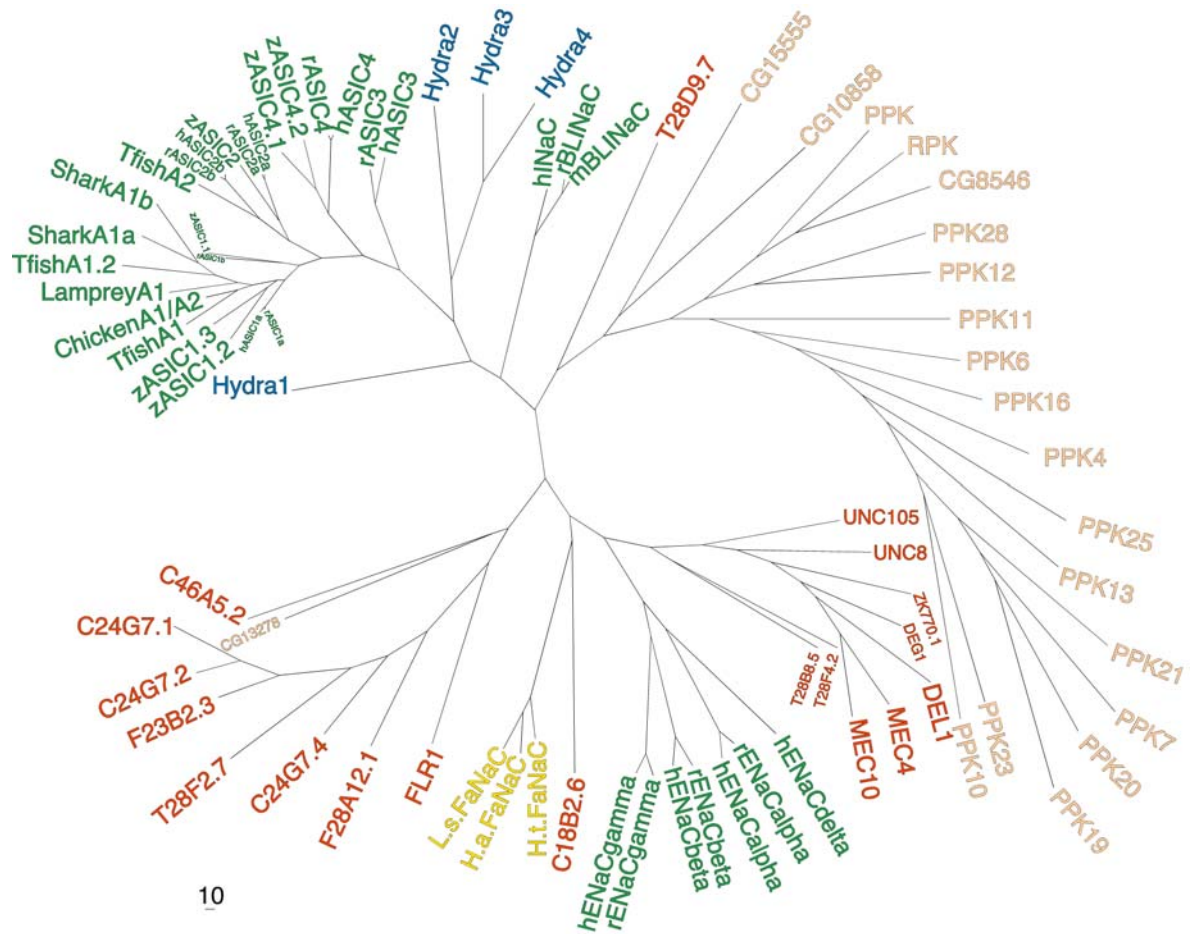
```

rat ASIC1a
rat ASIC3
rat ASIC2a
H.a.FaNaC
HyNaC4
HyNaC3
HyNaC2
rat ENaC alpha
rat ENaC beta
rat ENaC gamma
rat BLiNaC
MEC-4

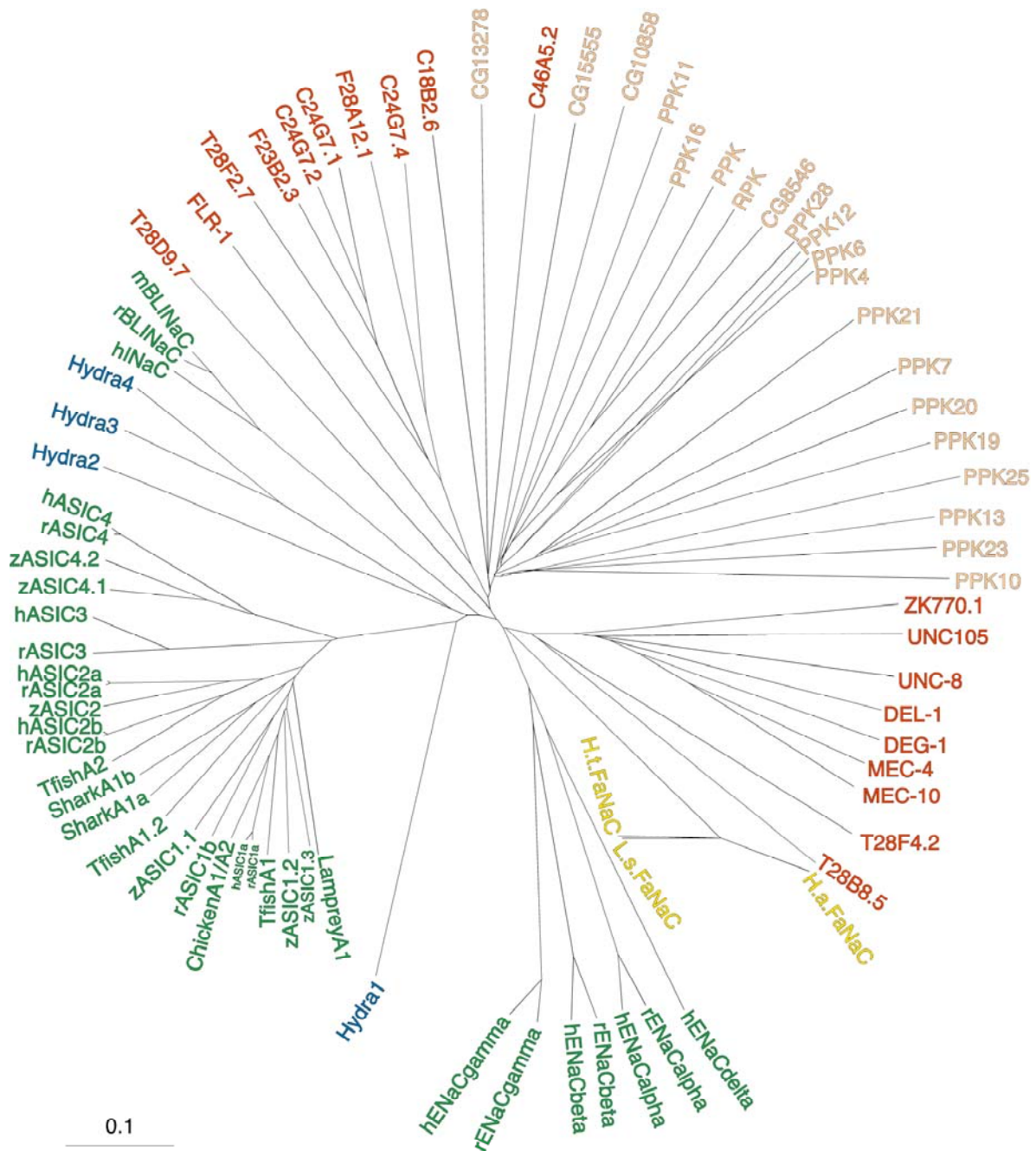
Appendix 1: Continuation from previous page.



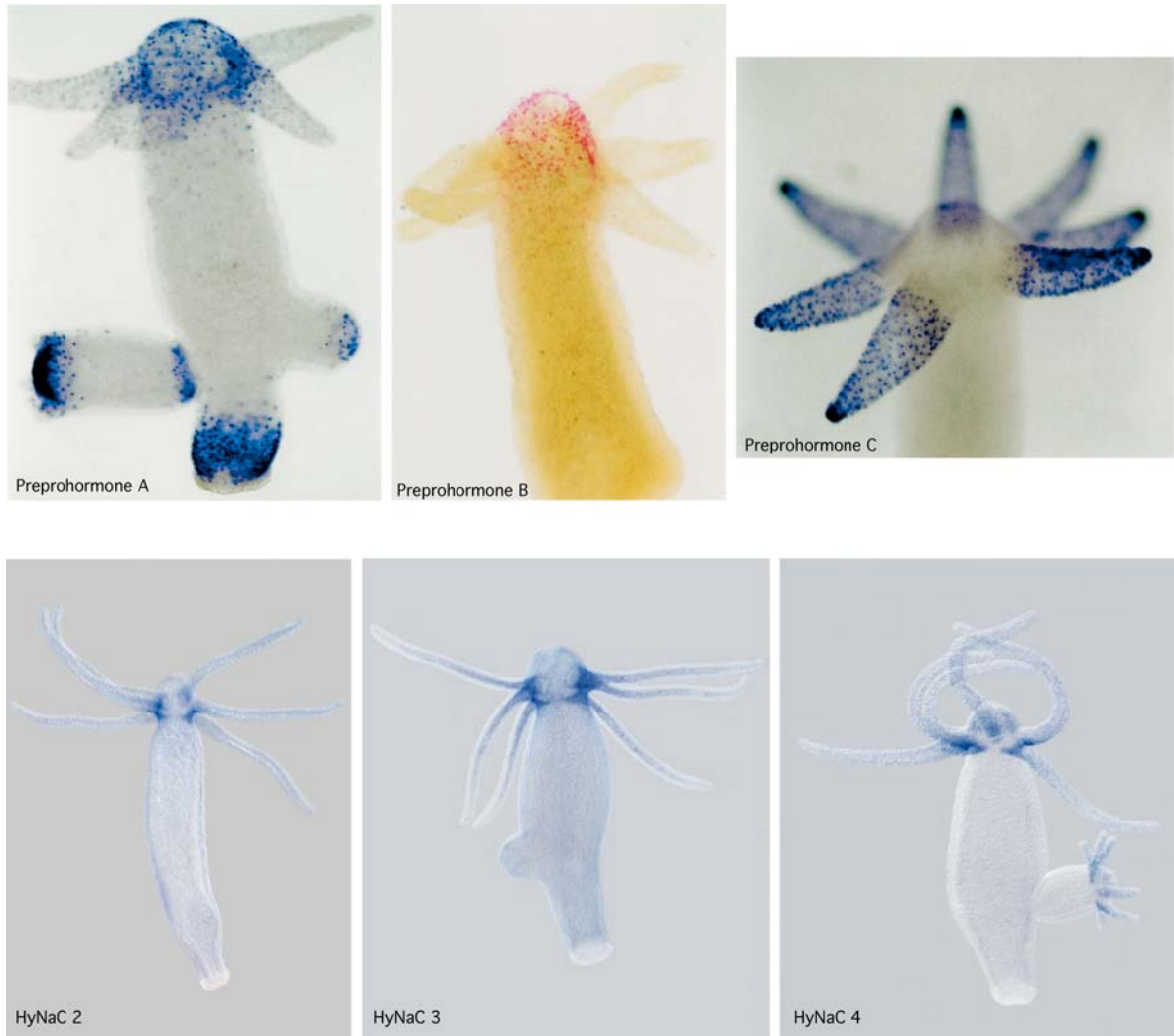
Appendix 3: Phylogenetic tree created with PAUP4.0b10 using the neighbor joining method. The colors represent animal groups from which the DEG/ENaC subunits were cloned (see Results Fig. 17). The branches are drawn so that their lengths are proportional to the evolutionary distance along that branch. The scale at the bottom relates the length of the branches to the distance, the number indicates the substitutions per site.



Appendix 4: Phylogenetic tree created with PAUP4.0b10 using the parsimony method. The colors represent animal groups from which the DEG/ENaC subunits were cloned (see Results Fig. 17). The branches are drawn so that their lengths are proportional to the evolutionary distance along that branch. The scale at the bottom relates the length of the branches to the distance, the number indicates the substitutions per site.



Appendix 5: Phylogenetic tree created with ClustalX 1.81 using the neighbor joining method. The colors represent animal groups from which the DEG/ENaC subunits were cloned (see Results Fig. 17). The branches are drawn so that their lengths are proportional to the evolutionary distance along that branch. The scale at the bottom relates the length of the branches to the distance, the number indicates the substitutions per site.



Appendix 6: In situ hybridizations reveal co-localization of HydraRFamides and HyNaC2-4 in the hypostome region. Top: Whole-mount in situ hybridizations of *Hydra* using cRNA probes coding for preprohormones A-C (from left to right) (Adapted from Hansen 2000.); Bottom: Whole-mount in situ hybridizations of *Hydra* using cRNA probes coding for HyNaC2-4 (from left to right). (Provided by A.KUHN and T.W. HOLSTEIN, Department of Molecular evolution and Genomics, Heidelberg.)

Sequence	Accession number
ASIC1a (human)	U78180
ASIC1a (rat)	U94403
ASIC1b (rat)	AJ309926
ASIC1a (shark)	AY956391
ASIC1b (shark)	AY956392
ASIC1 (chicken)	AY956393
ASIC1 (lamprey)	AY956390
ASIC1 (toadfish)	AY278028
ASIC1.2 (toadfish)	AY275840
ASIC1.1 (zebrafish)	AJ609615
ASIC1.2 (zebrafish)	AJ609616
ASIC1.3 (zebrafish)	AJ609617
ASIC2a (human)	U50352
ASIC2b (human)	NM_183377
ASIC2a (rat)	U53211
ASIC2b (rat)	AB049451
ASIC2 (chicken)	NM_001040467
ASIC2 (toadfish)	AY275841
ASIC2 (zebrafish)	AJ609618
ASIC3 (human)	AF095897

Appendix 7: List of accession numbers for the sequences used in the phylogenetic analysis.

(Continued on the next four pages.)

Sequence	Accession number
ASIC3 (rat)	AF013598
ASIC4 (human)	AJ271643
ASIC4 (rat)	AJ271642
ASIC4.1 (zebrafish)	AJ609619
ASIC4.2 (zebrafish)	AJ609620
BLINaC (mouse)	NM_021370
BLINaC (rat)	Y19034
C18B2.6	NM_076221
C24G7.1	NM_058895
C24G7.2	NM_058894
C24G7.4	NM_058892
C46A5.2	NM_068875
CG8546	NM_139868
CG10858	NM_139569
CG13278	NM_135965
CG15555	NM_143603
DEG-1	L33414
DEL-1	U76403
α ENaC (human)	X76180
α ENaC (rat)	X70521

Sequence	Accession number
β ENaC (human)	X87159
β ENaC (rat)	X77932
γ ENaC (human)	X87160
γ ENaC (rat)	X77933
δ ENaC (human)	U38254
F23B2.3	NM_069189
F28A12.1	NM_072829
FaNaC (<i>Helix aspersa</i>)	X92113
FaNaC (<i>Helisoma trivolvis</i>)	AF254118
FaNaC (<i>Lymnea stagnalis</i>)	AF335548
FLR-1	AB012617
HyNaC1	AM393879
HyNaC2	AM393878
HyNaC3	AM393880
HyNaC4	AM393881
INaC	AJ252011
MEC-4	X58982
MEC-10	L25312
PPK	Y16225
PPK4	NM_206137

Sequence	Accession number
PPK6	NM_137617
PPK7	NM_135172
PPK10	NM_001038805
PPK11	NM_001038798
PPK12	NM_137828
PPK13	NM_001014495
PPK16	NM_001038797
PPK19	AY226547
PPK20	NM_143448
PPK21	NM_143447
PPK23	NM_001014749
PPK25	NM_206044
PPK28	NM_001014748
RPK	Y12640
T28B8.5	NM_059829
T28D9.7	NM_062901
T28F2.7	NM_058795
T28F4.2	NM_059698
UNC-8	U76402
UNC-105	NM_063301

Appendix 7: Continuation from the previous three pages.

Sequence	Accession number
ZK770.1	U97404

Appendix 7: Continuation from the previous four pages.

LEBENS LAUF

seit Mai 2007 angestellt bei der Flyion GmbH in Tübingen als wissenschaftlicher Mitarbeiter

Studium

2004 - 2007 Promotion an der Eberhard-Karls-Universität Tübingen und der Julius-Maximilians-Universität Würzburg zum Thema „Phylogenetic and electrophysiological characterization of new ion channel subunits from *Hydra magnipapillata* belonging to the DEG/ENaC gene family“

September 2003 Diplom in Biologie an der Eberhard-Karls-Universität Tübingen; Diplomarbeit „Die Muskulatur der Vorderextremität von *Monias benschi* (Oustalet & Grandidier, 1903) (Mesornithidae, Aves) Die Schulter- und Oberarmmuskulatur im Vergleich mit Vertretern aus den Familien Gruidae, Rallidae, Megapodiidae, Ardeidae und Corvidae“

1997 – 2003 Studium der Biologie an der Eberhard-Karls-Universität Tübingen; Hauptfach Zoologie, Nebenfächer Parasitologie und Pharmakologie

Berufsausbildung

1994 – 1996 Ausbildung zum Versicherungskaufmann:
Basler-Versicherungen in Stuttgart; Kaufmännische Gesellenprüfung

Schulausbildung

1985 – 1994 Besuch des Gymnasiums in Ehingen/ Do.:
Abschluss mit der Allgemeinen Hochschulreife

1981 – 1985 Besuch der Christoph-von-Schmid Grundschule in Oberstadion

Tübingen, 25. Mai 2007